

In presenting the dissertation as a partial fulfillment of the requirements for an advanced degree from the Georgia Institute of Technology, I agree that the Library of the Institution shall make it available for inspection and circulation in accordance with its regulations governing materials of this type. I agree that permission to copy from, or to publish from, this dissertation may be granted by the professor under whose direction it was written, or, in his absence, by the dean of the Graduate Division when such copying or publication is solely for scholarly purposes and does not involve potential financial gain. It is understood that any copying from, or publication of, this dissertation which involves potential financial gain will not be allowed without written permission.

EFFECTS OF SURFACE HEAT TRANSFER
AND SPATIAL PROPERTY DEPENDENCE
ON THE OPTIMUM PERFORMANCE OF A
THERMOELECTRIC HEAT PUMP

A DISSERTATION

Presented to

The Faculty of the Graduate Division

by

Lawrence J. Ybarrondo

In Partial Fulfillment

of the Requirements for the Degree

Doctor of Philosophy in the School of Mechanical Engineering

Georgia Institute of Technology

June, 1964

62
12 R

EFFECTS OF SURFACE HEAT TRANSFER
AND SPATIAL PROPERTY DEPENDENCE
ON THE OPTIMUM PERFORMANCE OF A
THERMOELECTRIC HEAT PUMP

Approved: _____

U
Date approved by Chairman: 4/10/64

ACKNOWLEDGEMENTS

I cannot conceive of a better time or place to sincerely and gratefully thank the many people who have contributed to the writing of this dissertation by giving me more than my share of moral and financial support. I especially want to express my gratitude to: my wife for her patience and understanding; my advisor, Dr. J. E. Sunderland, whose guidance, encouragement and assistance were fundamental to the writing of this dissertation.

Finally and certainly not least, I wish to express my gratitude to: the Walter P. Murphy Foundation; the National Science Foundation; the Ford Foundation; the Mechanical Engineering Department at Georgia Tech; and the Roy C. Ingersoll Research Center for its generous financial support.

TABLE OF CONTENTS

	Page
ACKNOWLEDGMENTS	ii
LIST OF TABLES	vi
LIST OF ILLUSTRATIONS	vii
ABSTRACT	x
NOMENCLATURE	xiii
 Chapter	
I. INTRODUCTION	1
Thermoelectric Effects	
Thermoelectric Devices	
Objectives	
II. PREVIOUS RESEARCH	13
Historical-General	
Insulated Thermoelement with Finite Fins	
Thermoelements with Surface Heat Transfer and Finite Fins	
Thermoelements with Spatially Dependent Properties	
Summary of Previous Research	
III. CHARACTERIZATION OF THE PHYSICAL SYSTEM	20
Description of a Thermoelectric Device	
Differential Equation for the Temperature Distribution	
Thermal Boundary Conditions	
Summary of Assumptions	
IV. THE EFFECT OF FINITE HOT AND FINITE COLD JUNCTION FINS ON THE PERFORMANCE OF A THERMOELECTRIC HEAT PUMP	31
Physical System and Relevant Assumptions	
Temperature Distribution	
Performance Criteria	
Analysis of Results	
Conclusions	
V. OPTIMIZED PERFORMANCE OF A THERMOELECTRIC HEAT PUMP WITH SURFACE HEAT TRANSFER AND FINITE FINS	47

Chapter	Page
Physical System and Relevant Assumptions	
Temperature Distribution	
Performance Criteria	
Results	
Analysis of Results	
Conclusions	
VI. EFFECT OF SPATIAL PROPERTY DEPENDENCE ON THE PERFORMANCE OF A HEAT PUMP	76
1. Introduction to Spatial Property Dependence	
2. Physical System and Relevant Assumptions	
3. Effect of Spatially Dependent $\rho(x)$ on the Performance Criteria: S and k constant	
3a. Optimized No-Load Temperature Difference for $\rho(u) = \bar{\rho} [1 + \gamma_{\rho} (u - \frac{1}{2})]$	
3b. Optimized Heat Pumped for $\rho(u) = \bar{\rho} [1 + \gamma_{\rho} (u - \frac{1}{2})]$	
3c. Optimized C.O.P. for $\rho(u) = \bar{\rho} [1 + \gamma_{\rho} (u - \frac{1}{2})]$	
4. Effect of Spatially Dependent $k(x)$ on the Performance Criteria: ρ and S constant	
4a. Optimized No-Load Temperature Difference for $k(u) = \bar{k} [1 + \gamma_k (\frac{1}{2} - u)]$	
4b. Optimized Heat Pumped for $k(u) = \bar{k} [1 + \gamma_k (\frac{1}{2} - u)]$	
4c. Optimized C.O.P. for $k(u) = \bar{k} [1 + \gamma_k (\frac{1}{2} - u)]$	
5. Effect of Spatially Dependent $S(x)$ on the Performance Criteria: ρ and k constant	
5a. Optimized No-Load Temperature Difference for $S(u) = \bar{S} [1 + \gamma_S (u - \frac{1}{2})]$	
5b. Optimized Heat Pumped for $S(u) = \bar{S} [1 + \gamma_S (u - \frac{1}{2})]$	
5c. Optimized C.O.P. for $S(u) = \bar{S} [1 + \gamma_S (u - \frac{1}{2})]$	
6a. Effect of a Simultaneous Variation of $S(x)$ and $\rho(x)$ on the Performance Criteria: k constant	
6b. Optimized θ_{NL} , Q_i^* , and C.O.P. for Variable $S(u)$ and $\rho(u)$	
7a. Performance Criteria and the Variation of $S(x)$ and $\rho(x)$ such that Z remains constant	
7b. Optimized θ_{NL} , Q_i^* , and C.O.P. for Variable $S(u)$ and $\rho(u)$ and constant Z	
8. Simultaneous Variation of $S(x)$, $\rho(x)$, and $k(x)$	
8a. Performance Criteria for Variable $\rho(u)$, $k(u)$, and $S(u)$	
8b. Summary of Results	
VII. SUMMARY	134
APPENDIX	
A. Derivation of Differential Equation for One-Dimensional Temperature Distribution in an Inhomogeneous Thermo-element	138

APPENDIX	Page
B. Physical Significance of the Fin Conductance and Equations for the Maximum Performance of a Completely Insulated Thermoelement	143
C. Definitions of Constants in Chapter V	145
D. Discussion of the Green's Function	147
E. Discussion of a Numerical Optimizing Technique	152
LITERATURE CITED	153
OTHER REFERENCES	155
VITA	156

LIST OF TABLES

Table	Page
1. Heat Transfer Coefficients h ($W/cm^2-^{\circ}K$) for Several Values of u_L and L	61

LIST OF ILLUSTRATIONS

Figure	Page
1. Thermoelectric Effects	4
2. Thermoelectric Devices	9
3. A Basic Thermoelectric Heat Pump	21
4. A Single-Element Thermoelectric Heat Pump	21
5. Single Thermoelement used as a Heat Pump	32
6. Optimum No-Load Temperature Difference versus Hot Junction Fin Conductance	41
7. Optimum Heat Pumped versus Hot Junction Fin Conductance	42
8. C.O.P. versus Hot Junction Fin Conductance for Optimum Heat Pumped	43
9. Optimum C.O.P. versus Hot Junction Fin Conductance	44
10. Heat Pumped versus Hot Junction Fin Conductance for Optimum C.O.P.	45
11. Single Thermoelement with Surface Heat Transfer Used as a Heat Pump	49
12. Typical Temperature Distribution in a Thermoelement for Optimum Heat Pumping	49
13. Optimum Heat Pumped, $(Q_1^*)_{opt}$ versus Heat Pumped at Optimum C.O.P. with $u_L = 1$	63
14. Optimum C.O.P., $(C.O.P.)_{opt}$ versus C.O.P. at Optimum Heat Pumped with $u_L = 1$	64
15. Optimum Heat Pumped, $(Q_1^*)_{opt}$ versus Heat Pumped at Optimum C.O.P. with $u_L = 3$	66
16. Optimum C.O.P., $(C.O.P.)_{opt}$ versus C.O.P. at Optimum Heat Pumped with $u_L = 3$	67

LIST OF ILLUSTRATIONS (continued)

Figure		Page
17.	Optimum Heat Pumped, $(Q_1^*)_{opt}$ versus Heat Pumped at Optimum C.O.P. with $u_L = 5$	69
18.	Optimum C.O.P., (C.O.P.) _{opt} versus C.O.P. at Optimum Heat Pumped with $u_L = 5$	70
19.	Optimum Heat Pumped, $(Q_1^*)_{opt}$ versus Heat Pumped at Optimum C.O.P. with $u_L = 20$	71
20.	Optimum C.O.P., (C.O.P.) _{opt} versus C.O.P. at Optimum Heat Pumped with $u_L = 20$	72
21.	Optimum No-Load Temperature Difference versus Fraction of Element Insulated for Various Values of u_L	74
22.	Dependence of the Seebeck Coefficient, Electrical Resistivity and Thermal Conductivity on Carrier Concentration	77
23.	An Insulated Inhomogeneous Thermoelement Used as a Heat Pump	79
24.	Assumed Spatial Dependence of $\rho(x)$	82
25.	Assumed Spatial Dependence of $k(x)$	92
26.	Assumed Spatial Dependence of $S(x)$	101
27.	Effect of the Distribution of $S(u)$, $\rho(u)$, and $k(u)$ with Position on the Optimum No-Load Temperature Difference	114
28.	Effect of the Distribution of $S(u)$, $\rho(u)$, and $k(u)$ with Position on Heat Pumping	115
29.	Effect of the Distribution of $S(u)$, $\rho(u)$, and $k(u)$ with Position on the Coefficient of Performance	116
30.	Effect of the Distribution of $S(u)$ and $\rho(u)$ with Position on the Optimum No-Load Temperature when $S^2(u)/\rho(u)$ is Constant	123
31.	Effect of the Distribution of $S(u)$ and $\rho(u)$ with Position on Heat Pumping when $S^2(u)/\rho(u)$ is Constant	124

LIST OF ILLUSTRATIONS (Continued)

Figure		Page
32.	Effect of the Distribution of $S(u)$ and $\rho(u)$ with Position on the Coefficient of Performance when $S^2(u)/\rho(u)$ is Constant	125
33.	Energy Balance for a Differential Thermoelement .	140
34.	Illustration of a Numerical Optimizing Technique	152

ABSTRACT

The objectives of this study are to investigate the effects of finite fins, surface heat transfer with finite fins, and the spatial dependence of the Seebeck coefficient, electrical resistivity, and thermal conductivity on the optimum performance of a thermoelectric heat pump.

The first portion of the investigation presents analytical solutions for the steady-state temperature difference, heat pumping capacity, and coefficient of performance of a thermoelement used as a thermoelectric heat pump with finite hot and cold junction fins. The latter three expressions are also optimized with respect to the electrical current. The longitudinal surface of the thermoelement is insulated, the surface heat transfer coefficient over the hot and cold junction fins being arbitrary. A numerical example is worked in which performance curves are compared for cases of infinite and finite fin conductance at the junctions of a simple thermoelectric heat pump. A method of augmenting device performance by realistic fin design is shown; or, conversely, a method of economizing on fin size and the anticipated decrease in device performance is shown.

The second phase of the analysis presents equations for the steady-state temperature distribution, optimum heat pumping capacity, optimum coefficient of performance and optimum no-load temperature difference for a single element thermoelectric heat pump with constant properties. Part of the longitudinal surface of the thermoelement is

convectively cooled; fins of varying size exist at the hot and cold junctions; and three different surface heat transfer coefficients can be arbitrarily selected, one for the hot-junction fins, one for the fins at the cold junction, and one for the surface of the thermoelement. It is shown that surface heat transfer can be used to substantially increase the heat pumping capacity and, in some cases, the coefficient of performance is improved. The effect of fin size at the junctions of the thermoelement on performance is shown. An example is presented in which optimized performance curves are compared for devices using fins with infinite and finite conductances and where the thermoelements have varying amounts of surface heat transfer. The results are presented in dimensionless form so that they apply for many different conditions. The results show that gains in heat pumping capacity of the order of 300 percent to 400 percent are possible.

The third phase of this research ascertains quantitatively how the spatial dependence of the Seebeck coefficient, electrical resistivity, and thermal conductivity affect the optimized no-load temperature difference, optimized coefficient of performance and the optimized rate of heat removal of thermoelectric heat pumps. The longitudinal surface of the thermoelement is insulated. The fin conductance at the hot and cold junctions is infinite. The effect of the spatial dependence of each property on the performance criteria is analyzed individually and then in physically appropriate combinations. It is shown that certain small linear variations in the Seebeck coefficient and the electrical resistivity act to increase all the performance criteria. However, small linear variations in the thermal conductivity (consistent with the variations in the

Seebeck coefficient and the electrical resistivity) decrease the performance criteria. In addition, it is shown that the spatial dependence of the thermal conductivity is not nearly as important as the dependence of the electrical resistivity and the Seebeck coefficient. Therefore, a net increase in the performance criteria should be possible through the use of controlled spatial property dependence. Finally, all three thermoelectric properties are assumed to have a small linear spatial dependence (consistent with the physical principles governing their interrelationships) and analytical equations describing the performance criteria of a thermoelement used as a heat pump are developed. These equations may be used to compute the performance criteria of a thermoelement with inhomogeneous thermoelectric properties over a wide range of parameter values.

NOMENCLATURE

English Letters		Units
A	cross-sectional area of thermoelement	cm ²
A _c	surface area of cold-junction fin	cm ²
A _h	surface area of hot-junction fin	cm ²
B _k	function defined in Chapter VI, Section 4c	dimensionless
C ₁ , C ₂	constants of integration	dimensionless
D _m , E _m	constants defined in Appendix C (m=1,2,3,4)	dimensionless
F _m	constants of integration (m=1,2,3,4)	dimensionless
G(u, ε)	Green's function	dimensionless
h	convective heat transfer coefficient	W/cm ² -°K
H _c	heat conductance of cold-junction fin, $h_c A_c L/kA_c$	dimensionless
H _h	heat conductance of hot-junction fin, $h_h A_h L/kA_h$	dimensionless
I	electrical current	amps
J	electrical current density	amps/cm ²
k	thermal conductivity with zero current	W/cm-°K
L	length of thermoelement	cm
p	perimeter of thermoelement	cm
P _i	electrical power input	watts
Q _i	heat transferred to cold junction	watts
Q _o	heat transferred from hot junction	watts
R _m	constants defined in Appendix C (m=1,2,3,4)	dimensionless
S	Seebeck coefficient	volts/°K

T	absolute temperature	°K
T'	environment temperature	°K
u	position variable $u = x/L$ (Chapters IV and VI) $u = (x/L)(hpL^2/kA)^{1/2}$ (Chapter V)	dimensionless
\bar{u}	$u_L - u_V$	dimensionless
v	length of insulated section of thermoelement	cm
V	voltage	volts
W_m	constants defined in Appendix C (m=1,2,3,4)	dimensionless
x	position variable	cm
y	current $y = ISL/kA$ (Chapter IV) $y = ISL/kAu_L$ (Chapter V)	dimensionless
z	figure of merit, $S^2/\rho k$	°K ⁻¹
z_m	constants defined in Appendix C (m=1,2,...15)	dimensionless

Greek Letters

α	material parameter, $1/z(T'_c - T'_h)$ (Chapters IV and V) current, ISL/kA (Chapter VI, Section 3)	dimensionless
β	function defined in Chapter VI, Section 6a	dimensionless
β_1	function defined in Chapter VI, Section 8	dimensionless
$\gamma_p, \gamma_k, \gamma_s$	$\Delta\beta/\bar{\rho}, \Delta k/\bar{k}, \Delta S/\bar{S}$ respectively	dimensionless
$\gamma'_p, \gamma'_k, \gamma'_s$	$\gamma_p/(1 - \frac{\gamma_p}{2}), \gamma_k/(1 + \frac{\gamma_k}{2}), \gamma_s/(1 - \frac{\gamma_s}{2})$ respectively	dimensionless
ϵ_k	function defined in Chapter VI, Section 4b	dimensionless

θ	temperature variable, $\theta = (T - T'_c)/(T'_c - T'_h)$ (Chapters IV and V) $\theta = (T - T'_h)/T'_c$ (Chapter VI)	dimensionless
λ	current $\lambda = \sqrt{\alpha \gamma_s}$ (Chapter VI, Section 5) $\lambda = \sqrt{\frac{\alpha \gamma_s}{1 + \frac{\gamma_k}{2}}}$ (Chapter VI, Section 8)	dimensionless
Π	Peltier coefficient	volts
ρ	electrical resistivity	ohm-cm
τ	Thomson coefficient	volts/ $^{\circ}$ K
φ	temperature parameter, $T'_c/(T'_c - T'_h)$ (Chapters IV and V)	dimensionless
φ_{ρ}	function defined in Chapter VI, Section 3a	dimensionless
φ_k	function defined in Chapter VI, Section 4a	dimensionless
ψ	function defined in Chapter VI, Section 8a	dimensionless

Subscripts

a	refers to material a
b	refers to material b
c	refers to cold junction
h	refers to hot junction
L	refers to position $x = L$
v	refers to position $x = v$

Superscripts

*	denotes a dimensionless quantity
-	denotes an average quantity

Other symbols used are defined in the text.

CHAPTER I

INTRODUCTION

The thermoelectric effects are concerned with the direct conversion of electricity into heat; and conversely, the direct conversion of heat into electricity. Most of the factors entering into a consideration of thermoelectric effects have been known for over a hundred years. Not until the recent development of semiconductor materials did it become possible to utilize thermoelectric effects to fabricate thermoelectric heat pumps and thermoelectric generators that have important practical utility. Thus, in the past several years there has been a renewed interest in thermoelectric principles and completely new products based on these principles are being developed. For instance, in regions where electricity is plentiful, cooling or heating living areas by the direct conversion of electricity to a thermal effect by a thermoelectric heat pump is a distinct possibility. In the electronics industry, small battery operated thermoelectric refrigerators may be the answer to the cooling of electronic components.

For a period of several years, much research has been carried out for the purpose of improving the performance of thermoelectric devices. This research is generally divided into the categories of developing better and cheaper materials or making the greatest use of existing materials. This analysis will be concerned with both areas of research. The first part of the analysis is an attempt to determine: (1) if a

more effective design can be achieved by the use of direct heat transfer between the longitudinal surface of the thermoelement and its environment (2) a realistic design that will indicate how much the performance of a device is impaired by use of finite fins. The second phase of this analysis is an attempt to determine if the spatial dependence of thermoelectric properties can be used to improve the performance of a thermoelectric heat pump.

The behavior of a thermoelement subjected to heat transfer along its longitudinal surface has been investigated previously. But these investigations were made with boundary conditions that are not entirely realistic and the effect of finite fins on device performance was not considered. The effect of spatial property dependence on device performance has not been investigated to the author's knowledge. In fact, spatial property dependence has generally been considered undesirable under any condition of operation.

At this point, it might be expedient to briefly review the thermoelectric effects and their application to thermoelectric heat pumps and thermoelectric generators.

Thermoelectric Effects

The term, "thermoelectric effect," implies the reversible phenomena which occur at the junctions of dissimilar metals and throughout the bodies of conductors in which finite temperature differences exist. The principles and theory underlying thermoelectric effects were not established by one man at one time, but by several scientists working over a span of many years. The three thermoelectric effects are the Seebeck effect, Peltier effect and Thomson effect.

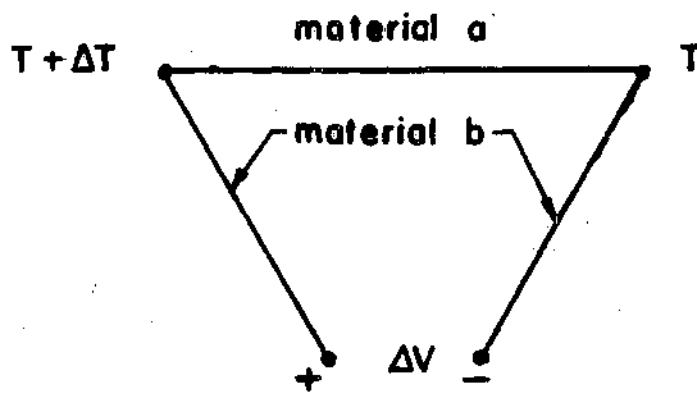
In 1821 Thomas J. Seebeck observed the first of the reversible thermoelectric effects. Seebeck discovered the existence of thermoelectric currents while experimenting with the electromagnetic effects associated with bismuth-copper and bismuth-antimony circuits. He discovered that when two dissimilar metals are connected to form an open circuit, as shown in Fig. 1a, and one of the junctions is at a higher temperature than the other, an emf (called the Seebeck emf) exists. This may be described mathematically by

$$\Delta V = S_{ab} \Delta T \quad (1-1)$$

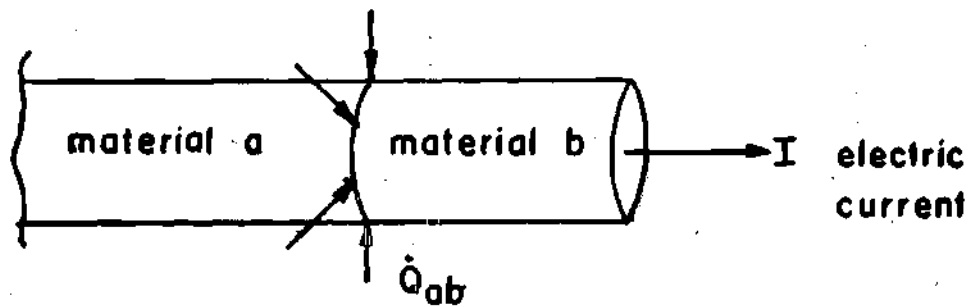
Where S_{ab} is a coefficient of proportionality called the Seebeck coefficient. This is more commonly, but erroneously, called the thermoelectric power. The relative Seebeck coefficient, S_{ab} is defined as

$$S_a - S_b = S_{ab} = \lim_{\Delta T \rightarrow 0} \frac{\Delta V}{\Delta T} = \frac{dV}{dT} \quad (1-2)$$

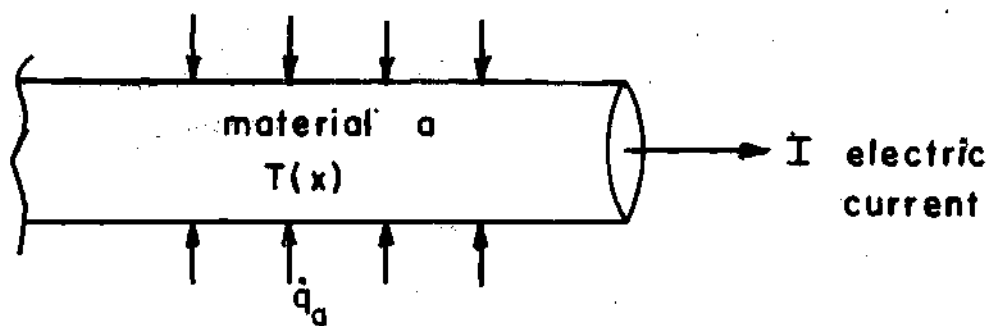
The Seebeck coefficient depends on the choice of materials a and b and represents for a given material combination, the net change in thermal emf caused by a unit temperature difference. The change in potential may be either positive or negative in the direction of the temperature gradient. Therefore, the magnitude and sign of, S_{ab} , are both important. It is expedient to assign an absolute Seebeck coefficient to all materials relative to an arbitrary reference material (usually lead) such that the Seebeck coefficient of the junction of two materials is the difference between the two absolute Seebeck coefficients of the material. It is well to distinguish between the Seebeck effect, which refers to the net



a) Seebeck Effect



b) Peltier Effect



c) Thomson Effect

Fig. 1. Thermoelectric Effects

conversion of thermal energy into electrical energy with the appearance of an electric current and the Seebeck emf, which refers to the net thermal electromotive force set up in a thermocouple under zero current conditions.

In 1834 Peltier discovered unusual thermal effects when he introduced small external electric currents in Seebeck's bismuth-antimony thermocouple. He found that when a current is passed through the junction of two dissimilar metals in one direction, heat is absorbed, and the junction is cooled (i.e., it acts as a heat sink). When the current is reversed, the junction is heated (i.e., it acts as a heat source) and rejects heat to the surroundings. The Peltier effect, then, refers to the reversible rejection or absorption of heat which usually takes place when an electric current crosses a junction between two dissimilar metals. Peltier observed that for a given current the rate of absorption or liberation of heat at the junction of the materials is proportional to the current and depends on the materials forming the junction. Thus, in Fig. 1b, the rate at which Peltier heat is absorbed is given by

$$\dot{Q}_{ab} = \Pi_{ab}I \quad (1-3)$$

where I is the current and Π_{ab} is a coefficient of proportionality known as the Peltier coefficient. Note that Π is the reversible heat which is absorbed or liberated at the junction when current passes through the junction in unit time; it has dimensions of voltage. The temperature of the junction and the materials comprising the junction determine the direction and magnitude of the Peltier coefficient; however, Π at one junction does not depend on the temperature of the other junction. Thus

(similar to the relative Seebeck coefficient S_{ab}) as shown in reference (3), a relative Peltier coefficient is defined as

$$\Pi_{ab} = \Pi_a - \Pi_b \tag{1-4}$$

such that Π_{ab} of the junction of two materials is the difference between the absolute Peltier coefficients of the materials a and b respectively.

William Thomson, later known as Lord Kelvin, realized that a relationship should exist between the Seebeck and Peltier coefficients. In 1857, Thomson attempted to derive such a relationship and collaterally conducted an experiment which demonstrated the existence of a third thermoelectric effect, now called the Thomson effect. Thomson passed an electric current through a closed circuit formed by a single homogeneous conductor which was subjected to a temperature gradient. He found the I^2R heat to be slightly augmented, or decreased, from the cold junction to the hot junction, or from the hot junction to the cold junction, depending upon the direction of the current and the material under test; this discrepancy was due to the third effect. The Thomson effect refers to the reversible absorption or liberation of heat along a conductor with a temperature gradient when an electric current flows through the conductor. Thus, in Fig. 1c, the rate at which Thomson heat is absorbed is

$$\dot{q}_a = \tau_a I \frac{dT}{dx} \tag{1-5}$$

where \dot{q}_a is the rate of heat absorption per unit length of material a, dT/dx is the temperature gradient, and τ_a is a coefficient of proportionality known as the Thomson coefficient depending on the properties of

material a only. Note that τ represents the rate at which heat is absorbed, or liberated per unit temperature difference per unit current.

Kelvin was first to demonstrate that there is a definite relationship between the three reversible thermoelectric effects. He assumed that the irreversible I^2R and heat-conduction effects could be disregarded in a thermodynamic derivation of the relationship between the three reversible coefficients. Although Kelvin's relations are correct, his analysis is not considered rigorous. A rigorous development of these same relations is accomplished using irreversible thermodynamics (see for example Callen). The first and second Kelvin relations are, respectively,

$$\Pi_a = T_a S_a \quad (1-6)$$

$$\tau_a = T_a \frac{dS_a}{dT} \quad (1-7)$$

These relations are important, since they express the Peltier and Thomson coefficients in terms of the more easily measured Seebeck coefficient.

Thermoelectric Devices

Thermoelectric effects are utilized in two basic types of thermoelectric devices:

1. A thermoelectric heat pump is a device which utilizes an electrical energy input to pump thermal energy across a temperature gradient.
2. A thermoelectric generator is a device which converts thermal energy into electrical energy.

This analysis will be concerned exclusively with the performance

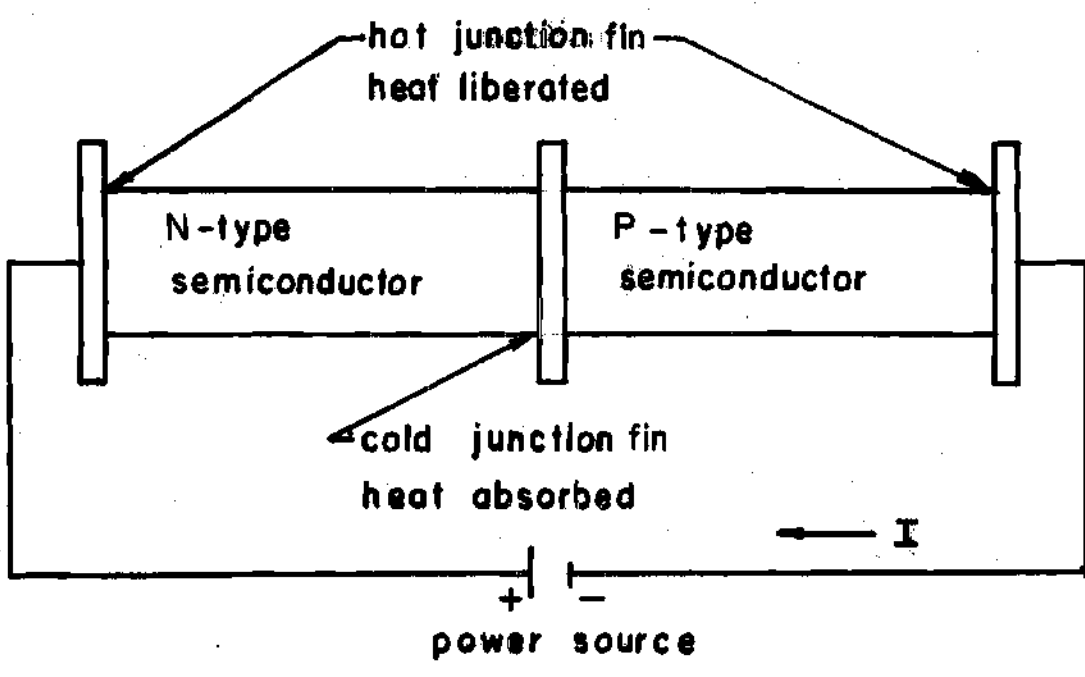
of a thermoelectric heat pump.* However, for the sake of completeness a representative device of each type will be described briefly.

Thermoelectric Heat Pump

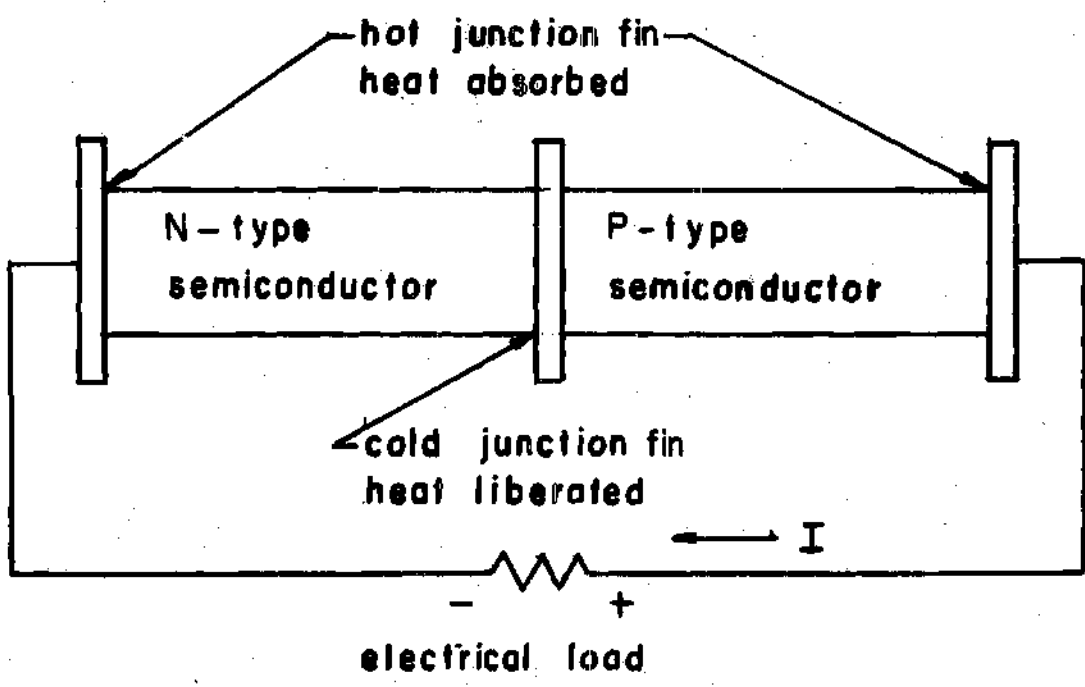
A typical heat pump is shown in Fig. 2a. Notice that the heat pump is an assembly of three basic components with distinctly different functions: (1) the thermoelements through which the heat is pumped; (2) fins or heat exchangers generally made of copper or aluminum; (3) the power supply equipment (represented by a d-c battery) necessary to transform and rectify the commonly available high-voltage a-c electric current to a low-voltage d-c supply to the heat pump. By the use of a P-type thermoelectric element and an N-type thermoelectric element in a d-c series arrangement, heat may be pumped from source to sink. When electrical power is delivered to the circuit, Peltier heat is liberated at the hot junction and absorbed at the cold junction, and therefore a temperature difference is established between the junctions. Thomson heat is absorbed and liberated along the length of the elements.

At the cold-junction fin heat from the source to be cooled is transferred to the junction and made available for transformation into electrical work; the temperature of the cold-junction fin must be lower than the temperature of the heat source and this temperature difference is an important design variable. Similarly, the temperature of the hot-junction fin must be higher than that of the heat sink, which is usually either air

*In the remainder of this analysis the word "thermoelectric" in reference to a heat pump or generator will be omitted frequently for brevity.



a) Thermoelectric Heat Pump



b) Thermoelectric Generator

Fig. 2. Thermoelectric Devices

or water. The net effect of the operation of the heat pump for a given electrical power input is a certain rate of heat removal from the source, and a higher rate of heat rejection to the sink. The thermoelectric heat pump is classified as a refrigerator (or cooling device) if the primary purpose is to remove heat from the heat source. At the same time, however, there is always the possibility of operating the pump as a warming device. For a given thermoelectric heat pump, three major design criteria are of interest: First, the maximum temperature difference that may be established with the cold junction thermally insulated from the cold environment. Second, the maximum amount of heat that may be pumped from the cold environment. Third, the maximum attainable ratio of heat pumped to electrical power input. This ratio is defined as the coefficient of performance.

A typical thermoelectric generator is shown in Fig. 2b. When a heat source is applied to the hot-junction fin, the Seebeck effect causes a current to flow through the electrical load. The Peltier heat is absorbed at the hot junction and liberated at the cold junction, and the Thomson heat is liberated or absorbed along the length of the elements. In designing a given generator, two problems are of interest: First, the maximum thermal efficiency, Second, the maximum electrical power output.

As stated before, only the thermoelectric heat pump is considered in this investigation. However, the temperature distribution equations derived in Chapters IV and V in this dissertation apply equally well to the thermoelectric generator problem. Thus, it is possible for future researchers to determine the effect of surface heat transfer* and finite

*Surface heat transfer is used in this paper to denote heat transfer from the longitudinal surface of a thermoelement.

fins on the performance of a thermoelectric generator by changing the junction boundary conditions given in this dissertation and using the temperature distribution equations derived herein.

Objectives

The objectives of this investigation are:

1. To determine the effect of finite fins on the optimum performance of a thermoelectric heat pump.
2. To determine the combined effect of finite fins and surface heat transfer on the optimum performance of a thermoelectric heat pump.
3. To determine the effect of spatial property dependence on the optimum performance of a thermoelectric heat pump.

In each of the three objectives, the effect in question is measured by comparing the optimum performance criteria of a heat pump embodying the effect in question to the corresponding optimum performance criteria of an idealized heat pump; that is, a heat pump with constant properties, infinite hot and cold junction fins, and zero surface heat transfer. Throughout this dissertation, the performance criteria are optimized with respect to the electrical current input I ; that is, I is adjusted to optimize the desired useful effect for a given set of conditions. Comparison of optimum performances is made because it is the most desirable criterion for measuring the effects being investigated.

However, adherence to the most desirable comparison procedure places severe restrictions upon the type of mathematical models that may be solved and compared analytically. It becomes extremely difficult to

obtain analytical expressions for the optimum current and therefore for the optimum performance, even for physical systems with relatively simple mathematical expressions describing the temperature distribution. For most of the mathematical models analyzed in this dissertation it is possible to obtain analytical expressions for the optimum performance. All exceptions are clearly indicated.

CHAPTER II

PREVIOUS RESEARCH

Historical - General

The discovery of the scientific principles that form the basis of the development of the thermoelectric heat pump was followed by a long period of inactivity. Then, in 1911, the first mathematical analysis of a Peltier heat pump was published by Altenkirch (1). Unfortunately, the technology received no impetus until the last decade when semi-conductors were developed with thermoelectric properties that are superior to those of the metals and alloys that were used previously. As a result, the next analysis of a thermoelectric heat pump published by Gelhoff, et al. (2) in 1950 followed almost 40 years after the initial analysis and about 150 years after the discovery of the thermoelectric effects. In 1957 Ioffe (3) published the first book devoted solely to thermoelectrics. Since publication of Ioffe's book, there has been a rapid and continuing development of a thermoelectric technology. Most of the research effort in the thermoelectric area has been directed toward the development of new materials with a much smaller portion of the effort being directed toward device design. The research effort in this dissertation is primarily directed toward device design.

Insulated Thermoelement with Finite Fins

In applications using thermoelectric heat pumps, space, weight, and cost considerations make it essential to limit the size of fins

that are used to transfer heat between the device and its environments. However, such limitations inherently reduce the amount of heat pumped and the coefficient of performance. It is desirable to know how much the performance of a device is impaired by the use of finite fins.

An investigation by Brandt (4) considered a nonlinear mathematical model of a thermoelectric power generator. The model had an infinite hot-junction fin and finite cold-junction fin. Brandt (4) considered only a radiative energy exchange between the cold-junction fin and its environment; he did not specifically evaluate the effect of the finite cold-junction fin on generator performance.

An investigation by Rollinger and Sunderland (5) evaluated the effect of a finite hot-junction fin on the performance of a thermoelectric generator. The analysis assumed the cold-junction fin was infinite, and did not consider the effect of finite fins on the performance of a thermoelectric heat pump. An analysis by Crosby et al. (6) investigated a thermoelectric heat pump with finite hot and finite cold junction fins. The investigation was concerned primarily with optimizing Peltier heat pumping with respect to the length-to-area ratio for a given current. It did not consider the effect of finite hot and finite cold-junction fins on the coefficient of performance.

A paper by Zito (7) considered a physical model of a thermoelectric heat pump that had finite fins. Zito assumed that the finite fins could exchange energy with their environments by convection and/or radiation. He did not evaluate the effect of the finite fins on the performance of the heat pump. Furthermore, the analysis of Zito did not consider or evaluate the effect of finite fins on the optimum performance of a heat pump.

An analysis by Ybarrondo and Sunderland (8) investigated the effects

of finite fins on the optimized performance of a thermoelectric generator. The analysis indicated that finite fins could significantly affect the performance of a generator.

A very interesting discussion on thermoelectric heat exchangers was given by Mackey (9); his paper was a feasibility study. He discussed heat transfer surfaces, feasibility of natural convection and radiation, and forced convection insofar as these factors are related to the heat exchange between a thermoelectric device and its surroundings. His analysis showed that the hot-junction fins of most thermoelectric heat pumps with a "figure of merit" (Z)* less than or equal to $3 \times 10^{-3} \text{ } ^\circ\text{K}^{-1}$ will probably be water-cooled or will be cooled by air blown over a compact heat exchanger with extended surfaces. In addition, cooling the hot-junction fin by natural convection and/or radiation will prove practical for most thermoelectric devices only when the figure of merit approaches $5 \times 10^{-3} \text{ } ^\circ\text{K}^{-1}$.

Thermoelements with Surface Heat Transfer and Finite Fins

This section of the analysis will be concerned with making the greatest use of existing materials, specifically the optimum utilization of existing materials relative to the thermal system. As mentioned, the first analysis of a heat pump was made by Altenkirch (1) and more refined solutions were given by Gehlhoff et al. (2), Ioffe (3) and others. Many simplifying assumptions were made in these analyses. Of particular interest here is the assumption neglecting all external heat transfers except those at the hot and cold junctions. External heat transfers were

* See nomenclature for an explanation of this symbol.

neglected because it was assumed that they would have a deleterious effect on performance; it has been demonstrated analytically that surface heat transfer can be utilized to substantially improve the performance of thermoelectric devices.

Analyses by Harmon et al., (10) and Kaganov et al. (11) have included convective surface heat transfer between a thermoelement and its environment. However, both these analyses were concerned primarily with establishing a theoretical basis for the accurate measurement of thermoelectric properties and were not concerned with using surface heat transfer to augment device performance. An analysis by Parrott (12) considered surface heat transfer along the entire length of a thermoelement. However Parrott did not indicate the effect of surface heat transfer on performance. Parrott's analysis was not an attempt to determine if surface heat transfer could be a useful mechanism for improving performance. He was only concerned with establishing an accurate theoretical model for comparison of experimental data.

The investigation by Brandt (4) considered the effect of surface heat transfer on the power output of a power generator. His work covered surface heat transfer by radiation; for the conditions he studied, surface heat transfer had a deleterious effect on the efficiency. He did not report the effect surface heat transfer had on the power output of a generator or on the performance of a heat pump. Furthermore, his model did not include finite fins. In a paper by Ybarrondo and Sunderland (8) analytical expressions were given for predicting the improvements in performance of a power generator that could be attained using surface heat transfer; the analysis also assumed finite fin conductances at both

junctions but did not consider applications involving heat pumping.

An analysis by Nottage et al. (13) attempted to determine if surface heat transfer could be a useful mechanism for improving generator performance. However, the authors came to the conclusion the "system" efficiency could be increased if the surface heat loss from the thermoelement was used to power a thermodynamic conversion process which was more efficient than the thermoelectric generator with zero surface heat transfer. No attempt was made by the authors to explicitly determine how surface heat transfer affected the performance of the generator itself; but this effect could be deduced from their work for one condition of operation; the authors model did not include finite fins. A paper by Rollinger and Sunderland (14) presented results which showed how the performance of a heat pump could be improved through the use of surface heat transfer. The analysis assumed a fixed temperature difference between the hot and cold junctions and an infinite cold-junction fin; it did not consider the effect of finite fins on the performance of a heat pump.

Thermoelements with Spatially Dependent Properties

The thermoelectric properties electrical resistivity $\rho(x)$, Seebeck coefficient $S(x)$, and thermal conductivity $k(x)$ of a semiconductor can be made spatially dependent by appropriate doping (CuBr is a typical doping agent). For the sake of simplicity, it is assumed the resulting spatial dependence is axial only.

The effect of spatially dependent properties on the performance of a thermoelectric heat pump has never been investigated to the author's

knowledge. This may be due in part to the fact that semiconductor material is assumed to be homogeneous; homogeneity is generally controlled during preparation. However, the fact that semiconductor materials are not or may not be homogeneous has been mentioned by several authors. In a paper by T. C. Harman, et al. (15), the positional dependence of electrical resistivity was shown as a function of several preparation techniques. An excellent paper by Domenicali (16) derived differential equations for the positional dependence of ρ , S , and k in three dimensions. Domenicali did not solve these equations, discuss the effect of spatial dependence of properties on device performance, or indicate a method of using spatially dependent properties to advantage. It should be added that he intended only to present the basic principles of thermoelectricity.

An analysis by W. H. Clingman (17) indicated the possibility of spatially dependent properties. The principles of irreversible thermodynamics and the calculus of variations were employed to derive an expression for the optimum coefficient of performance that is valid for positional dependent properties. However, Clingman considered the thermoelectric properties to vary with position only across a given cross-section of the thermoelement; he did not consider the property values to vary along the longitudinal axis of the thermoelement. The expression for optimum coefficient of performance presented by Clingman was not evaluated for his type of spatially dependent properties - only for constant properties. Further, the analysis did not consider the effect of spatial dependence or attempt to use this dependence to advantage. A recent analysis by B. Varga et al. (18) solved the dynamical equations

governing the performance of thermoelectric and thermomagnetic heat pumps and compared the maximum no-load temperature difference of the two types of pumps for several operating conditions. The authors assumed that S , ρ and k were independent of position whenever magnetic field effects were present. In the absence of a magnetic field the authors assumed ρ and k were independent of position but allowed S to be spatially dependent. The authors showed that this dependence leads to an increase in the maximum no-load temperature difference; the effect of a spatially dependent Seebeck coefficient on the heat pumping capacity and coefficient of performance was not discussed.

Summary of Previous Research

This brief review of previous research indicates rather clearly that there are three problems that have not been investigated adequately.

The effect of a finite hot-junction fin and a finite cold-junction fin on the performance of a thermoelectric heat pump has not been adequately treated.

While the advantageous use of surface heat transfer has been considered previously, an adequate mathematical model of a physical system utilizing both surface heat transfer and finite fins has not been developed.

Finally, the possibility of using positional dependent thermoelectric properties to improve heat pump performance has not been investigated. In fact, inhomogeneity of thermoelectric properties has generally been considered undesirable.

CHAPTER III

CHARACTERIZATION OF THE PHYSICAL SYSTEM

Description of a Thermoelectric Device

A basic thermoelectric device is shown in Fig. 3. This device consists of two thermoelectric semiconductors to which electrical and thermal connections are made by means of metal straps. By the use of a P-type thermoelectric element and an N-type thermoelectric element in an electrical d-c. series arrangement heat may be pumped from source to sink.

For simplicity it is assumed that the electrical, geometrical, and thermal properties of the P and N elements of the device are identical except for the absolute thermoelectric coefficients which are assumed opposite and equal. Thus, only one half of the physical model has to be considered in the analysis (see Fig. 4) and the mathematical model will be simplified considerably; the element removed is assumed to be replaced by a perfect electrical conductor.

Before proceeding with a discussion of the nomenclature in Fig. 4, there are several basic assumptions which must be mentioned. It is assumed that the hot and cold junction fins have negligibly small electrical resistance and Seebeck coefficient. In addition, the electrical resistance, thermal resistance and Seebeck coefficient of connecting wires between the thermoelement(s) are assumed negligibly small. Both these assumptions are reasonable because the fins are made of copper or

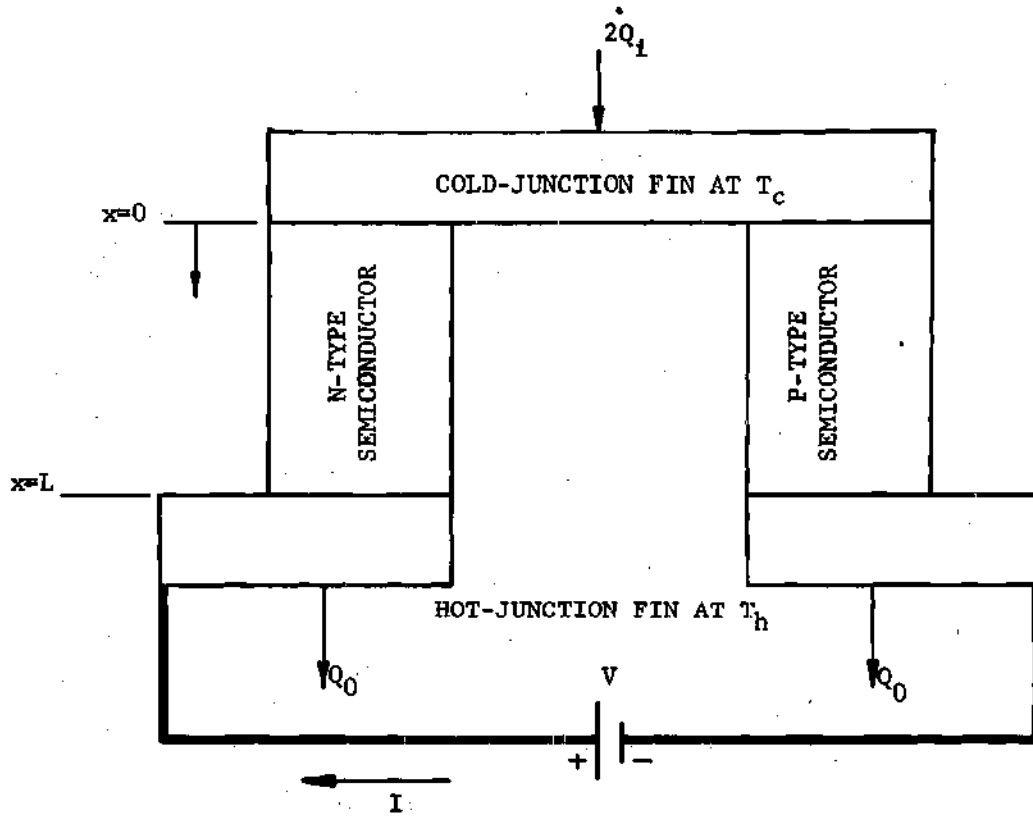


Fig. 3. A Basic Thermoelectric Heat Pump.

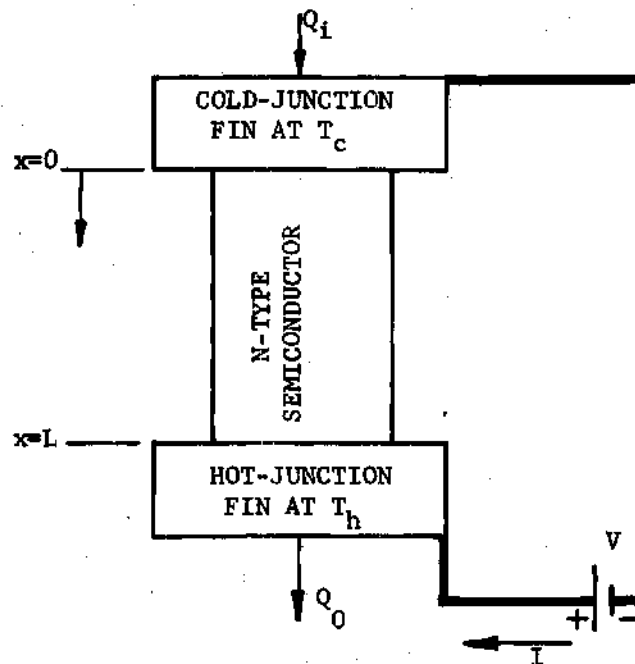


Fig. 4. A Single-Element Thermoelectric Heat Pump.

aluminum and the wires of copper almost exclusively. Within the thermoelement, it is assumed that fluxes of heat and electric current normal to the longitudinal axis of the thermoelement are negligible. Because the cross-sectional area of the thermoelement is considered constant throughout this analysis, the assumption of one-dimensional electric current flow is reasonable. This analysis will consider thermoelements that are convectively cooled along a portion of their longitudinal length. Thus the assumption of a one-dimensional heat flux (along the longitudinal axis) will be true only if the heat flux through the longitudinal surface is not significant. In defense of this assumption it should be noted that the use of a one-dimensional mathematical model for studying the heat transfer characteristics of fins with constant cross-sectional area leads to analytical results which agree very favorably with experimental data.

For the sake of simplicity, it is assumed that the entire cold-junction fin is at a temperature T_c and the entire hot-junction fin is at a temperature T_h ; that is, both fins are isothermal. In regard to this last assumption note that the fins of the thermoelement are generally made of copper or aluminum. Since this is a steady-state analysis, the assumption of isothermal fins is a good assumption. Furthermore the temperature distribution in the fins would be very small for steady-state operation and would certainly be a second order effect. Hence there is little reason to believe that the results of an analysis with a simplified model (neglecting second order effects) will not be effectively reproduced by a more refined model as long as both models include all the first order effects.

The reader will find the following explanation of basic nomenclature more meaningful by referring to Fig. 4. The rate at which heat is transferred to the cold-junction fin is designated as Q_i . The temperature of the isothermal cold-junction fin is the same as the temperature at $x = 0$ and is always designated as T_c . The temperature distribution in the thermoelement is designated by $T(x)$. The temperature of the isothermal hot-junction fin is the same as the temperature at $x = L$ and is always designated as T_h . The rate at which heat is transferred from the hot-junction fin is designated as Q_o . The electric current, I , is defined as positive in the positive x -direction. The source voltage, V , is defined such that the rate at which electrical energy enters the system is given by the product of the voltage and the current.

Differential Equation for the Temperature Distribution

The general partial differential equations which describe the steady-state temperature distribution in an inhomogeneous, anisotropic thermoelement have been derived from the principles of irreversible thermodynamics by Domenicali (16). In shorthand notation these equations can be written

$$\frac{\partial}{\partial x_i} \left(k_{ij} \frac{\partial T}{\partial x_j} \right) - T \frac{\partial}{\partial x_i} \left(s_{ij} J_j \right) + \rho_{ij} J_i J_j = 0 \quad (3-1)$$

where $i, j = 1, 2, 3$

In Eq. (3-1), k_{ij} is the thermal conductivity matrix (for zero electrical current), ρ_{ij} is the isothermal electrical resistivity matrix,

S_{ij} is the Seebeck matrix, J_i, J_j is the electrical current density and T is the absolute temperature. Equation (3-1) is non-linear because k_{ij}, ρ_{ij} , and S_{ij} are generally functions of temperature; they also depend on position. The general solution to Eq. (3-1) has not been found. However many special cases of Eq. (3-1) have been solved.

In this analysis, only isotropic thermoelectric elements will be considered which means that $\rho_{ij} = k_{ij} = S_{ij} = 0$ for $i \neq j$. Furthermore, the assumption that heat and current fluxes only exist parallel to the longitudinal axis means that $k = k_{11} = k_{22} = k_{33}, \rho = \rho_{11} = \rho_{22} = \rho_{33}$, and $S = S_{11} = S_{22} = S_{33}$. Unfortunately the differential equation for the one-dimensional temperature distribution in a thermoelement with convective heat transfer along a portion of its longitudinal surface can not be obtained by reducing Eq. (3-1). This results from the fact that the convective heat transfer effect is accounted for as a boundary condition in the multidimensional case whereas it appears in the differential equation in the one-dimensional case.

A derivation of the one-dimensional partial differential equation for the non-steady state temperature distribution in a thermoelement subjected to convective heat transfer is given in Appendix A. Assuming steady-state conditions, the resulting ordinary differential equation (A-15) is

$$\frac{d}{dx} \left[k(x,T) A(x) \frac{dT}{dx} \right] - IT \left. \frac{\partial S}{\partial x} \right|_T - IT \left. \frac{\partial S}{\partial T} \right|_x \frac{dT}{dx} - hP(x)(T-T') + \frac{I^2 \rho(x,T)}{A(x)} = 0 \quad (3-2)$$

In Eq. (3-2), the first term represents the gradient of the heat conducted in the element; the second term, represents the "Volume Peltier effect"*; the third term, represents the usual Thomson effect; the fourth term represents the convective heat transfer from the longitudinal surface of the element; and the fifth term, represents the Joule heating effect.

Although Eq. (3-2) is a considerable mathematical simplification of Eq. (3-1) it is still non-linear and very difficult to solve. Of course, there are a large number of special cases of Eq. (3-2) which may be solved.

For instance Gray (19), Parrott (12), and Norwood (20) have all studied the effect of temperature dependent S , ρ , and k on the performance of a fully insulated homogeneous thermoelement used as a heat pump. Their results generally concur with the conclusion that the assumption of temperature dependent properties introduces second-order effects. These second-order effects do not seriously affect the results arrived at by using temperature independent properties - when the heat pump is operated at a value of electrical current less than or equal to the optimum electrical current for a given performance criteria. The analysis of Norwood (20) is particularly interesting because besides illustrating graphically the veracity of the above statement, his results illustrate the effect of the temperature dependence of S , ρ , and k individually.

Several interesting special cases of Eq. (3-2) have been solved by Brandt (4) and Rollinger (21). In particular both these authors have studied the effect of variable cross-sectional area and surface

*See Domenicali (16), page 108, Eq. 94.

heat transfer on the performance of thermoelectric devices. For the conditions he studied, Brandt showed that shape by itself does not affect the power output and thermal efficiency of a generator under matched load conditions; Rollinger reached analogous conclusions for the heat pump. In addition, Brandt showed that a conical shaped element together with surface heat transfer reduced the efficiency of a generator. Rollinger derived optimum expressions for the performance of a heat pump with surface heat transfer and an arbitrary cross-sectional area; he did not evaluate the expressions.

In view of the objectives of this dissertation and considering the "special cases" mentioned in the last two paragraphs, it is assumed that all thermoelements in this analysis have temperature independent S , ρ , and k and a constant cross-sectional area. These assumptions reduce Eq. (3-2) to

$$A \frac{d}{dx} \left[k(x) \frac{dT}{dx} \right] - IT \frac{dS}{dx} - hP (T - T') + \frac{I^2 \rho(x)}{A} = 0 \quad (3-3)$$

This differential equation forms the basis for the analyses in the following chapters; additional simplifications are made as indicated in each chapter.

Thermal Boundary Conditions

The purpose of this section is to give the reader an insight and a physical understanding of the boundary conditions that will be used to solve various forms of Eq. (3-3) in the following chapters. It has been the experience of the author that the thermal boundary conditions frequently cause a great deal of difficulty.

Referring to Fig. 4, it is noted that the thermoelement has three boundary surfaces: the longitudinal surface of the thermoelement and the radial surfaces at $x = 0$ and $x = L$. In this analysis, the longitudinal surface is assumed to exchange energy with its environment by convection only.* As mentioned previously, the effect of convection along the longitudinal surface of the thermoelement is taken into account in the differential Eq. (3-3) and does not enter into the boundary conditions.

The Peltier effect occurs at the radial surfaces at $x = 0$ and $x = L$ because these surfaces are the junctions of two different conductors. At each of these junctions an energy balance relating the various energy fluxes is made and gives the usual boundary conditions**

$$Q_i = IS(0)T_c - k(0)A \left. \frac{dT}{dx} \right|_{x=0} - I^2 r_i A \quad (3-4a)$$

$$Q_o = -IS(L)T_h + k(L)A \left. \frac{dT}{dx} \right|_{x=L} + I^2 r_o A \quad (3-4b)$$

In Eq. (3-4a), the first term is the Peltier heat absorbed; the second term is the heat conducted into the junction through the element; and the third term is the Joulean heat produced by electrical contact resistance in the junction. The sum of these terms, Q_i , is the heat absorbed from the environment at the cold junction; a completely analogous statement applies to Eq. (3-4b).

*See Carslaw (23) p. 21 for a discussion of radiation heat transfer at this boundary.

**See Parrott (12) or Rollinger (21).

In this analysis two modifications of Eqs. (3-4a) and (3-4b) are made. First, electrical contact resistances at the junctions are neglected; that is, $r_i = r_o \cong 0$. This is a very good assumption if reasonable care is exercised in assembling the heat pump and the length to cross-sectional area ratio is small. Second, as a matter of personal preference Q_i and Q_o are both considered positive; some authors consider the heat removed from the hot junction, Q_o , as negative. With these two changes, Eqs. (3-4a) and (3-4b) become

$$Q_i = IS(0)T_c - k(0)A \left. \frac{dT}{dx} \right|_{x=0} \quad (3-5a)$$

$$Q_o = IS(L)T_h - k(L)A \left. \frac{dT}{dx} \right|_{x=L} \quad (3-5b)$$

where Q_i and Q_o are both positive quantities.

In some of the following analyses, the effect of finite hot and finite cold junction fins on performance is considered. For these analyses Eqs. (3-5a) and (3-5b) take the form

$$Q_i = h_c A_c (T_c^f - T_c) = IS(0)T_c - k(0)A \left. \frac{dT}{dx} \right|_{x=0} \quad (3-6a)$$

$$Q_o = h_h A_h (T_h - T_h^f) = IS(L)T_h - k(L)A \left. \frac{dT}{dx} \right|_{x=L} \quad (3-6b)$$

For an explanation of the additional symbols in Eqs. (3-6a) and (3-6b) see the Nomenclature.

In Chapters IV and V, Eqs. (3-6a) and (3-6b) are used as boundary conditions. However in Chapter VI, a specified cold junction temperature

T_c together with Eq. (3-5a) are used as boundary conditions.

Summary of Assumptions

In formulating the mathematical description of the thermoelectric heat pump shown in Fig. 4, the following basic assumptions have been made:

1. The electrical, geometrical, and thermal properties of the P and N elements in Fig. 3 are identical except for the absolute thermoelectric coefficients which are assumed equal and opposite; this allows analysis of the simplified pump in Fig. 4.
2. The cold and hot junction fins have negligibly small electrical resistance and Seebeck coefficient.
3. The electrical resistance, thermal resistance, and Seebeck coefficient of connecting wires are negligible.
4. Fluxes of heat and electric current normal to the longitudinal axis of the thermoelement are negligible within the thermoelement.
5. The cross-sectional area of the thermoelement is constant.
6. The hot and cold junction fins are isothermal.
7. The thermoelement is an isotropic material and the Seebeck coefficient, electrical resistivity, and thermal conductivity are not functions of temperature.
8. The electrical contact resistance at the hot and cold junctions is negligible.

Generally speaking, most of the assumptions in this chapter have been made because it is felt that their inclusion would only introduce second-order effects. These effects would needlessly complicate the

desired analytical solutions or entirely preclude the possibility of an analytical solution to a realistic first-order effect. In addition, it is felt that the assumptions made will provide an accurate mathematical model of the physical system while providing analytical solutions yielding a better physical insight into the effect being investigated.

CHAPTER IV

THE EFFECT OF FINITE HOT AND FINITE COLD JUNCTION FINS
ON THE PERFORMANCE OF A THERMOELECTRIC HEAT PUMP

The purpose of this chapter is twofold. First, the quantitative effect of finite hot and cold junction fins on the performance of a thermoelectric heat pump is determined. Second, the performance of a heat pump with finite fins at the hot and/or cold junction to the performance if one or both fins are infinite is compared.

In this chapter analytical solutions are given for the steady-state temperature distribution, no-load temperature difference, heat pumping capacity and coefficient of performance of a thermoelement used as a thermoelectric heat pump with finite fins. A numerical example is worked in which performance curves are compared for cases of infinite and finite fin conductance at the junctions of a simple thermoelectric heat pump.

Physical System and Relevant Assumptions

The physical system considered in this analysis is a single-element thermoelectric heat pump (see Fig. 5). At the cold junction, fins are exposed to a cold environment at the temperature T_c' . At the hot junction, fins are exposed to a hot environment at the temperature T_h' . The longitudinal surface of the element is perfectly insulated. The surface heat-transfer coefficient is denoted by h_c for the cold-junction fin and h_h for the hot-junction fin.

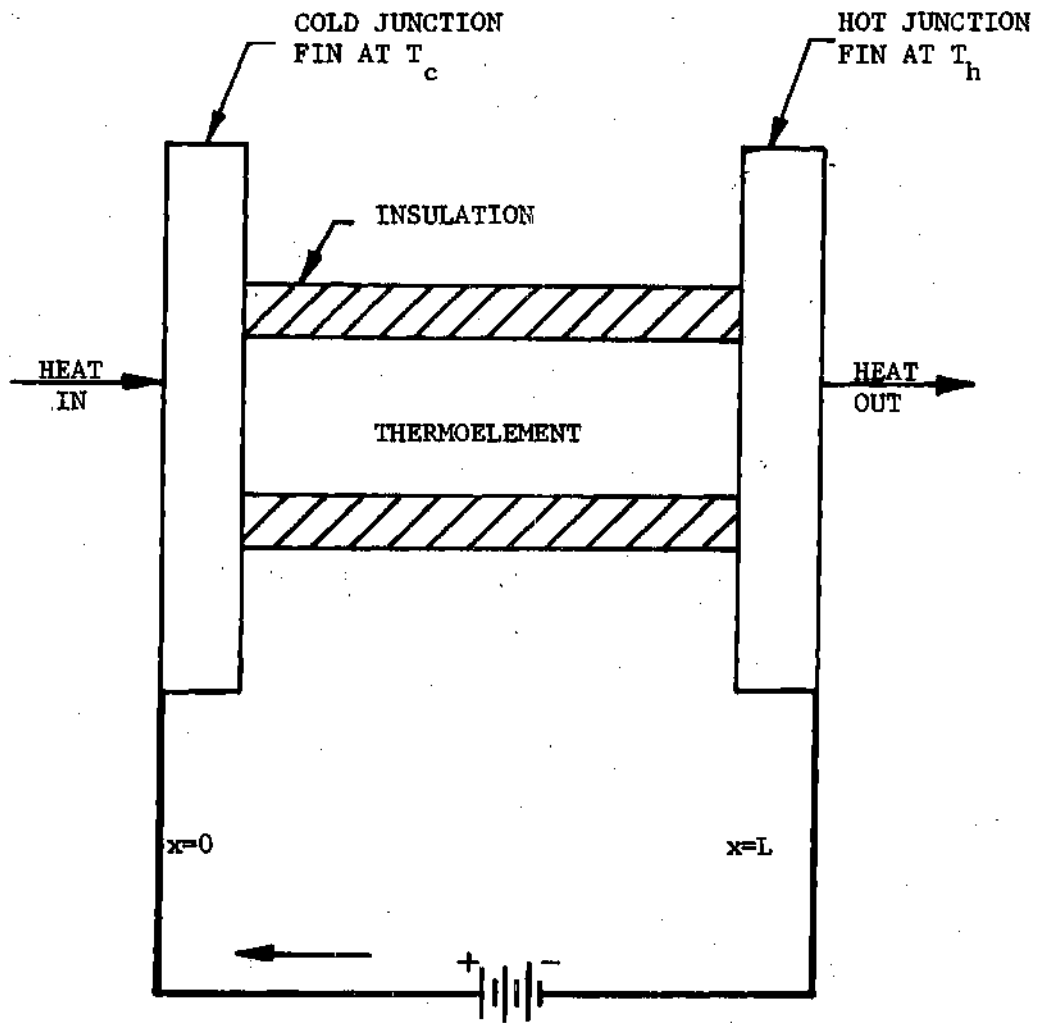


Fig. 5. Single Thermoelement Used as a Heat Pump;

It is assumed that the cross-sectional area A , the Seebeck coefficient S , the electrical resistivity ρ and the thermal conductivity k are constant. Thermal and electrical contact resistances are neglected. Further, it is assumed that the electrical leads that complete the circuit have zero thermal conductivity, Seebeck coefficient and electrical resistivity. Finally it is assumed that the flow of heat and electricity in the thermoelement is one-dimensional and that the fin surfaces are isothermal.

Temperature Distribution

The differential equation for the steady-state temperature distribution in the thermoelement is reduced from Eq. (3-3) to

$$kA \frac{d^2T}{dx^2} + \frac{I^2\rho}{A} = 0 \quad (4-1)$$

Equation (4-1) is subject to the following boundary conditions:

$$T(0) = T_c \quad (4-2 a)$$

$$T(L) = T_h \quad (4-2 b)$$

Since the temperatures of the environments T_c' and T_h' are specified, the junction temperatures T_h and T_c are not known. In order to find T_h and T_c , it is necessary to take an energy balance at the hot and cold junctions. Thus, at the cold junction,

$$-kA \left. \frac{dT}{dx} \right|_{x=0} + IST_c = h_c A_c (T_c' - T_c) \quad (4-3 a)$$

at the hot junction,

$$-kA \left. \frac{dT}{dx} \right|_{x=L} + IST_h = h_h A_h (T_h - T_h') \quad (4-3b)$$

If boundary conditions (4-2) and (4-3) are applied to the general solution (4-1), the unknown temperature distribution may be solved explicitly. Before determining this relationship, it is helpful to reduce the number of parameters by defining the following dimensionless quantities. The dimensionless temperature θ , position u , and parameters α , ϕ , H_c , and H_h are defined by

$$\theta = \frac{T - T_c'}{T_c' - T_h'} \quad (4-4a)$$

$$u = \frac{x}{L} \quad (4-4b)$$

$$y = \frac{ISL}{kA} \quad (4-4c)$$

$$\alpha = \frac{1}{2(T_c' - T_h')} \quad (4-4d)$$

$$\phi = \frac{T_c'}{(T_c' - T_h')} \quad (4-4e)$$

$$H_c = \frac{h_c A_c L}{kA} \quad (4-4f)$$

$$H_h = \frac{h_h A_h L}{kA} \quad (4-4g)$$

Utilizing the dimensionless quantities, equation (4-1) becomes

$$\frac{d^2\theta}{du^2} + y^2\alpha = 0 \quad (4-5)$$

The boundary conditions (4-2) and (4-3) become

$$\theta(0) = \theta_c \quad (4-6a)$$

$$\theta(1) = \theta_h \quad (4-6b)$$

$$-\left. \frac{d\theta}{du} \right|_{u=0} + y(\theta_c + \phi) = -H_c \theta_c = Q_i^* \quad (4-6c)$$

$$-\left. \frac{d\theta}{du} \right|_{u=1} + y(\theta_h + \phi) = H_h (\theta_h + 1) = Q_o^* \quad (4-6d)$$

Solving equation (4-1) subject to boundary conditions (4-6a) and (4-6b) gives

$$\theta = -\frac{y^2 \alpha}{2} u^2 + \left\{ \theta_h - \theta_c + \frac{y^2 \alpha}{2} \right\} u + \theta_c \quad (4-7)$$

Equation (4-7) gives the temperature distribution in terms of θ_c and θ_h as well as other parameters. By making use of equation (4-6c) and (4-6d), the following expressions may be determined for the hot and cold junction temperatures

$$\theta_c = \frac{\{y^2 \alpha / 2 - y\phi\} \{1 + H_h - y\} - \{H_h - y^2 \alpha / 2 - y\phi\}}{H_h + H_c + (H_c + y)(H_h - y)} \quad (4-8)$$

$$\theta_h = \frac{\{y^2 \alpha / 2 - y\phi\} - \{H_h - y^2 \alpha / 2 - y\phi\} \{1 + H_c + y\}}{H_h + H_c + (H_c + y)(H_h - y)} \quad (4-9)$$

Equations (4-7) - (4-9) can be used to determine the steady-state temperature distribution in the thermoelement for any value of y , H_c , H_h , α and ϕ .

Performance Criteria

The no-load temperature difference, heat pumped, and coefficient of performance are the important performance criteria of a thermoelectric heat pump. The no-load temperature difference, θ_{NL} , is defined as the temperature difference between the hot-junction environment and the cold-junction ($T'_h - T_c$), when the cold junction is insulated from its environment. Letting $H_c = 0$ in equation (4-8) and applying the above definition gives

$$\begin{aligned} -(\theta_c + 1) &= \theta_{NL} \\ &= \frac{(\alpha/2)y^3 + \left[1 - \alpha - \beta - (\alpha/2)H_h\right] y^2 + H_h(\beta - 1)y}{-y^2 + H_h(y + 1)} \end{aligned} \quad (4-10)$$

The rate of heat pumped from the cold environment equals Q_i^* and can be determined by combining equations (4-6a), (4-7), (4-8), and (4-9). Thus

$$Q_i^* = \frac{(\alpha H_c/2)y^3 - H_c \left[\beta + \alpha(1 + H_h/2) \right] y^2 + \beta H_c H_h y + H_c H_h}{-y^2 + (H_h - H_c)y + H_h(H_c + 1) + H_c} \quad (4-11)$$

The coefficient of performance (C.O.P.) is defined as the ratio of the heat pumped to the total electrical power input; it is given by

$$\text{C.O.P.} = \frac{h_c A (T'_c - T_c)}{IS(T_h - T_c) + I^2 \rho L/A} \quad (4-12)$$

By combining equations (4-8), (4-9), and (4-11), it can be shown that

$$\text{C.O.P.} = \frac{(\alpha H_c/2)y^3 - H_c \left[\beta + \alpha(1 + H_h/2) \right] y^2 + \beta H_h H_c y + H_h H_c}{(\alpha/2)(H_h - H_c)y^3 + \left[(H_h + H_c)(\beta + \alpha) + H_h(\alpha H_c - 1) \right] y^2 - H_h H_c y} \quad (4-13)$$

For any given set of conditions, in order to find the value of current y that will optimize any given performance criterion, the first derivative of equations (4-10), (4-11), and (4-13) with respect to y can be set equal to zero. Thus, the optimum value of the current y_{opt} that will yield the optimum no-load temperature difference can be shown from equation (4-10) to satisfy the following equation

$$y^4 - 2H_h y^3 + H_h(H_h - 1)y^2 - \frac{4H_h}{a} \left[1 - \phi - \alpha \left\{ 1 + \frac{H_h}{2} \right\} \right] y - \frac{2H_h^2}{a} (\phi - 1) = 0 \quad (4-14)$$

For the optimum heat pumped from equation (4-11) y_{opt} must satisfy

$$y^4 - 2(H_h - H_c)y^3 - \left[H_h(1 - H_h) + H_c \left\{ 5 + 4H_h + \frac{2\phi}{a} \right\} \right] y^2 - \frac{4}{a} \left[H_h - \left\{ \phi + \alpha \left(1 + \frac{H_h}{2} \right) \right\} \right] \left\{ H_h(H_c + 1) + H_c \right\} y + \frac{2H_h}{a} \left[H_h - H_c - \phi \left\{ H_h(H_c + 1) + H_c \right\} \right] = 0 \quad (4-15)$$

From equation (4-13), for the optimum value of C.O.P., y_{opt} must satisfy

$$\begin{aligned} & \frac{\alpha}{2} \left[2(\alpha + \phi) + \frac{\alpha}{2} (H_h + H_c) - 1 \right] y^4 - \alpha \left[H_c + \phi (H_h - H_c) \right] y^3 \\ & + \left[(\alpha + \phi) \left\{ H_c - \phi(H_h - H_c) \right\} + H_h \left\{ \alpha H_c (1/2 - \phi) + \phi \right\} \right] y^2 \\ & + \left[\frac{3}{2} \alpha (H_c - H_h) \right] y^2 - 2 \left[(H_h + H_c) (\phi + \alpha) \right. \\ & \left. + H_h (\alpha H_c - 1) \right] y + H_h H_c = 0 \end{aligned} \quad (4-16)$$

Each of the equations (4-14) and (4-15) has only one real positive root. Equation (4-16) has two real positive roots; however, the larger is physically insignificant. For the values of the parameters used in this analysis, the real positive roots of equations (4-14) - (4-16) are between 0 and 1.

Equations (4-11) - (4-16) are sufficient to determine the optimum performance of a completely insulated thermoelement with unknown hot and cold junction temperatures, arbitrary hot and cold junction fin surface areas, and arbitrary surface heat-transfer coefficients over the hot and cold junction fins. Unfortunately, owing to the complexity of the equations, it is difficult to interpret the quantitative results in a general manner. Therefore in order to evaluate the effect of finite fins on the performance, specific numerical examples are used. The following constants are used in the examples:

$$S = 212 \times 10^{-6} \text{V/}^{\circ}\text{K}$$

$$\rho = 1.0 \times 10^{-3} \text{ ohm-cm}$$

$$k = 15.0 \times 10^{-3} \text{W/cm-}^{\circ}\text{K}$$

$$Z = 3.0 \times 10^{-3} / ^{\circ}\text{K}$$

$$T_c' = 273^{\circ} \text{K}$$

$$T_h' = 300^{\circ} \text{K}$$

$$L = 2.54 \text{ cm}$$

$$A = 0.317 \text{ cm}^2$$

In dimensionless form, these values give $\beta = -10.11$ and $\alpha = -12.34$. The dimensionless fin parameters H_c and H_h are not assumed equal and are allowed to vary in the following combinations: $H_c = 4$, with $H_h = 1, 2, \dots, 300$; $H_c = 10$, with $H_h = 1, 2, \dots, 300$; $H_c = 20$, with $H_h = 1, 2, \dots, 300$; $H_c = 200$, with $H_h = 1, 2, \dots, 300$; and $H_c = 300$, with $H_h = 1, 2, \dots, 300$.

For these conditions, the performance criteria of the thermoelement were calculated and divided by the corresponding maximum possible values*: $(\theta_{NL})_{max} = -2.801$, $(Q_i^*)_{max} = -3.145$, $(C.O.P.)_{max} = 1.134$. Expressions from which these maximum values may be obtained are given in Appendix B. The results are given in Figs. 6 through 10. The effect of the thermal-fin conductance on optimum no-load temperature difference, optimum heat pumped and optimum C.O.P. is shown in Figs. 6, 7, and 9, respectively. Fig. 8 illustrates the variation of the C.O.P. with thermal-fin conductance for the condition of optimum heat pumped. Fig. 10 shows the variation of heat pumped with thermal-fin conductance for the condition of optimum C.O.P.

Analysis of Results

It is helpful to discuss the results of this analysis with some idea of typical values for the hot and cold junction fin conductances. It is shown in Appendix B that a 0.635 cm by 0.635 cm thermoelement has a fin conductance (H_c or H_h) of about 50 for natural convection in air

*In this chapter and in Chapters V and VI, note that the word "maximum" refers exclusively to the optimized performance criteria of a completely insulated homogeneous thermoelement with infinite hot and cold junction fin conductances.

and about 250 for forced-convection in air.

Fig. 6 illustrates that increasing H_h beyond about 35 will not significantly increase the optimum no-load temperature difference. In addition, it shows that the assumption of an infinite hot-junction fin can be reasonably accurate for an H_h of about 35 or greater.

Fig. 7 shows that for a given H_c , increasing H_h beyond about 50 does not increase the heat pumped appreciably. For example, if $H_c = 200$ and $H_h = 50$, the heat pumping capacity would be increased only 5 per cent by increasing H_h to 200. This increase in H_h could be accomplished by either increasing the fin surface area by a factor of 4, or by using forced convection instead of free convection in air. Similarly, for a given H_h , only a small increase in heat pumped is to be gained by increasing H_c from 20 to 200.

Fig. 8 shows that the C.O.P. for optimum heat pumping is virtually independent of the hot and cold fin conductances for H_h about 5 or greater. It should be noted that in this figure the heat pump is operating under conditions that will give the optimum possible heat removal from the cold environment.

Fig. 9 shows that for a given H_c , increasing H_h above 50 does not increase the C.O.P. appreciably. Similarly for a given H_h only a small increase in C.O.P. is obtainable by raising H_c from 20 to 200. It can be seen in Fig. 10 the heat pumped for optimum C.O.P. is virtually independent of the hot and cold fin conductances for $H_h > 10$.

Conclusions

An analysis has been presented that can be used to predict the

Normalized Optimum No-Load Temperature

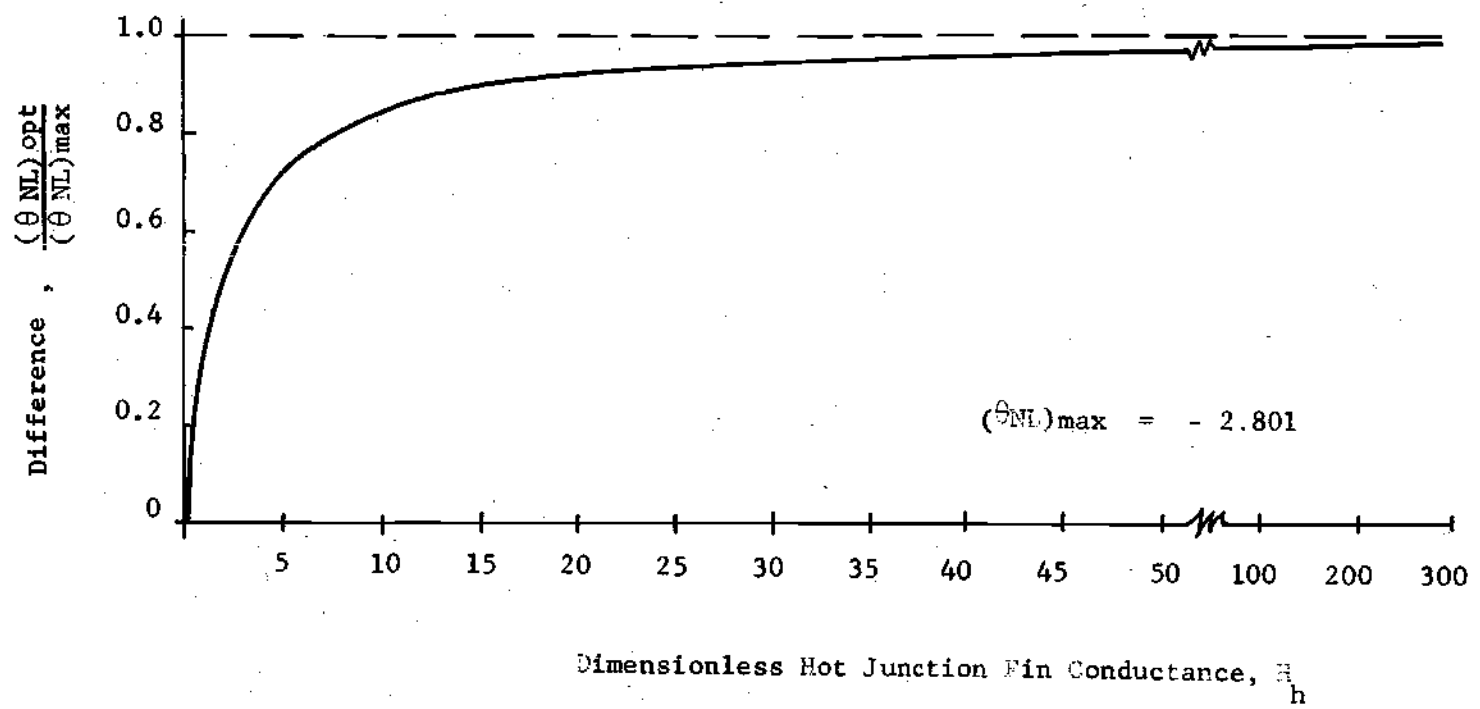


Fig. 6. Optimum No-Load Temperature Difference vs. Hot-Junction Fin Conductance.

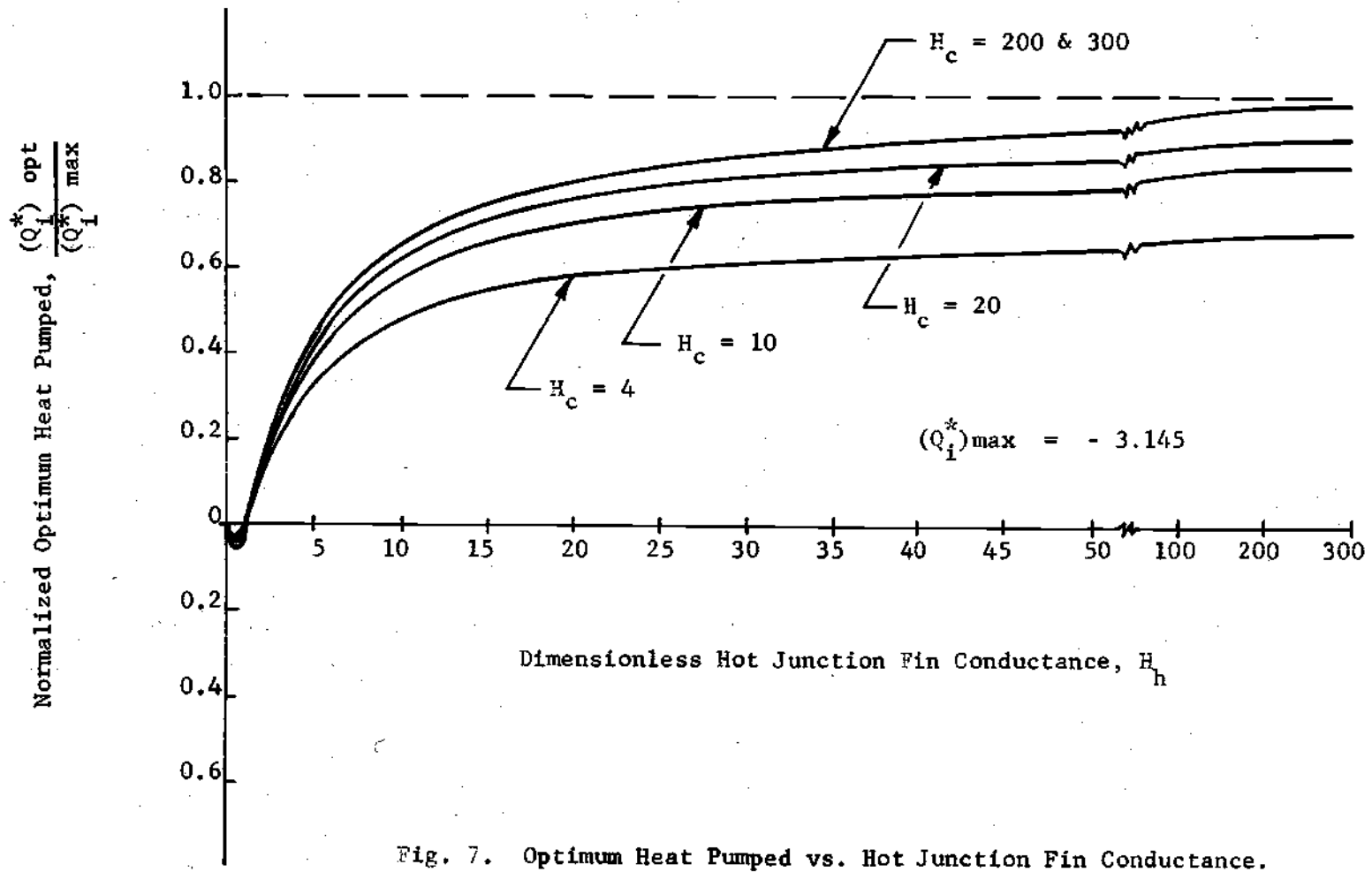


Fig. 7. Optimum Heat Pumped vs. Hot Junction Fin Conductance.

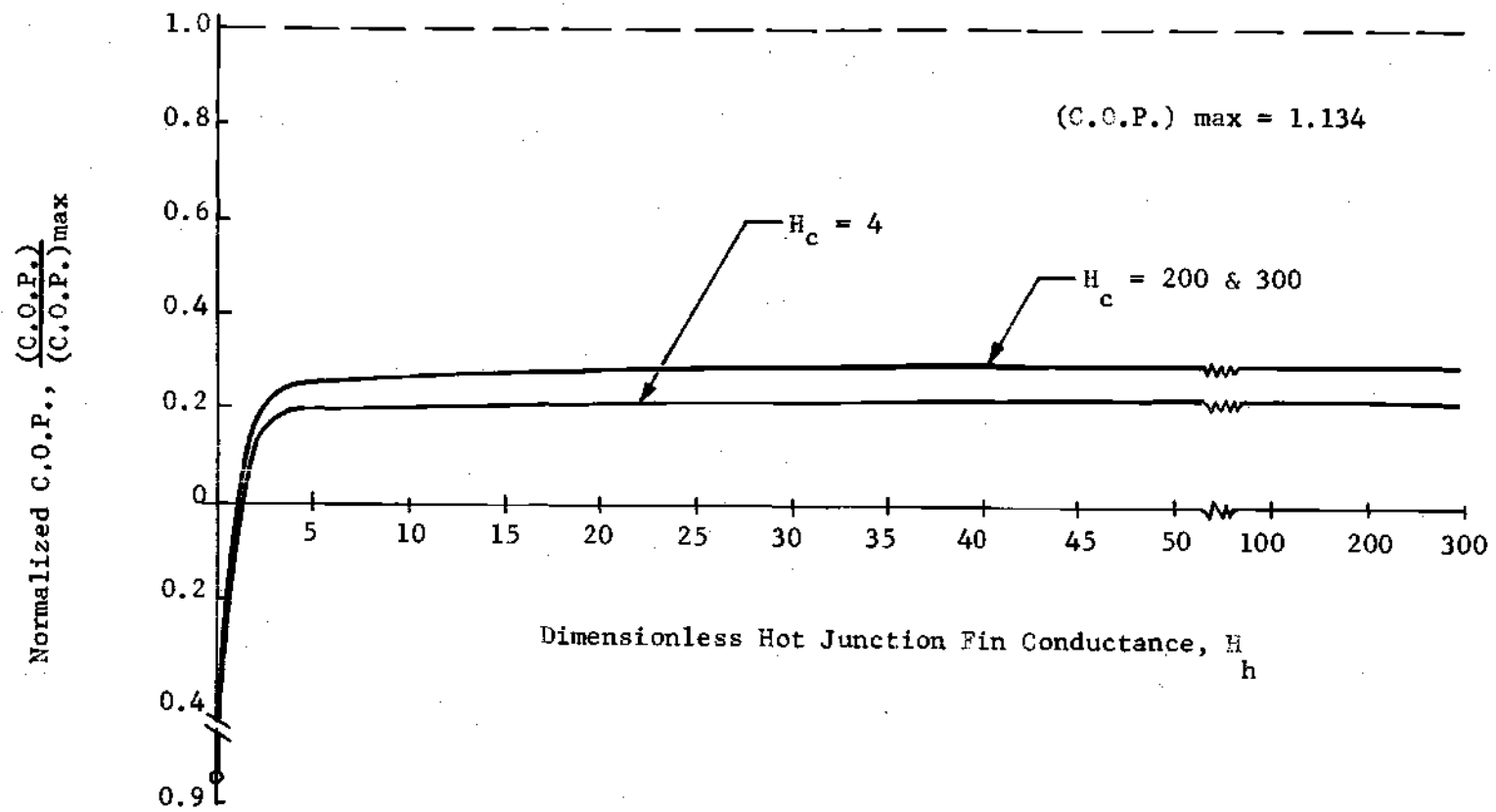


Fig. 8. C.O.P. vs. Hot Junction Fin Conductance for Optimum Heat Pumped.

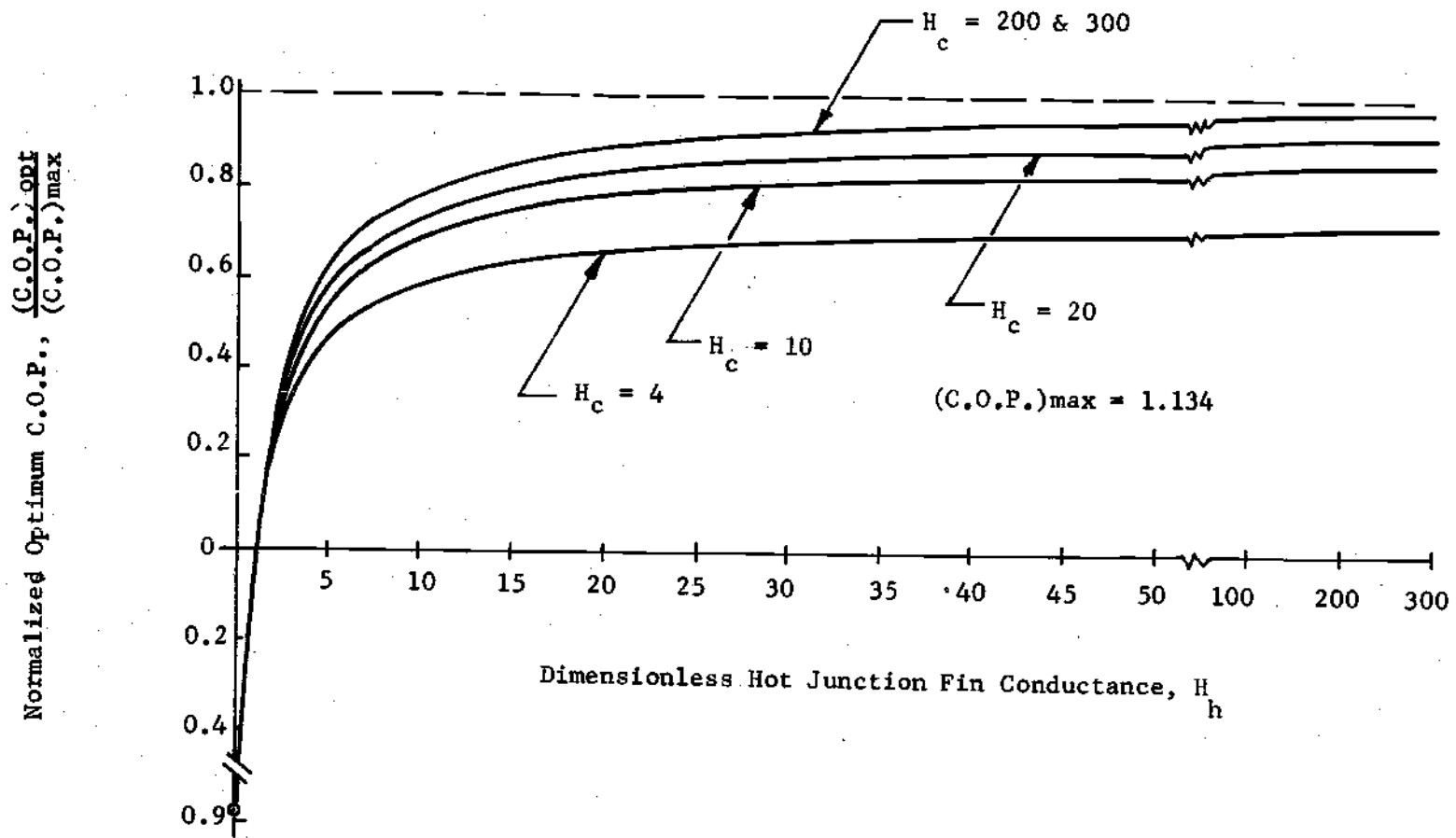


Fig. 9. Optimum C.O.P. vs. Hot Junction Fin Conductance.

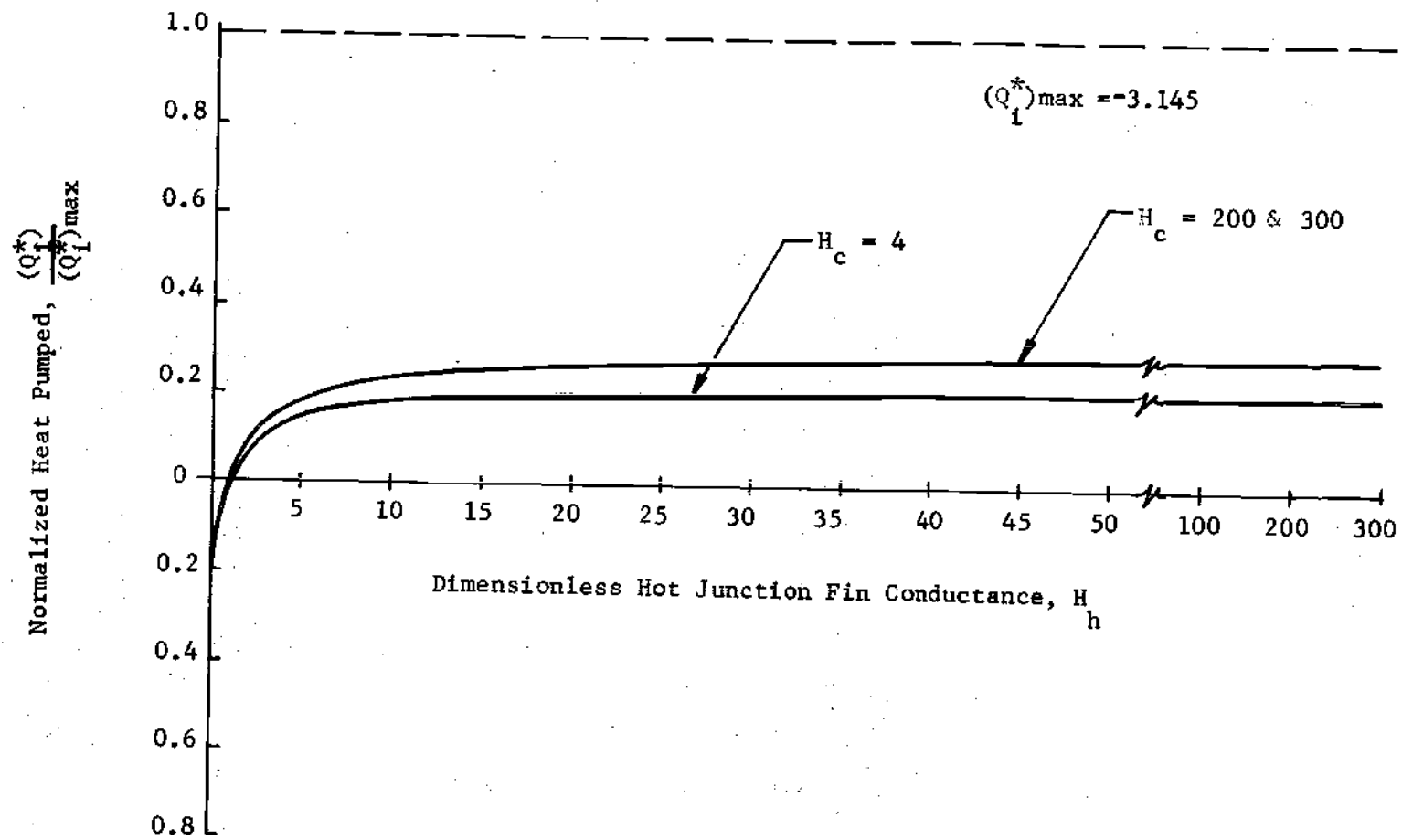


Fig. 10. Heat Pumped vs. Hot Junction Fin Conductance for Optimum C.O.P.

performance of a completely insulated thermoelectric heat pump operating with finite fins at the hot and cold junctions. The results show that the performance of an element may be altered significantly depending on the values of the dimensionless parameters, H_h and H_c . The results were applied to a numerical example. For the set of conditions considered, increasing the fin conductances H_c and H_h to a value greater than 20 would improve the performance by only a small amount. For other design applications curves similar to those presented in this chapter can be constructed, and, from these curves, the amount of fin surface area needed can be determined.

CHAPTER V

OPTIMIZED PERFORMANCE OF A THERMOELECTRIC HEAT PUMP
WITH SURFACE HEAT TRANSFER AND FINITE FINS

The purpose of this chapter is to capitalize more fully on the gains in performance that can be attained through surface heat transfer; determine the quantitative effect of finite fins on the performance of a thermoelectric heat pump using surface heat transfer; and compare the performance of a heat pump using surface heat transfer and having finite fins to the performance of a completely insulated heat pump with infinite fins.

In this chapter, equations are presented for the steady-state temperature distribution, optimum heat pumping capacity, optimum coefficient of performance, and optimum no-load temperature difference for a single element thermoelectric heat pump with constant properties. Part of the longitudinal surface of the thermoelement is convectively cooled; fins of varying size exist at the hot and cold junctions; and three different surface heat transfer coefficients can be arbitrarily selected, one for the hot-junction fins, one for the fins at the cold junction, and one for the surface of the thermoelement. The effect of fin size at the junctions of the thermoelement on performance is shown. An example is presented in which optimized performance curves are compared for devices using fins with infinite and finite conductance and where the thermoelements have varying amounts of surface heat transfer. The results

given are presented in dimensionless form so that they apply for many different conditions.

Physical System and Relevant Assumptions

The physical system considered in this analysis is a single-element thermoelectric heat pump (see Fig. 11). At the cold junction, fins are exposed to a cold environment at the temperature T_c^i ; at the hot junction, fins are exposed to a hot environment at the temperature T_h^i . The longitudinal surface of the thermoelement is divided into two parts; one part of length v , is perfectly insulated; the second part of length $(L-v)$, is exposed to convection with the hot environment. The fraction of the surface insulated can be arbitrarily varied. The surface heat transfer coefficient h is not assumed to be the same throughout the system.

It is denoted by h_c for the cold-junction fin, h in the region $v \leq x \leq L$, and h_h for the hot-junction fin. It is assumed that the cross-sectional area A , the Seebeck coefficient S , the (isothermal) electrical resistivity ρ , and the thermal conductivity k (for zero electrical current) are constant. Thermal and electrical contact resistances, as well as the Thomson effect, are neglected. It is also assumed that the electrical leads which complete the circuit have zero thermal conductivity, Seebeck coefficient, and electrical resistivity. Finally, it is assumed that the flow of heat and electricity in the thermoelement is one dimensional and the fin surfaces are isothermal.

Temperature Distribution

The differential equations for the steady state temperature

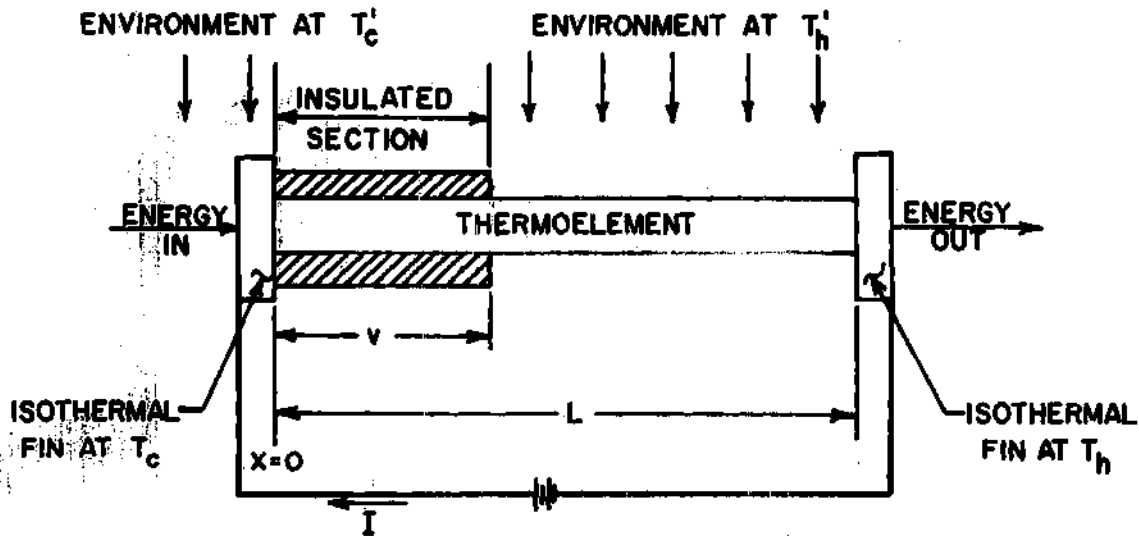


Fig. 11. Single Thermoelement with Surface Heat Transfer Used as a Heat Pump.

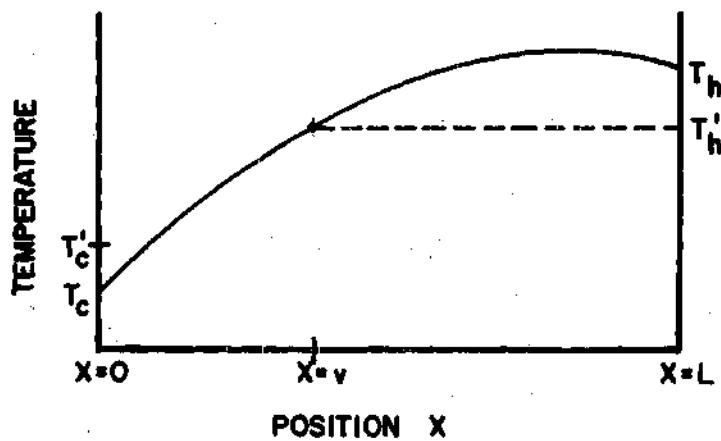


Fig. 12. Typical Temperature Distribution in a Thermoelement for Optimum Heat Pumping.

distribution in the two parts of the thermoelement are:

$$kA \frac{d^2 T_1}{dx^2} + \frac{I^2 \rho}{A} = 0 \quad 0 \leq x \leq v \quad (5-1)$$

$$kA \frac{d^2 T_2}{dx^2} - hp(T_2 - T'_h) + \frac{I^2 \rho}{A} = 0 \quad v \leq x \leq L \quad (5-2)$$

In equation (5-2), the first term is the result of heat conduction; the second term results from the heat transferred by convection; the third term results from Joule heating. These differential equations are subject to the following boundary conditions:

$$T_1(0) = T_c \quad (5-3a)$$

$$T_1(v) = T_2(v) \quad (5-3b)$$

$$T_2(L) = T'_h \quad (5-3c)$$

$$\left. \frac{dT_1}{dx} \right|_{x=v} = \left. \frac{dT_2}{dx} \right|_{x=v} \quad (5-3d)$$

Because only the cold and hot junction environment temperatures, T'_c and T'_h , are specified, it is necessary to take an energy balance at the cold and hot junctions to determine the junction temperatures T_c and T_h . Thus, at the cold junction,

$$-kA \left. \frac{dT_1}{dx} \right|_{x=0} + IST_c = h_c A_c (T'_c - T_c) \quad (5-4a)$$

At the hot junction,

$$-kA \left. \frac{dT_2}{dx} \right|_{x=L} + IST_h = h_h A_h (T_h - T_h') \quad (5-4b)$$

In equation (5-4a), the first term is equal to the heat conducted from the thermoelement to the cold junction; the second term is the Peltier heat absorbed at the junction; the sum of these two terms equals the energy convected to the cold-junction fin by the environment. It should be noted that the entire surface of the fin at the cold junction is assumed to be at a temperature equal to the cold-junction temperature; similarly, the entire hot-junction fin surface is assumed to be at a temperature equal to the hot-junction temperature.

If boundary conditions (5-3) and (5-4) are applied to the solutions of equations (5-1) and (5-2), the unknown temperature distributions, T_1 and T_2 , may be determined. Before solving for the temperature distributions, it is helpful to reduce the number of parameters by defining the following dimensionless quantities. Thus, the dimensionless temperature θ , the dimensionless position u , and the dimensionless current y , are defined by

$$\theta = \frac{T - T_c'}{T_c' - T_h'} \quad (5-5)$$

$$u = \frac{x}{L} \left(\frac{hpL^2}{kA} \right)^{\frac{1}{2}} \quad (5-6)$$

$$y = \frac{ISL}{kAu_L} \quad (5-7)$$

Making use of the above definitions, equations (5-1) and (5-2) become

$$\frac{d^2\theta_1}{du^2} + y^2 a = 0 \quad 0 \leq u \leq u_v \quad (5-8)$$

$$\frac{d^2\theta_2}{du^2} - \theta_2 + y^2 a - 1 = 0 \quad u_v \leq u \leq u_L \quad (5-9)$$

The boundary conditions (5-3) and (5-4) become

$$\theta_1(0) = \theta_c \quad (5-10a)$$

$$\theta_1(u_v) = \theta_2(u_v) = \theta_v \quad (5-10b)$$

$$\theta_2(u_L) = \theta_h \quad (5-10c)$$

$$\left. \frac{d\theta_1}{du} \right|_{u=u_v} = \left. \frac{d\theta_2}{du} \right|_{u=u_v} \quad (5-10d)$$

$$Q_1^* = -H_c \theta_c = u_L (\theta_c + \phi) y - u_L \left. \frac{d\theta_1}{du} \right|_{u=0} \quad (5-11a)$$

$$Q_0^* = H_h (\theta_h + 1) = u_L (\theta_h + \phi) y - u_L \left. \frac{d\theta_2}{du} \right|_{u=u_L} \quad (5-11b)$$

The general solutions of equations (5-1) and (5-2) are

$$\theta_1 = -\frac{ay^2 u^2}{2} + F_1 u + F_2, \quad 0 \leq u \leq u_v \quad (5-12)$$

$$\theta_2 = F_3 e^u + F_4 e^{-u} + y^2 a - 1, \quad u_v \leq u \leq u_L \quad (5-13)$$

where F_m ($m=1,2,3,4$) are constants of integration. Solving equations (5-12) and (5-13) subject to boundary conditions (5-10a) - (5-10d), yields

$$\theta_1 = -\frac{\alpha y^2 u^2}{2} + \left[\frac{\alpha y^2}{2} u_v^2 + \theta_v - \theta_c \right] \frac{u}{u_v} + \theta_c \quad 0 \leq u \leq u_v \quad (5-14)$$

$$\theta_2 = \frac{\left[\theta_v (e^{-\dot{u}} - 1) + \theta_h (e^{\dot{u}} - 1) + 2 \{1 - \cosh(\dot{u})\} (y^2 \alpha - 1) \right] e^u}{2 \sinh(\dot{u}) (e^{u_L} - e^{u_v})}$$

$$+ \frac{\left[\theta_v e^{u_L} - \theta_h e^{u_v} + (e^{u_L} - e^{u_v}) (1 - y^2 \alpha) \right] e^{-u}}{2 \sinh(\dot{u})}$$

$$+ y^2 \alpha - 1 \quad u_v \leq u \leq u_L \quad (5-15)$$

The temperature distributions, θ_1 and θ_2 , are given in terms of θ_c , θ_v , and θ_h as well as other variables. By making use of equation (5-10d), the following expression can be determined for θ_v .

$$\theta_v = \frac{\left[y^2 \alpha u_v \left\{ (u_v/2) + \tanh(\dot{u}/2) \right\} + u_v \left\{ (\theta_h / \sinh(\dot{u})) - \tanh(\dot{u}/2) \right\} \right] + \theta_c}{1 + u_v \coth(\dot{u})} \quad (5-16)$$

Applying boundary conditions (5-11a) and (5-11b), and solving for the cold and hot junction temperatures,

$$\theta_c = \frac{(y^2 \alpha E_3 - y u_L \theta + E_4) (H_h - y u_L - D_1) + E_2 (y^2 \alpha D_3 - y u_L \theta - D_4)}{(H_c + y u_L + E_1) (H_h - y u_L - D_1) - D_2 E_2} \quad (5-17)$$

$$\theta_h = \frac{(-y^2 \alpha D_3 + y u_L \theta + D_4) (H_c + y u_L + E_1) - D_2 (y^2 \alpha E_3 - y u_L \theta + E_4)}{(H_c + y u_L + E_1) (H_h - y u_L - D_1) - D_2 E_2} \quad (5-18)$$

The terms E_m and D_m ($m=1,2,3,4$) depend on the distances L and v as shown in Fig. 11; expressions for these terms are given in Appendix C.

Equations (5-14) - (5-18) can be used to determine the steady-state temperature distribution in the thermoelement for all values of α , ϕ , u_v , u_L , H_c , H_h , and y .

Performance Criteria

The heat pumped, coefficient of performance (C.O.P.) and no-load temperature difference are the important performance criteria of a thermoelectric heat pump. The rate of heat pumped from the cold environment, Q_1 , can be determined by taking an energy balance at the cold junction. This has already been determined in dimensionless form in equation (5-11 a). Using equations (5-14), (5-16), (5-17), and (5-18), the following expression for Q_1^* can be found.

$$Q_1^* = \frac{(y^2 \alpha E_3 - y u_L \phi + E_4) \left\{ (H_h - y u_L - D_1) \left[y u_L + E_1 \right] - D_2 E_2 \right\}}{(H_c + y u_L + E_1) (H_h - y u_L - D_1) - D_2 E_2} - \frac{(y^2 \alpha D_3 - y u_L \phi - D_4) E_2 H_c}{(H_c + y u_L + E_1) (H_h - y u_L - D_1) - D_2 E_2} + y u_L \phi - E_4 - y^2 \alpha E_3 \quad (5-19)$$

Before continuing the development of the performance criteria equations, it is important to discuss briefly the convective energy flux to or from the element along its longitudinal surface. This can be accomplished with the aid of Fig. 12 which represents a typical temperature distribution in a thermoelement. It is clear that energy will be convected from all parts of the element in the region $v \leq x \leq L$ only if

$$T_v < T_h \quad (5-20a)$$

or, in dimensionless form, if

$$\theta_v \leq -1 \quad (5-20b)$$

Thus, the distance v along the element should not be less than the value of x where $T'_h = T'_v$ (or $\theta_v = -1$) if energy is to be convected from the element. The increased heat pumping capacity that may be attained by removing insulation from the surface of the element is more readily understood by referring to Fig. 12 and equation (5-4a). If energy is removed from the surface of the thermoelement ($T_v \leq T'_h$), the temperature distribution in Fig. 12 will tend to lose the hump, i.e., the temperatures in the region $v \leq x \leq L$ will be smaller. In addition, the gradient at $x=0$ will become smaller. If the gradient at $x=0$ becomes smaller, equation (5-4a) clearly shows more heat can be pumped than if the element is completely insulated. This discussion is based on the assumption that the cold-junction temperature can be maintained relatively constant; this is a realistic assumption if the fin sizes are sufficiently large. It is also possible to remove some insulation from the surface of the element near the cold junction so that additional energy may be convected to the element from the cold environment. A preliminary analysis by the author indicates that the amount of insulation that may be removed is so small that it has a negligible effect on performance.

The C.O.P. is defined as the ratio of the heat pumped to the total electrical power input; it is given by

$$\text{C.O.P.} = \frac{IST_c - \left. \frac{dT_1}{dx} \right|_{x=0}}{\frac{I^2 PL}{A} + IS(T_h - T_c)} = \frac{Q_i}{\frac{I^2 PL}{A} + IS(T_h - T_c)} \quad (5-21)$$

The first term in the denominator is the electrical energy dissipated in Joulean heat; the second term is the power dissipated in overcoming the Seebeck voltage due to the temperature difference across the element. Combining equations (5-17), (5-18) and (5-19), equation (5-21) becomes

$$\text{C.O.P.} = \frac{Q_1^*}{y^2 u_L^2 \alpha + y u_L (\theta_h - \theta_c)} \quad (5-22)$$

The no-load temperature difference, θ_{NL} , is defined as the temperature difference between the hot-junction environment and the cold junction ($T_h' - T_c$), when the cold junction is insulated from its environment. Letting $H_c = 0$ in equation (5-17) and applying the above definition,

$$\theta_{NL} = -(\theta_c + 1)$$

$$= \frac{(y^2 \alpha E_3 - y u_L \phi + E_4)(D_1 + y u_L - H_h) + E_2 (D_4 + y u_L \phi - y^2 \alpha D_3)}{(y u_L + E_1)(H_h - y u_L - D_1) - D_2 E_2} - 1 \quad (5-23)$$

For any given set of conditions, in order to find the value of the dimensionless current y that will optimize any given performance criterion, the first derivative of equations (5-19), (5-22), and (5-23) with respect to y must be set equal to zero. Thus, the optimum value of the dimensionless current, y_{opt} , that will optimize the heat pumped can be shown from equation (5-19) to satisfy

$$y^4 - \frac{2E_6}{E_5} y^3 - \frac{(W_3 E_5 + W_2 E_6 + 3W_1 E_7) y^2}{W_1 E_5}$$

(equation continued)

$$-\frac{2(W_2 z_7 + W_4 z_5) y}{W_1 z_5} + \frac{W_4 z_6 - W_3 z_7}{W_1 z_5} = 0 \quad (5-24)$$

From equation (5-22), for the optimum C.O.P., y_{opt} must satisfy

$$\begin{aligned} y^6 + \frac{2W_2}{W_1} y^5 + \frac{\left[W_2(R_2 + \alpha u_L z_6) + 3W_3(R_1 - \alpha u_L z_5) - W_1(R_3 + \alpha u_L z_7) \right]}{W_1(R_1 - \alpha u_L z_5)} y^4 \\ + \frac{2 \left[W_3(R_2 + \alpha u_L z_6) - W_1 R_4 + 2W_4(R_1 - \alpha u_L z_5) \right]}{W_1(R_1 - \alpha u_L z_5)} y^3 \\ + \frac{\left[W_3(R_3 + \alpha u_L z_7) - W_2 R_4 + 3W_4(R_2 + \alpha u_L z_6) \right]}{W_1(R_1 - \alpha u_L z_5)} y^2 \\ + \frac{2W_4(R_3 + \alpha u_L z_7) y}{W_1(R_1 - \alpha u_L z_5)} + \frac{W_4 R_4}{W_1(R_1 - \alpha u_L z_5)} = 0 \quad (5-25) \end{aligned}$$

From equation (5-23), for the optimum value of θ_{NL} , y_{opt} must satisfy

$$\begin{aligned} y^4 - \frac{2z_{14}}{z_5} y^3 - \left[\frac{z_{12}}{z_1} + \frac{z_{14}(u_L^2 - z_2)}{z_1 z_5} + \frac{3z_{15}}{z_5} \right] y^2 \\ - 2 \left[\frac{z_{15}(u_L^2 - z_2)}{z_1 z_5} + \frac{z_{13}}{z_1} \right] y + \frac{z_{13} z_{14} - z_{12} z_{15}}{z_1 z_5} = 0 \quad (5-26) \end{aligned}$$

Quantities comprising part of the coefficients of the y terms, R_m ($m=1,2,3,4$), W_m ($m=1,2,3,4$), and z_m ($m=1,2,\dots,15$), are listed in Appendix C. The number of positive real roots in each of the equations (5-24) - (5-26) may be determined by evaluating the coefficients in these equations and using Descartes' rule. For the values of the parameters used

in this analysis, it can be shown that the physically significant real positive roots of equations (5-24) - (5-26) are between 0 and 1.

Equations (5-19) - (5-16) are sufficient to determine the optimum performance of a thermoelement subjected to convection along a portion of its length if the temperatures of the hot and cold environments are known. The hot and cold junction temperatures do not have to be given, and the device may have arbitrary hot and cold junction fin surface areas, and arbitrary surface heat transfer coefficients.

Results

The steady-state temperature distribution in a thermoelement with finite fins and with convective heat transfer between a portion of the surface of the thermoelement and the hot environment can be determined from equations (5-14) - (5-18). The heat pumped, coefficient of performance, and no-load temperature difference can be obtained from equations (5-19), (5-22), and (5-23), respectively. Using equations (5-24) - (5-26), it is possible to evaluate the C.O.P. for optimum heat pumping; and to evaluate the heat pumped for the condition of optimum C.O.P. These equations are long and therefore have not been solved in a general manner. The quantitative effect of varying conditions of surface heat transfer and finite fins on optimum performance can be determined best by discussing several examples. It must be emphasized that the examples to be discussed are not restricted to any one material, geometry, environmental temperature difference, or heat transfer coefficient because of the dimensionless character of the equations. The following material properties are assumed for the sole purpose of giving a

physical frame of reference for the examples. These properties are typical of commercial materials and are

$$S = 212 \times 10^{-6} \text{ V/}^\circ\text{K}$$

$$\rho = 0.001 \text{ } \Omega \text{ - cm}$$

$$k = 0.015 \text{ W/cm - }^\circ\text{K}$$

The environment temperatures selected are $T'_c = 250^\circ \text{ K}$ and $T'_h = 300^\circ \text{ K}$.

From these properties and temperatures it can be easily shown that $\alpha = -6.67$ and $\phi = -5.00$. Table 1 gives several values of u_L for various heat transfer coefficients* for thermoelements with equal circular cross-sections and varying lengths. It can be seen that $u_L = 3$ corresponds to an element of length 0.635 cm, diameter 0.635 cm and heat transfer coefficient equal to $0.0531 \text{ W/cm}^2\text{-}^\circ\text{K}$. This heat transfer coefficient could be obtained by forcing a liquid over the surface of the thermoelement. The same value of u_L could be obtained by increasing the length of the element to 1.91 cm and forcing a gas over the surface of the element so that $h = 0.00591 \text{ W/cm}^2\text{-}^\circ\text{K}$.

The dimensionless length of the element insulated, u_v , varies from zero, when the entire element is convectively cooled; to u_L , when the element is completely insulated. The dimensionless fin parameters H_c and H_h are assumed to be equal** and they range in value from 5 to 500. $H_c = 5$ corresponds to a high thermal resistance across the fin and $H_c = 500$ corresponds to a very low thermal resistance across the fin. Note that the entire fin surface is assumed to be at a constant

*See reference (22), page 393, table 13.1-1, for the physical significance of these h values.

**Chapter IV discusses the effect of unequal fin sizes on the optimum performance of an insulated heat pump.

temperature equal to the corresponding junction temperature.

For the conditions mentioned above, the performance criteria of the thermoelement were calculated and divided by the corresponding maximum values. The maximum values are obtained by considering a fully insulated element with infinite fins. These values are obtained from the given performance equations by setting $u_v = u_L$ and $H_c = H_h = \infty$. The results are $(Q_i^*)_{\max} = -0.875$, $(\text{C.O.P.})_{\max} = 0.321$, and $(\theta_{NL})_{\max} = -1.511$.

The optimum heat pumped, the heat pumped for the condition of optimum C.O.P., the optimum C.O.P., the C.O.P. for the condition of optimum heat pumping, and the optimum no-load temperature difference were calculated for $u_L = 1, 3, 5, \text{ and } 20$. The results are given in Figs. 13 through 21. The dimensionless fin conductance $H_c = H_h$ is used as a parameter in these figures. The end point of each curve where $u_v/u_L = 1$ represents the performance of a fully insulated element and serves as a convenient reference for two comparisons. First, when compared with any other point along the same curve, the end point illustrates the gain or decrease in performance attained by using surface heat transfer. Second, when compared with the point where the ordinate and abscissa are both one (1), the end point of any given curve illustrates the predicted performance for a fully insulated element with equal finite fins relative to a fully insulated element with infinite fins.

Analysis of Results

There are two modes of operation to consider in the design of thermoelectric heat pumps. The device may be operated to obtain the

Table 1. Heat Transfer Coefficients h ($W/cm^2 \cdot ^\circ K$)
for Several Values of u_L and L

u_L	$L = 0.635$ cm $d = 0.635$ cm	$L = 1.27$ cm $d = 0.635$ cm	$L = 1.91$ cm $d = 0.635$ cm
1	0.00591*	0.00148	0.000654
3	0.0531	0.0133	0.00591
5	0.148	0.0369	0.0164
20	2.36	0.591	0.262

* (1761.1 B/hr-ft²-^oR = 1 W/cm²-^oK)

optimum* rate of heat transfer from the cold junction or it may be operated under conditions that will give the optimum C.O.P. Fig. 13 shows how the rate of heat pumping depends on the fraction of the element insulated and the fin conductance, with $u_L = 1$, and for both conditions of operation. This value of u_L is considered very low and would be obtained using a short element with low heat transfer coefficients. With such small values of u_L , it can be seen that no appreciable gain in the heat pumping capacity can be achieved by using surface heat transfer. Fig. 13 shows that considerably more heat can be pumped when the device is operated at the optimum heat pumping capacity as compared to operation at optimum C.O.P. The variation of the rate of heat pumped with fin conductance can also be observed from Fig. 13.

Fig. 14 shows how the C.O.P. depends on fin conductance and surface heat transfer for the same conditions considered in Fig. 13. For values of fin conductance exceeding about 10, for the conditions considered, the C.O.P. is much larger when the device is operated under conditions that give the optimum C.O.P. as compared with operation at optimum heat pumping. It can also be seen that for $u_L = 1$, only small improvements in the C.O.P. are possible through the use of surface heat transfer. If the fraction of the element insulated (u_V/u_L) is 0.6 and if the fin conductance is 10, the optimum C.O.P. remains unchanged compared with a fully insulated element. However, if the device is operated under conditions giving optimum heat pumping, then the rate of heat pumping is

*The optimum rate of heat transfer from the cold junction is used here to refer to the maximum rate of heat transfer from the cold junction of a device utilizing finite fins. An analogous definition is used for the optimum C.O.P.

$u_L = 1$
 $(Q_i^*)_{MAX} = -0.875$
— OPTIMUM HEAT PUMPED
- - - HEAT PUMPED AT OPTIMUM C.O.P.

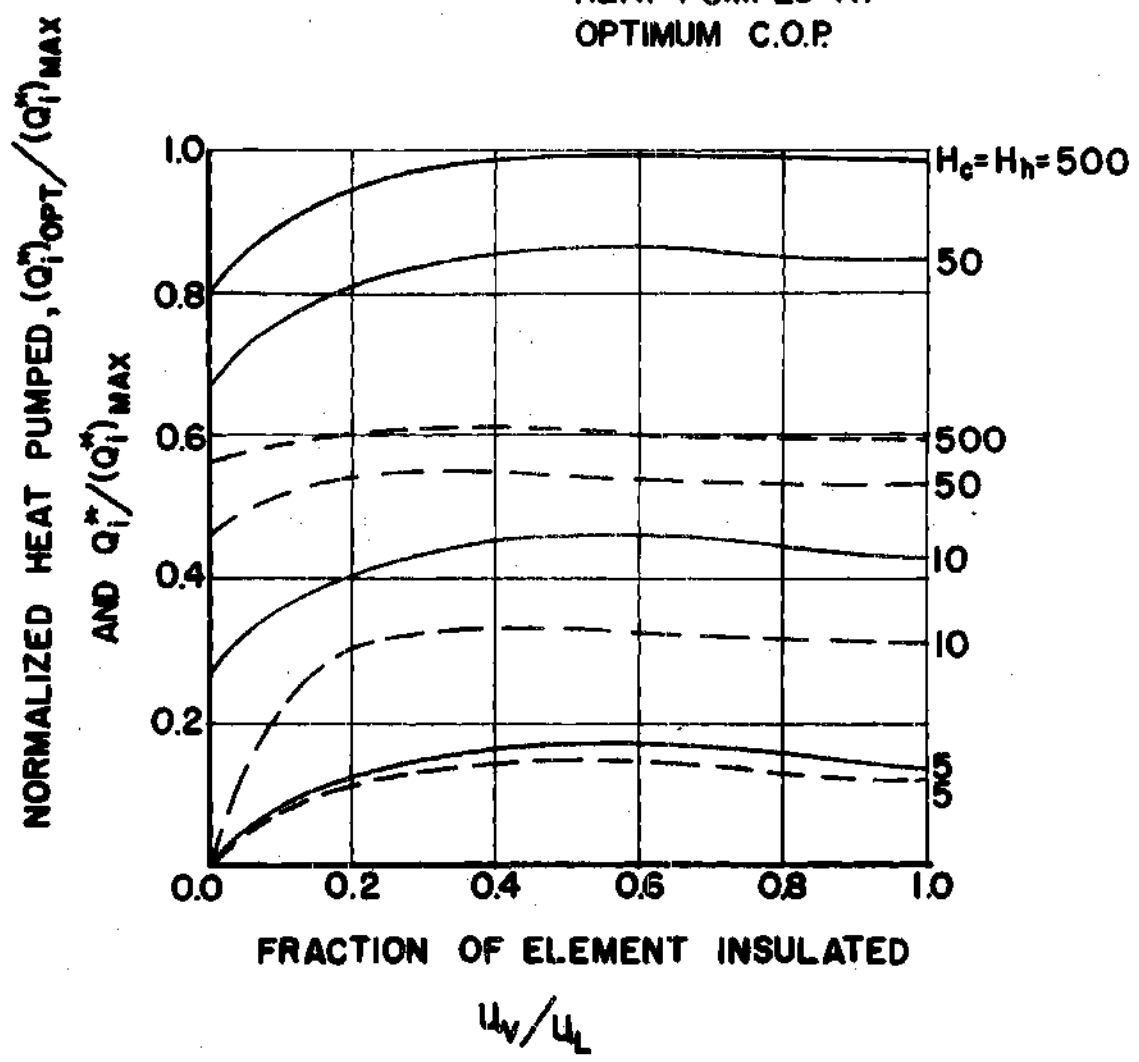


Fig. 13. Optimum Heat Pumped, $(Q_i^*)_{opt}$ versus Heat Pumped at Optimum C.O.P. with $u_L = 1$.

$u_L = 1$
 $(C.O.P.)_{MAX} = 0.321$
 ——— OPTIMUM C.O.P.
 - - - C.O.P. FOR OPTIMUM HEAT PUMPED

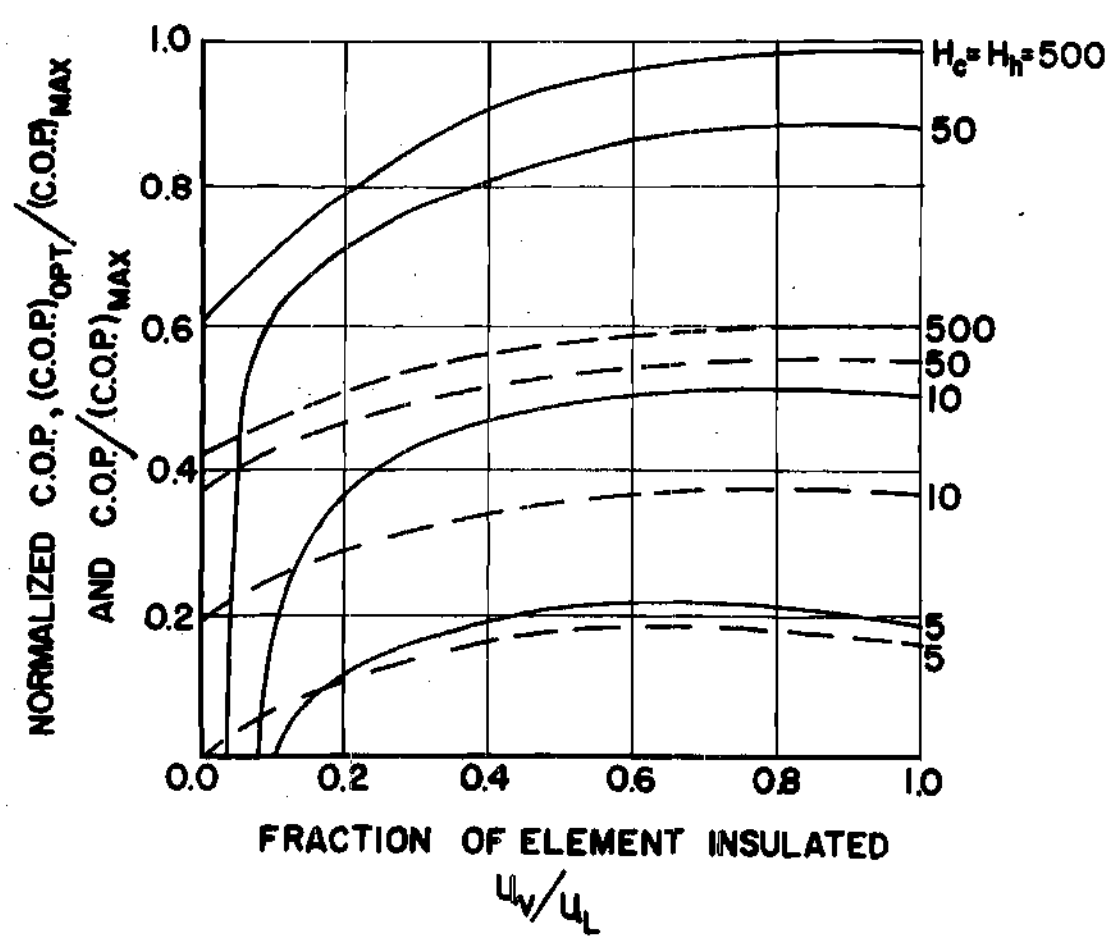


Fig. 14. Optimum C.O.P., $(C.O.P.)_{OPT}$ versus C.O.P. at Optimum Heat Pumped with $u_L = 1$.

increased by about six per cent through the use of surface heat transfer.

Figs. 15 and 16 give the same type of results shown in Figs. 13 and 14, except $u_L = 3$. It can be seen from Fig. 15 that for this larger value of u_L , significant improvements in the rate of heat pumping can be achieved through the judicious use of surface heat transfer. Gains in performance will be achieved only if part of the element is insulated. For example, for a device with a fin conductance of 10, if it is operated under conditions of optimum heat pumping, surface heat transfer will be beneficial only if $u_v/u_L > 0.12$. In Fig. 16, it can be seen that improvements in C.O.P. can be achieved by using surface heat transfer if the fin conductance is around 10 or less. For example, consider a circular element 0.635 cm long with a diameter of 0.635 cm. If part of the surface of the element is exposed to forced convection with a gas, the heat transfer coefficient could be around $0.053 \text{ W/cm}^2\text{°K}$ and $u_L = 3$. If the fin conductance H is 5, the ratio of fin-surface area to the cross-sectional area of the fin will be 2.2. If the element is operated to obtain the optimum C.O.P., Fig. 16 shows surface heat transfer will increase the optimum C.O.P. if $u_v/u_L > 0.36$. Specifically, if $u_v/u_L = 0.66$, the optimum C.O.P. will be nearly twice the value of the optimum C.O.P. for a corresponding fully insulated element. At the same time, Fig. 15 shows the heat pumped at optimum C.O.P. will be nearly three times the value for a corresponding fully insulated element with $H_c = H_h = 5$. Thus, it is possible to substantially increase both the optimum C.O.P. and the heat pumping capacity at optimum C.O.P. by using surface heat transfer.

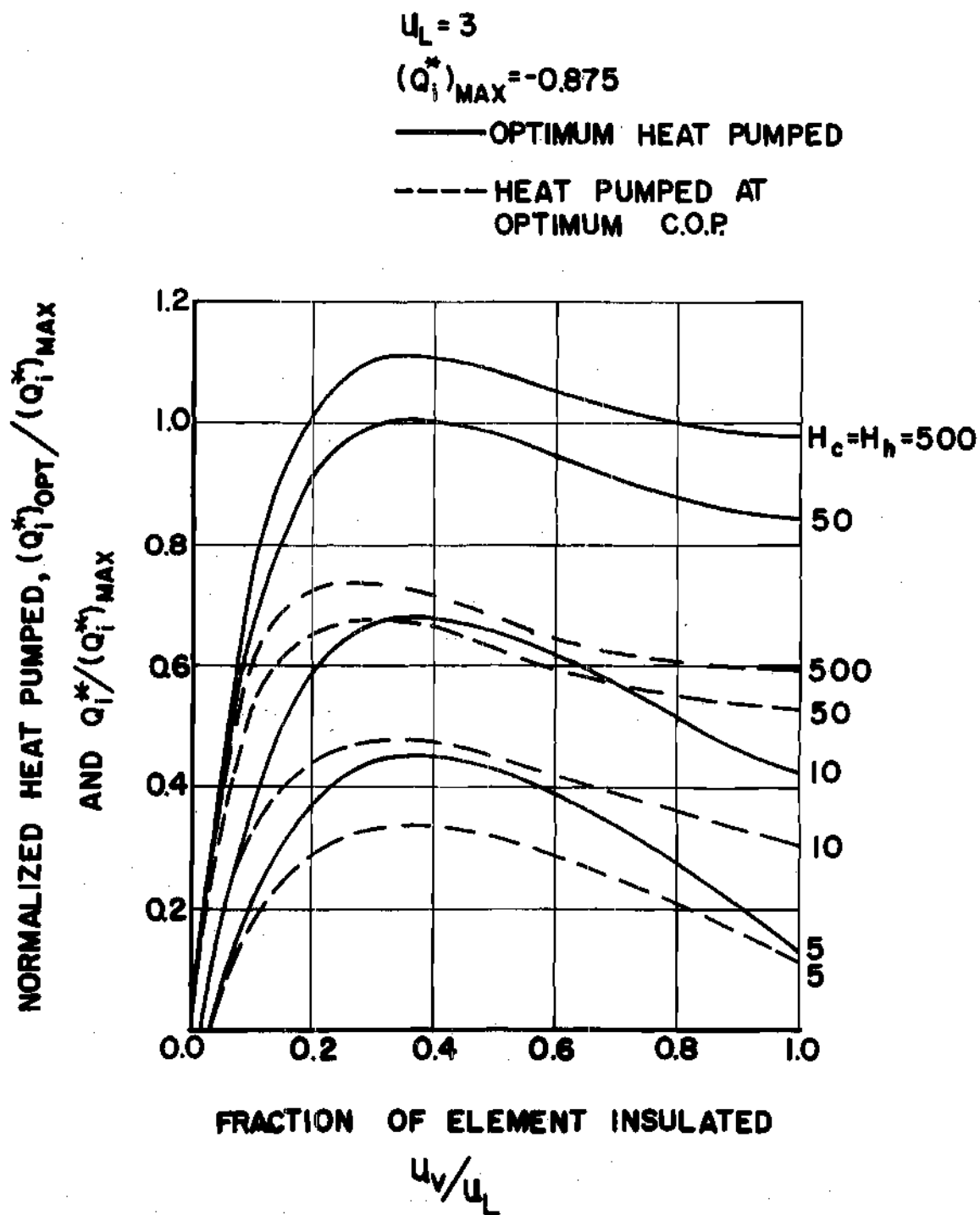


Fig. 15. Optimum Heat Pumped, $(Q_i^*)_{opt}$ versus Heat Pumped at Optimum C.O.P. with $u_L = 3$.

$u_L = 3$
 $(C.O.P.)_{MAX} = 0.321$

— OPTIMUM C.O.P.
 - - - C.O.P. FOR OPTIMUM
 HEAT PUMPED

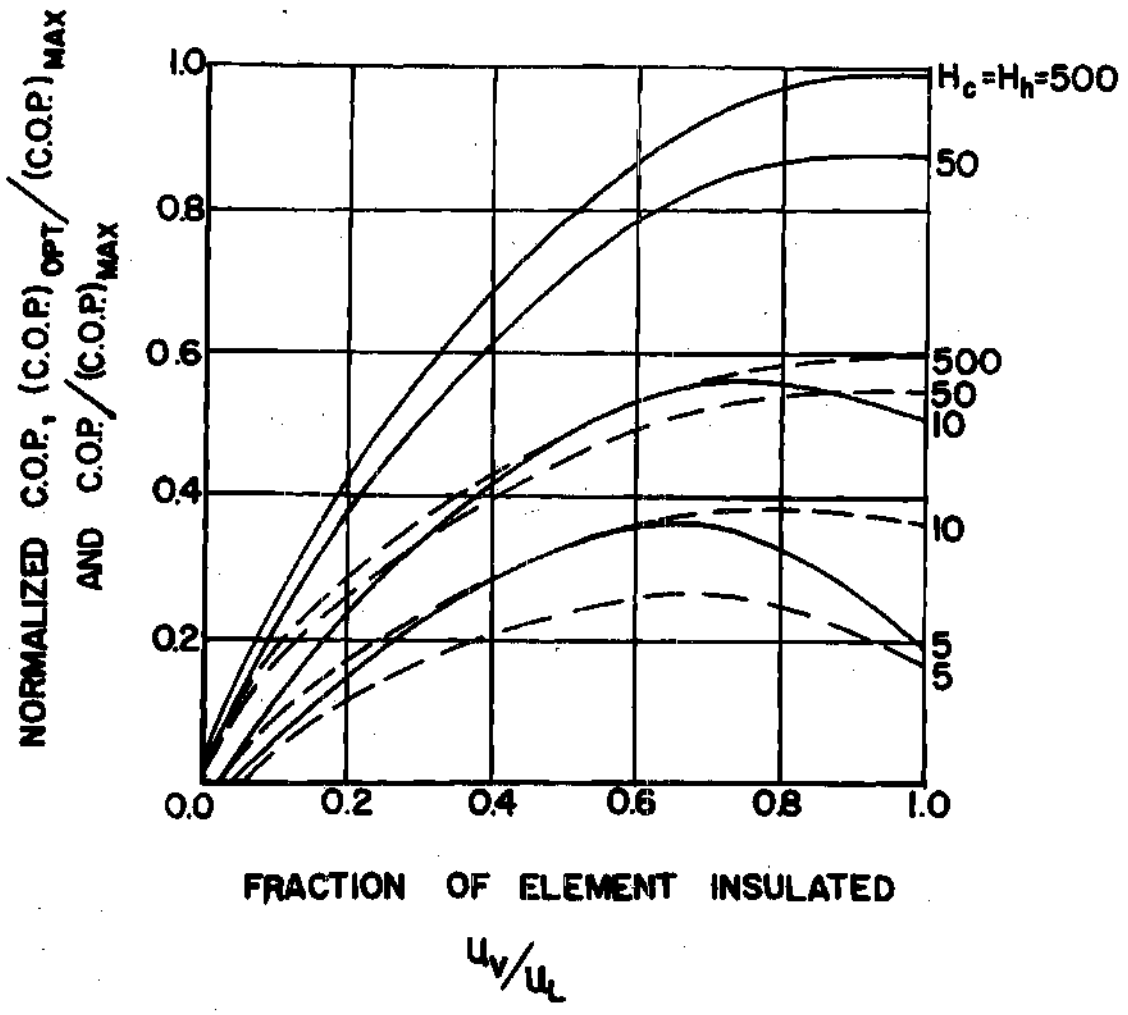


Fig. 16. Optimum C.O.P., $(C.O.P.)_{opt}$ versus C.O.P. at Optimum Heat Pumped with $u_L = 3$.

Figs. 17 and 18 give the rate of heat pumping and C.O.P. for $u_L = 5$. This value of u_L could be easily obtained, for example, by using a cylindrical element 1.27 cm long with a 0.635 cm diameter and by exposing it to free convection with a liquid so that $h = 0.0369 \text{ W/cm}^2\text{-}^\circ\text{K}$. Under these conditions, if the fin conductance H is 50, the ratio of the fin-surface area to the cross-sectional area of the element is about 16. If the device is operated under conditions giving the optimum heat pumping and if $u_v/u_L = 0.25$, then the rate of heat pumping will be increased by 61 per cent compared with the heat pumping capacity of a fully insulated element. Furthermore, the rate of heat pumping will be 37 per cent above the rate for a fully insulated element with infinite fin conductance. The increases in heat pumping capacity for the case considered will be accompanied by decreases in the C.O.P. which can be observed in Fig. 18.

Figs. 19 and 20 show the changes in performance that result by using surface heat transfer with $u_L = 20$. It can be seen from Fig. 19 that the heat pumping capacity can be increased by as much as a factor of five over the capacity of fully insulated elements. Fig. 20 shows that substantial reductions in C.O.P. occur if the device is operated under conditions giving the greatest gain in the heat pumping capacity. From Table 1 it can be seen that values of u_L as large as 20 can be obtained either by using elements with large values of L/A or by using a system that would give very large values of the heat transfer coefficient. Due to considerations involving cost, fabrication and performance, it is generally considered desirable to use elements with small values of L/A . Therefore, in order to obtain the maximum benefits from using surface

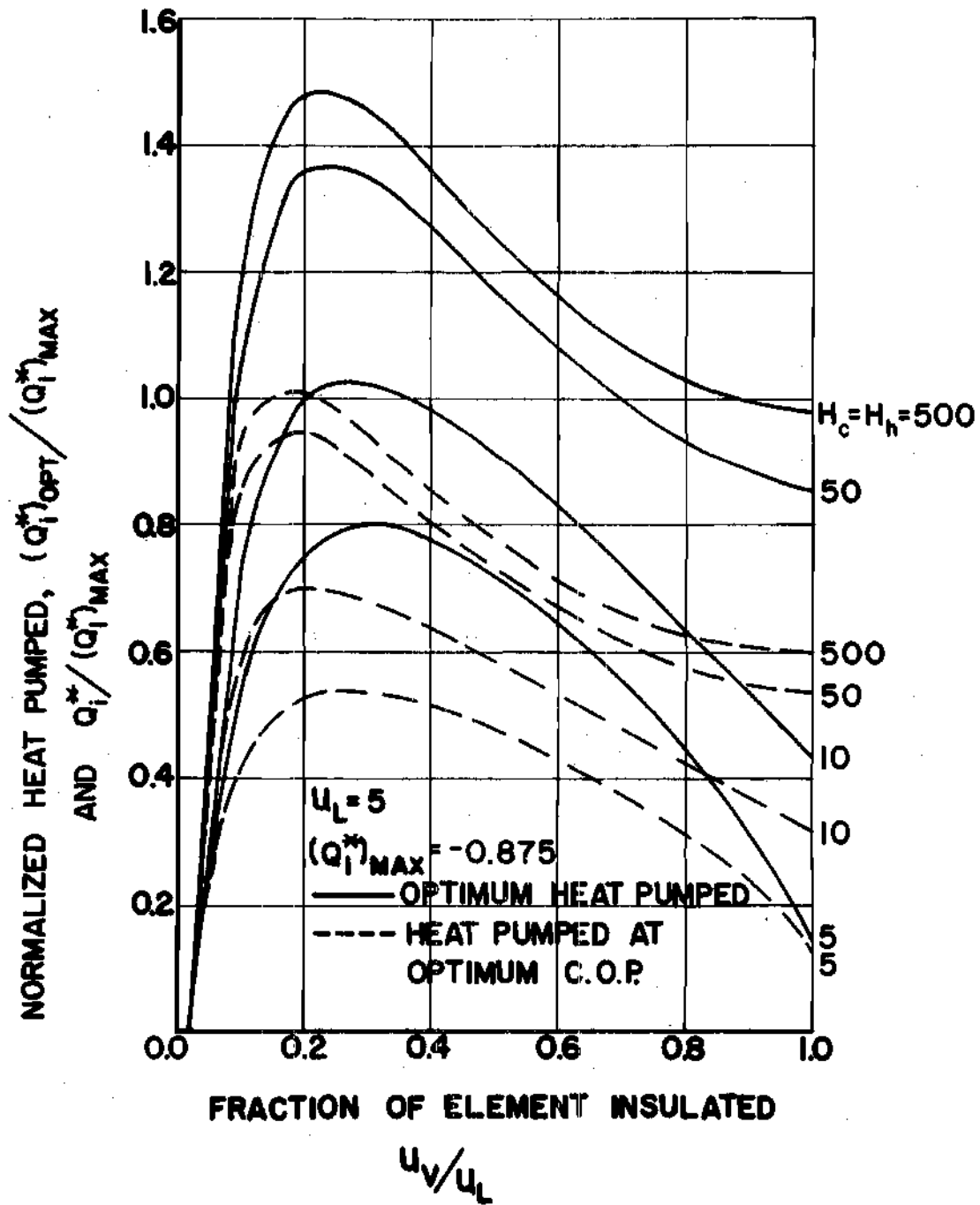


Fig. 17. Optimum Heat Pumped, $(Q_i^*)_{OPT}$ versus Heat Pumped at Optimum C.O.P. $(Q_i^*)_{MAX}^{opt}$ with $u_L = 5$.

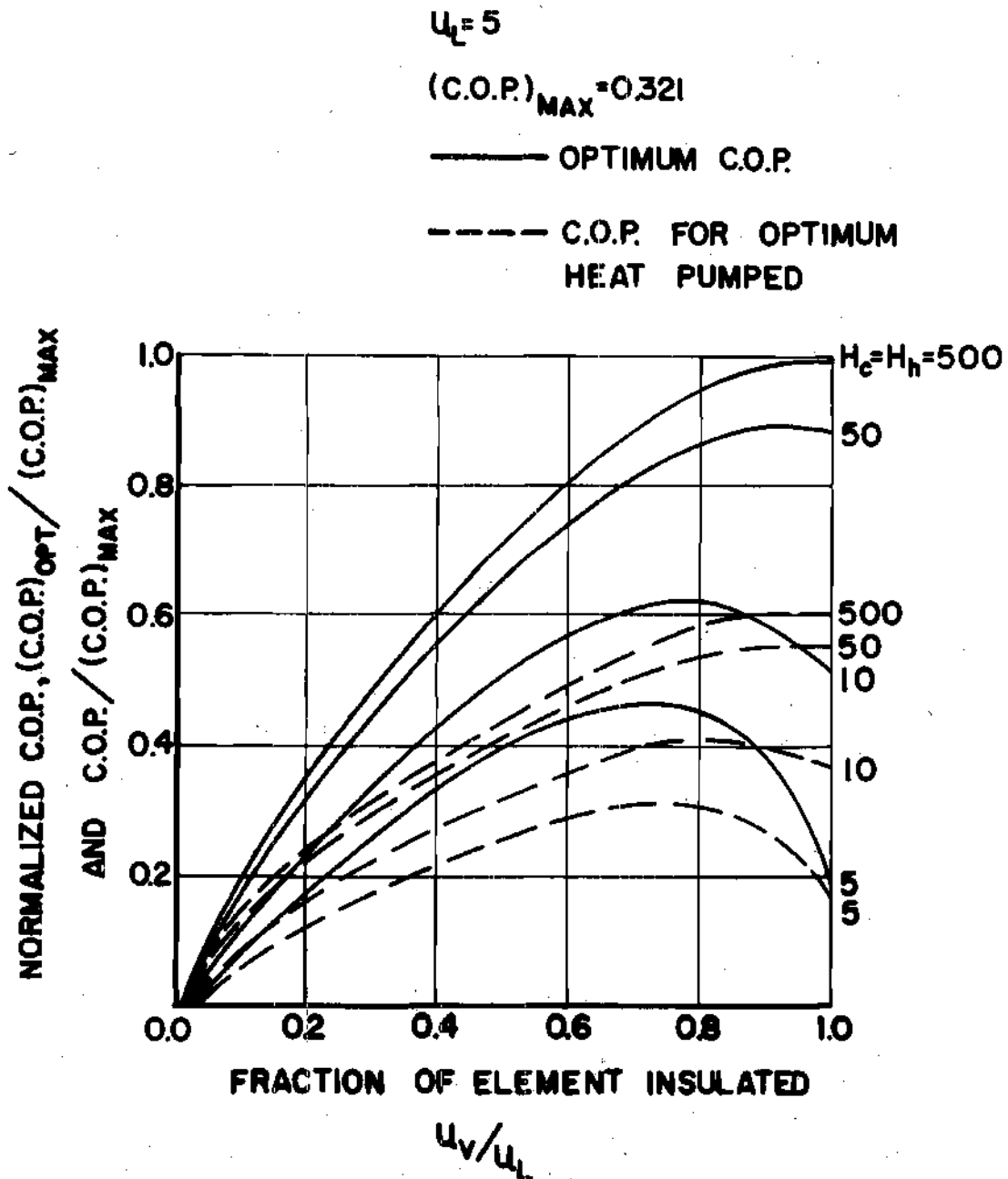


Fig. 18. Optimum C.O.P., $(C.O.P.)_{opt}$ versus C.O.P. at Optimum Heat Pumped with $u_L = 5$.

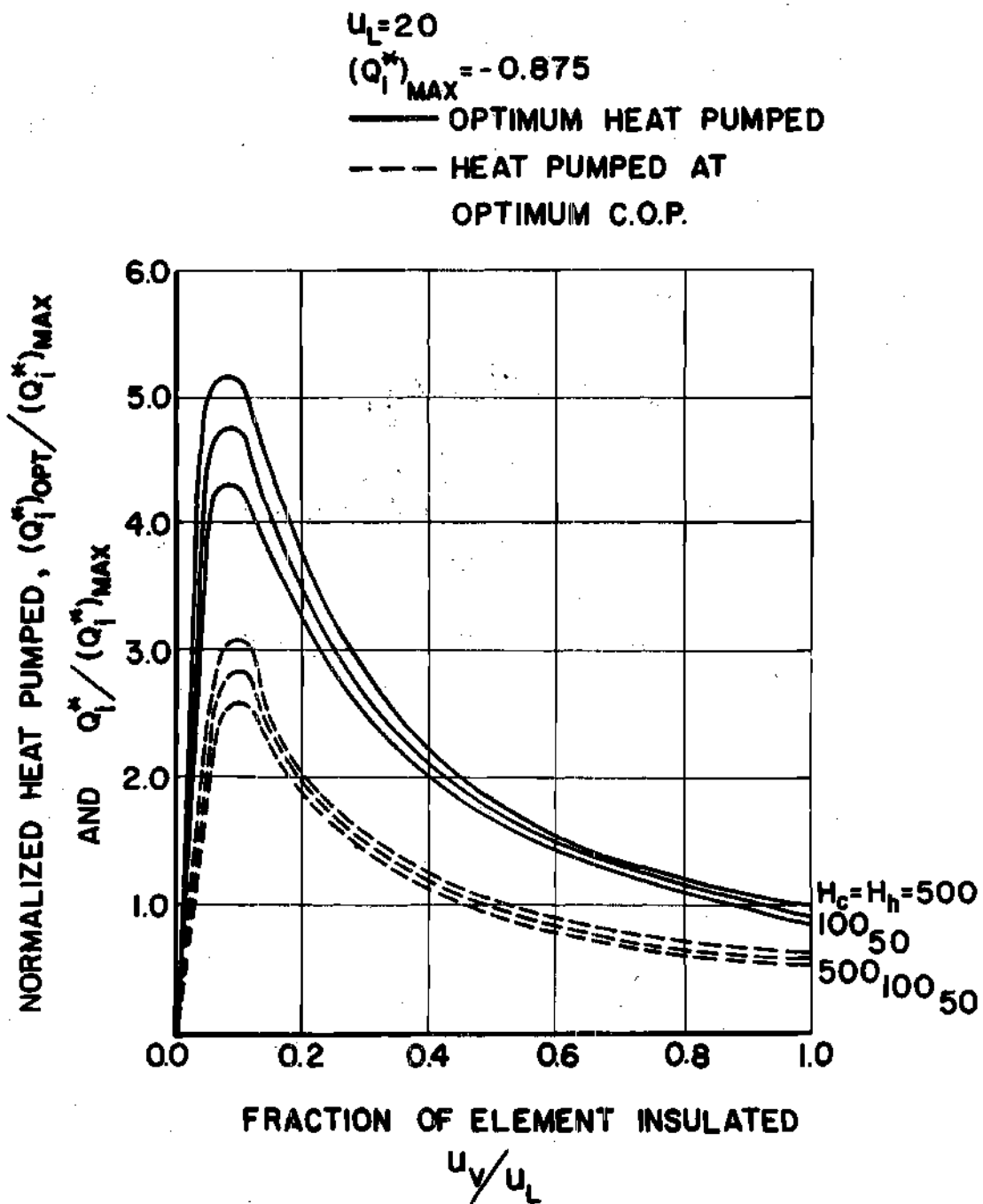


Fig. 19. Optimum Heat Pumped, $(Q_i^*)_{OPT}$ versus Heat Pumped at Optimum C.O.P. $(Q_i^*)_{MAX}$ with $u_L = 20$.

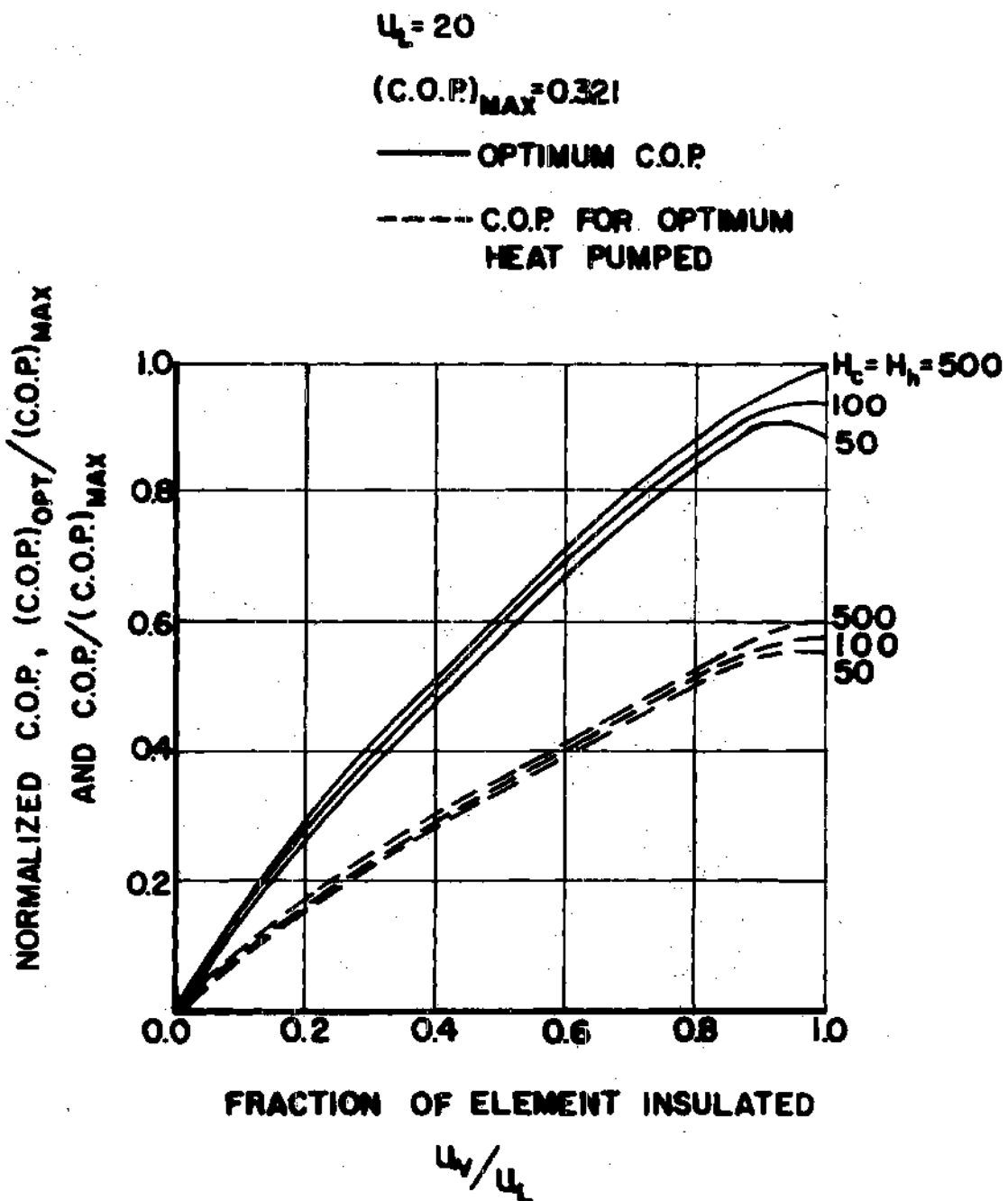


Fig. 20. Optimum C.O.P., $(C.O.P.)_{opt}$ versus C.O.P. at Optimum Heat Pumped with $u_L = 20$.

heat transfer, it would be desirable to design a system that would provide large heat transfer coefficients. If a portion of the thermoelement is exposed to convection with a boiling liquid (such as freon), it is possible to obtain values of the heat transfer coefficient in the range 0.1185 to $11.85 \text{ W/cm}^2\text{-}^\circ\text{K}$ (see reference 22).

Fig. 21 shows the optimum no-load temperature difference as a function of the fraction of the element insulated for various values of u_L and H^* . This figure shows the effect of u_L and dimensionless fin conductance on $(\theta_{NL})_{opt}$. As u_L increases the influence of the dimensionless fin conductance on $(\theta_{NL})_{opt}$ decreases.

Conclusions

The analysis presented can be used to predict the performance of thermoelectric heat pumps that have finite fins at the hot and cold junctions and are fully or partially insulated. The results show that substantial gains in heat pumping capacity and C.O.P. can be achieved when the thermoelement has insulation extending a specified distance along its surface from the cold junction. The effect of fin conductance on performance is also shown. One of the interesting aspects of the analysis is the significance of the value u_L . As u_L increases, the gains realized from surface heat transfer increase greatly and vice versa. For $u_L = 1$, surface heat transfer offers no improvements in performance compared to devices using fully insulated elements. However, for $u_L \geq 3$, large improvements in performance can result through the use of surface heat transfer. The results show that for $u_L = 3$ or 5 , if H is low (say 5 or 10), it is possible to use surface heat transfer to provide

*Note the suppressed zero for the ordinate.

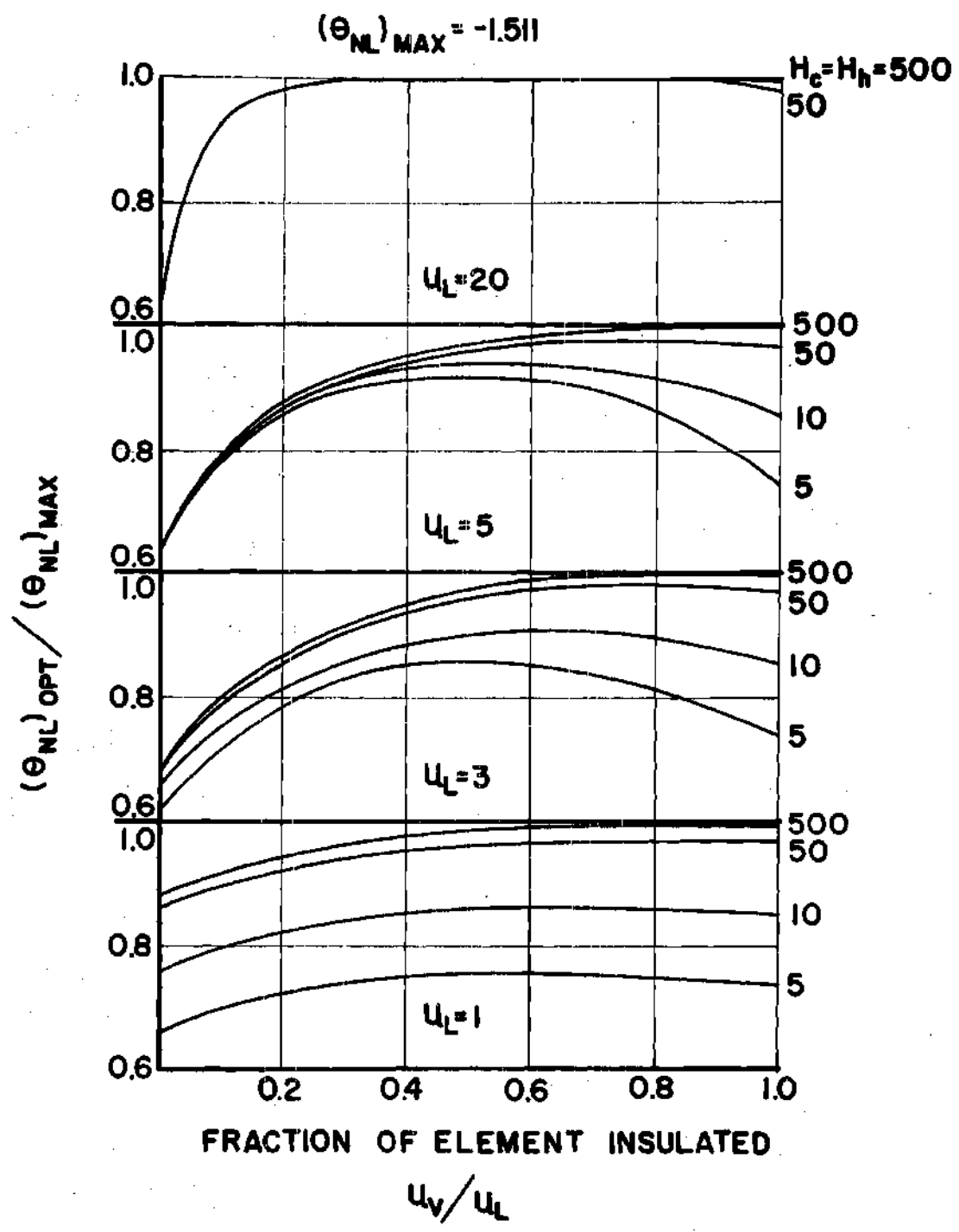


Fig. 21. Optimum No-Load Temperature Difference versus Fraction of Element Insulated for Various Values of u_L .

large increases in both C.O.P. and the rate of heat pumped. For values of H greater than about 50, surface heat transfer can be used to give greatly increased values of the heat pumping capacity, but this is often accompanied with large decreases in the C.O.P. This serious disadvantage may not be so important in applications where efficiency requirements are of secondary importance. It would also be possible to design a device in such a manner that the elements normally would be fully insulated, and exposed to surface heat transfer only to meet peak demands. Under normal conditions, the exposed surface of the elements could be insulated with a stagnant gas and the device could be operating near the maximum C.O.P. For peak demand conditions, a specific portion of the surface of the thermoelements could be exposed to forced convection with a liquid or a gas. It would, of course, be important to prevent electrical current from passing through the liquid.

The improvements in performance, resulting from the use of surface heat transfer predicted in this analysis, are conservative for two reasons. First, it is assumed that thermal and electrical contact resistance at the junction of the elements are negligible. Second, it is assumed that the fins used at the hot and cold junctions are isothermal. Thus, the actual benefits gained by using surface heat transfer should be somewhat greater than those predicted by this analysis.

CHAPTER VI

EFFECT OF SPATIAL PROPERTY DEPENDENCE ON THE PERFORMANCE OF A HEAT PUMP

1. Introduction to Spatial Property Dependence

The purpose of this section is to consider in detail the effect of spatial dependence of the thermoelectric properties $\rho(x)$, $k(x)$ and $S(x)$ on the performance of a heat pump. More specifically, this analysis seeks to determine if the spatial dependence of thermoelectric properties can be used to some advantage under certain conditions of operation. These properties are also temperature dependent but the purpose here is to first isolate the effect of spatially dependent properties.

The analysis is composed of three basic parts. First, only one of the three properties is considered a specified function of x ; the other two are considered constant. This procedure rotates until the effect of the spatial dependence of each individual property has been analyzed. Second, k is considered constant and $S(x)$ and $\rho(x)$ vary with position in such a manner that the figure of merit Z defined as $Z = S^2(x)/\rho(x)k$ remains a constant. Third, all three thermoelectric properties vary with position in a predetermined manner.

Before proceeding further, it is expedient to digress briefly and discuss some of the factors which cause a thermoelement to be inhomogeneous (not necessarily in a prescribed fashion) and hence to have spatially dependent properties. The following treatment is by no means a

complete explanation of the physical principles that govern the construction of a thermoelectric material and is intended only to give the reader a better physical insight into the problem at hand; see reference (24) or (25) for a complete treatment of the following discussion.

Fig. 22 is taken from Zoffe (3) and illustrates the dependence of the Seebeck coefficient S , electrical resistivity ρ , and thermal conductivity k on carrier concentration n . In Fig. 22 note that the electrical conductivity, $\frac{1}{\rho}$, can be increased by increasing the number of charge carriers; this may be effected by the use of appropriate doping agents or a variation in chemical composition. Conversely, the Seebeck coefficient decreases with increased carrier concentration. As a result, the product S^2/ρ passes through a maximum at a carrier concentration of about 10^{19} carriers/cm³.

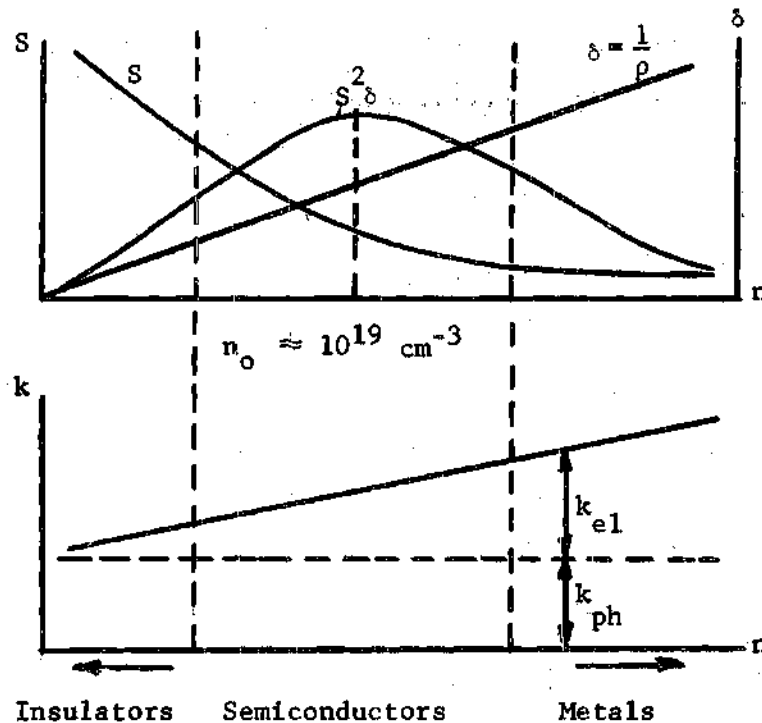


Fig. 22. Dependence of the Seebeck Coefficient, Electrical Resistivity and Thermal Conductivity on Carrier Concentration.

The thermal conductivity k of the thermoelement is seen to be composed of two components: k_{phonon} which is the lattice contribution to the thermal conductivity and is due to the propagation of energy in the form of atomic vibrations along the lattice; and $k_{\text{electronic}}$ which is the electronic component of the thermal conductivity and is due to the passage of charge carriers from a "hotter" region to a "colder" region. Fig. 22 illustrates that $k_{\text{electronic}}$ increases with increased carrier concentration and that k_{phonon} is independent of carrier concentration. Thus, Fig. 22 shows that the Seebeck coefficient, S , and the electrical resistivity, ρ , both decrease with increasing carrier concentration while the thermal conductivity, k , increases with increasing carrier concentration. It is interesting to note that in the region of interest here (semiconductors) the variation of S , ρ , and k with carrier concentration is roughly linear. In addition, in the semiconductor region, it can be seen from Fig. 22 that a change in carrier concentration brings about a larger change in S , and ρ than in k .

As mentioned earlier, changes in carrier concentration may be produced by the use of appropriate doping agents or a variation in chemical composition. Thus, it is desirable to determine whether improvements in the performance of thermoelectric devices can result by judiciously controlling carrier concentration such that predetermined spatially dependent properties result; such an analysis on a heat pump will be presented.

2. Physical System and Relevant Assumptions

The physical system to be considered in the following sections will be a single-element thermoelectric heat pump as shown in Fig. 23. It is

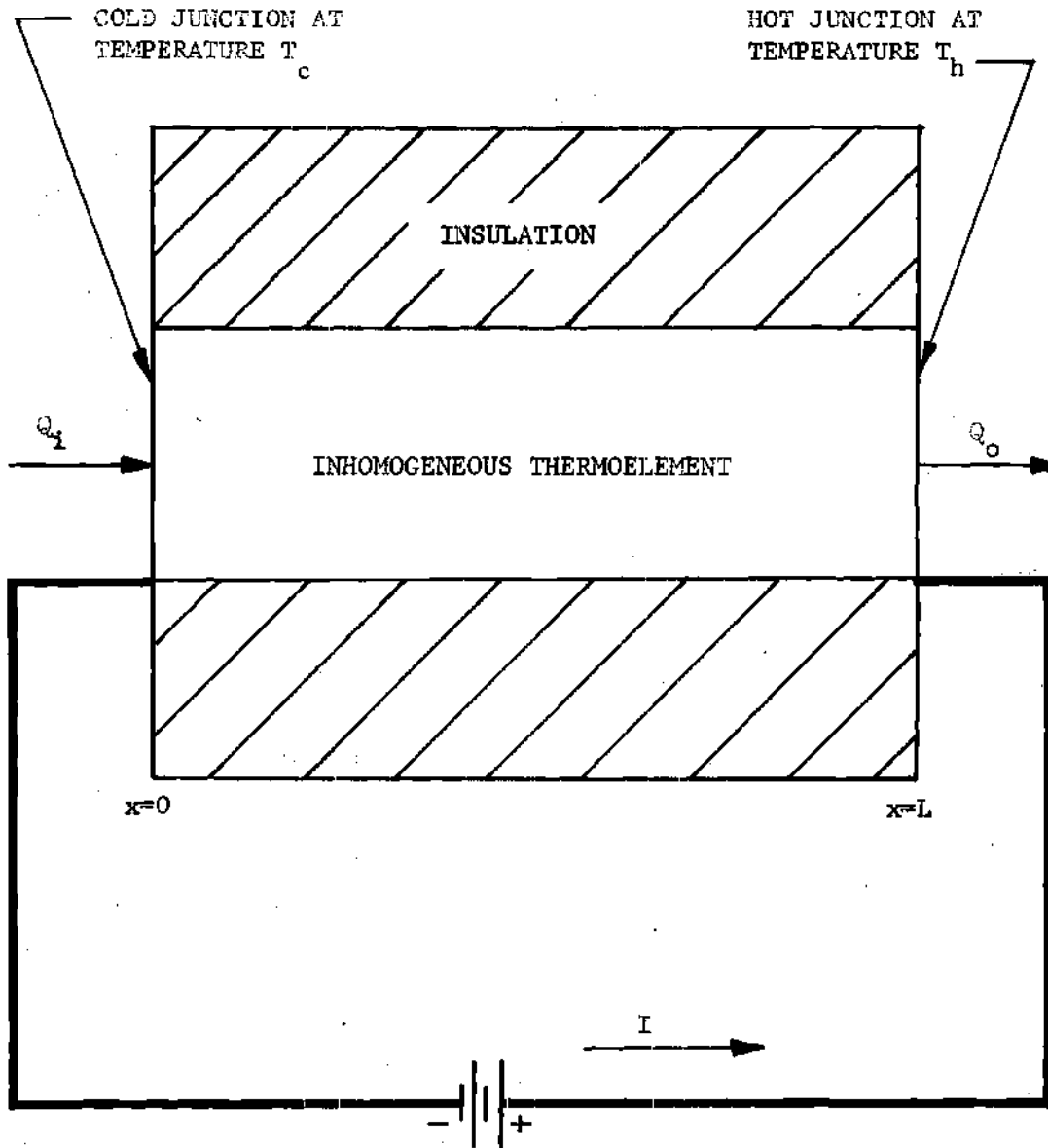


Fig. 23. An Insulated Inhomogeneous Thermoelement Used as a Heat Pump.

assumed that the cross-sectional area is constant; material properties are temperature independent and spatially dependent; the longitudinal surface of the element is insulated; steady-state conditions prevail; the electrical leads which complete the circuit have zero thermal conductivity, Seebeck coefficient, and electrical resistivity; the flow of heat and electricity in the thermoelement is one-dimensional; and the hot and cold junction fins have zero thermal resistance ($h_c = h_h = \infty$). The assumption of infinite fins is justified because this analysis seeks to determine the quantitative effects of spatially dependent properties on the performance criteria and is not concerned with the qualitative effects.

The differential equation describing the physical system above is obtained by applying the above assumptions to Eq. (3-2) and is

$$\frac{d}{dx} \left[k(x) A \frac{dT}{dx} \right] - IT \frac{dS}{dx} + \frac{I^2 \rho(x)}{A} = 0 \quad (6-1)$$

Equation (6-1) is subject to the boundary conditions

$$Q_i = IS(0) T_c - k(x) A \left. \frac{dT}{dx} \right|_{x=0} \quad (6-2a)$$

$$T(L) = T_h \quad (6-2b)$$

where T_c and T_h are specified constants. Equations (6-1) - (6-2) form the mathematical basis for the analysis in sections 3 through 8b.

In order to make the solutions of the system of equations (6-1) through (6-2) concise and general, two schemes are employed. First, most solutions to follow are obtained by using the Green's function (see

reference (26) or (27); a detailed solution of a differential equation using the Green's function is given in Appendix D. Second, all solutions are presented in non-dimensional form.

3. Effect of Spatially Dependent $\rho(x)$ on the Performance Criteria: S and k Constant

The purpose of this section is to examine the effect of a linear variation in $\rho(x)$ with axial position on the no-load temperature difference, the heat pumped, and the C.O.P. The Seebeck coefficient and thermal conductivity are constant. The electrical resistivity, $\rho(x)$, is assumed to vary linearly such that the average electrical resistivity $\bar{\rho}$ remains the same for all cases considered. Effectively, this section illustrates the effect of redistributing the electrical resistivity. Under these conditions, the resistance can be expressed by

$$\rho(x) = \bar{\rho} + \frac{\Delta \rho}{L} \left(x - \frac{L}{2}\right) \quad (6-3)$$

Graphically Eq. (6-3) appears as shown in Fig. 24.

The physical model to be studied in this section is shown in Fig. 23. The differential equation describing this system subject to the assumptions of this section is obtained by reduction of Eq. (6-1) and is

$$\frac{d^2 T}{dx^2} = - \frac{I^2 \rho(x)}{kA^2} \quad (6-4)$$

Equation (6-4) is subject to the boundary conditions (6-2a) and (6-2b). Before solving for the temperature distribution, it is helpful to reduce the number of parameters by defining the following dimensionless

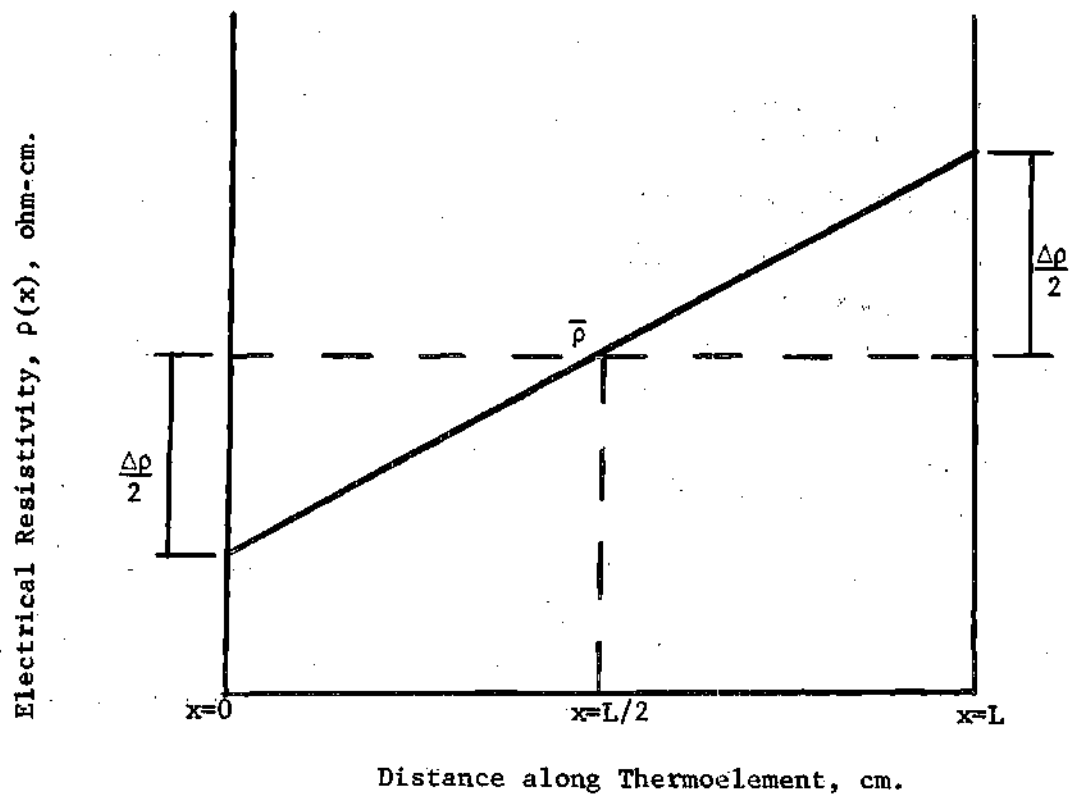


Fig. 24. Assumed Spatial Dependence of $\rho(x)$:

quantities. Thus, the dimensionless temperature θ , the dimensionless position u , the dimensionless current α and the dimensionless resistivity change γ_ρ , are defined by

$$\theta = \frac{T(x) - T_h}{T_h} \quad (6-5 a)$$

$$u = \frac{x}{L} \quad (6-5 b)$$

$$\alpha = \frac{ISL}{KA} \quad (6-5 c)$$

$$\gamma_\rho = \frac{\Delta\rho}{\bar{\rho}} \quad (6-5 d)$$

Making use of the above definitions, Eq. (6-3) becomes

$$\rho(u) = \bar{\rho} \left[1 + \gamma_{\rho} \left(u - \frac{1}{2} \right) \right] \quad (6-6)$$

Equation (6-4) becomes,

$$\frac{d^2\theta}{du^2} = -f(u) \quad (6-7)$$

and Eq. (6-2) becomes,

$$Q_i^* = \alpha(\theta_c + 1) - \frac{d\theta}{du} \Big|_{u=0} \quad (6-8a)$$

$$\theta(1) = \theta_h = 1 \quad (6-8b)$$

where

$$f(u) = \frac{r^2 L^2}{k A^2 T_h} \rho(u) = \frac{\alpha^2}{\bar{E} T_h} \left[1 + \gamma_{\rho} \left(u - \frac{1}{2} \right) \right]$$

Note that the notation \bar{E} means the figure of merit is defined using the average values $\bar{\rho}$, \bar{S} , and \bar{k} . Clearly the notation \bar{S} and \bar{k} is redundant at this point since they are both constant; however, it will prove convenient in correlating the various sections in this chapter.

Using the Green's function as outlined in Appendix D, the dimensionless temperature distribution $\theta(u)$, may be written as,

$$\theta(u) = \int_0^1 G(u, \epsilon) f(\epsilon) d\epsilon + \frac{(Q_i^* - \alpha)(1 - u)}{\alpha + 1} \quad (6-9)$$

where

$$G(u, \varepsilon) = \begin{cases} \frac{(1 - \varepsilon)(1 + \alpha u)}{1 + \alpha} & 0 \leq u \leq \varepsilon \\ \frac{(1 - u)(1 + \alpha \varepsilon)}{1 + \alpha} & \varepsilon < u \leq 1 \end{cases}$$

$$\text{and } f(\varepsilon) = f(u) \Big|_{u=\varepsilon}$$

It is interesting to note that Eq. (6-9) is actually the solution for the temperature distribution for any one-dimensional variation of electrical resistivity with position. In addition, the effect of a spatially dependent resistivity is conveniently confined to the first term in Eq. (6-9). Using the variation of $\rho(u)$ assumed in this section, Eq. (6-9) may be integrated to yield

$$\theta(u) = \frac{\alpha^2}{2 \bar{E} T_h} \left[u^2 \left(\frac{\gamma_\rho}{2} - 1 - \frac{\gamma_\rho u}{3} \right) + \left(\frac{1 + \alpha u}{1 + \alpha} \right) \left(\frac{1 - \gamma_\rho}{6} \right) \right] + \frac{(Q_1^* - \alpha)(1 - u)}{1 + \alpha} \quad (6-10)$$

3a. Optimized No-Load Temperature Difference for $\rho(u) = \bar{\rho} \left[1 + \gamma_\rho \left(u - \frac{1}{2} \right) \right]$

As mentioned previously, the dimensionless no-load temperature difference θ_{NL} , is defined as the dimensionless temperature difference that results between the hot and cold junctions when the cold junction is insulated from its environment so that $Q_1^* = 0$. Letting $Q_1^* = 0$ and $u = 0$ in Eq. (6-10) gives

$$\theta_{NL} = \frac{\alpha}{1 + \alpha} \left[1 - \frac{\alpha}{2 \bar{E} T_h} \left(1 - \frac{\gamma_\rho}{6} \right) \right] \quad (6-11)$$

where, by definition, $\theta_{NL} = -\theta(0) = -\theta_c$. The optimum no-load temperature difference occurs if

$$\frac{\partial \theta_{NL}}{\partial \alpha} = 0 \quad (6-12)$$

The current which yields the optimum value of θ_{NL} is

$$(\alpha)_{opt} = \sqrt{1 + \frac{2 \bar{\epsilon} T_h}{1 - \frac{\gamma_\rho}{6}}} - 1 \quad (6-13)$$

Substitution of Eq. (6-13) into Eq. (6-11) gives the optimum value of

θ_{NL} as

$$(\theta_{NL})_{opt} = \frac{\left(\sqrt{1 + \phi_\rho} - 1\right)^2}{\phi_\rho} \quad (6-14)$$

where

$$\phi_\rho = 2 \bar{\epsilon} T_h / \left(1 - \frac{\gamma_\rho}{6}\right)$$

In order to determine the effect of the spatially dependent $\rho(u)$ on

$(\theta_{NL})_{opt}$, it is expedient to compare $(\theta_{NL})_{opt}$ as given by Eq. (6-14) with

$(\theta_{NL})_{max}$ for constant electrical resistivity. Equation (6-14) gives

$(\theta_{NL})_{max}$ for constant electrical resistivity by letting $\gamma_\rho = 0$. Thus,

$$(\theta_{NL})_{max} = (\theta_{NL})_{opt} \Big|_{\gamma_\rho = 0} = \left(\sqrt{1 + 2 \bar{\epsilon} T_h} - 1\right)^2 / 2 \bar{\epsilon} T_h \quad (6-15)$$

Equations (6-14) and (6-15) can best be compared by assuming specific

values of the parameters \bar{z} and T_h , for various values of γ_ρ . For $\bar{z} = 3 \times 10^{-3} \text{ }^\circ\text{K}^{-1}$ and $T_h = 300^\circ \text{K}$, Fig. 27 illustrates the effect of a spatially dependent resistivity on the optimum no-load temperature difference (normalized with respect to $(\theta_{NL})_{\max}$). Fig. 27 shows that the effect of the assumed variation in $\rho(u)$ is always to increase θ_{NL} . Thus, a predetermined redistribution of electrical resistivity -- even though small -- acts to increase the optimum no-load temperature difference. It is important to note that a practical variation in $\rho(u)$ is confined to approximately $\gamma_\rho < 1$. Based on Eq. (6-6), variations of θ much greater than one (1) are not presently feasible. The region $\gamma_\rho > 1$ is included primarily for present interest and possible future use.

3b. Optimized Heat Pumped for $\rho(u) = \bar{\rho} \left[1 + \gamma_\rho \left(u - \frac{1}{2} \right) \right]$

In this section the effect of spatially dependent resistivity on the optimum amount of heat that a thermoelement can pump across a specified temperature difference is determined. The energy balance at the cold junction, Eq. (6-2a) has the form

$$Q_i^* = \alpha(\theta_c + 1) - \left. \frac{d\theta}{du} \right|_{u=0} \quad (6-2a)$$

or by letting $u = 0$ in Eq. (6-10),

$$\theta(0) = \theta_c = \frac{\alpha^2}{2 \bar{z} T_h} \left(\frac{1}{1 + \alpha} \right) \left(1 - \frac{\gamma_\rho}{6} \right) + \frac{Q_i^* - \alpha}{1 + \alpha} \quad (6-16)$$

Solving for Q_i^* ,

$$Q_i^* = \alpha(\theta_c + 1) + \theta_c - \frac{\alpha^2}{2 \bar{z} T_h} \left(1 + \frac{\gamma_\rho}{6} \right) \quad (6-17)$$

Inspection of Eq. (6-17) shows that the heat pumping capacity Q_i^* , increases as γ_ρ increases. In Eq. (6-17), the first term is due to the Peltier effect and is positive; the second term is due to heat conduction within the element and is negative; and the last term is due to Joule heating and is negative. Furthermore, only the last term contains the effect of variable $\rho(u)$. For positive γ_ρ , as γ_ρ increases, the Joule heating term decreases thus augmenting Q_i^* .

The optimum heat pumping occurs if

$$\frac{\partial Q_i^*}{\partial \alpha} = 0 \quad (6-18)$$

The current which yields the optimum value of Q_i^* is

$$(\alpha)_{\text{opt}} = \frac{\bar{z} T_h}{1 - \frac{\gamma_\rho}{6}} (\theta_c + 1) \quad (6-19)$$

Substitution of Eq. (6-19) into Eq. (6-17) gives the optimum value of $(Q_i^*)_{\text{opt}}$ as

$$(Q_i^*)_{\text{opt}} = \frac{\bar{z} T_h}{2(1 - \frac{\gamma_\rho}{6})} (\theta_c + 1)^2 + \theta_c \quad (6-20)$$

Again, inspection of Eq. (6-20) shows that $(Q_i^*)_{\text{opt}}$ increases as γ_ρ increases; the same conclusion is reached by inspection of Eq. (6-17).

The value $\gamma_\rho = 6$ does not have any practical significance because its existence implies a negative electrical resistivity at the cold junction.

The general effect of the assumed spatially dependent $\rho(u)$ on

$(Q_i^*)_{opt}$ was determined by inspection. However, it is interesting to compare $(Q_i^*)_{opt}$ as given by Eq. (6-20) with $(Q_i^*)_{max}$ for constant electrical resistivity; that is, let $\gamma_\rho = 0$ in Eq. (6-20) and obtain

$$(Q_i^*)_{max} = \frac{\bar{z} T_h}{2} (\theta_c + 1)^2 + \theta_c \quad (6-21)$$

Equations (6-20) and (6-21) are easily compared by assuming specific values of \bar{z} , T_c and T_h . For $T_c = 250^\circ \text{K}$, $T_h = 300^\circ \text{K}$ and $\bar{z} = 3 \times 10^{-3} \text{K}^{-1}$. Fig. 28 quantitatively illustrates that a spatially dependent resistivity, as given by Eq. (6-6), significantly increases both the optimum heat pumping capacity and the heat pumping capacity for the condition of optimum C.O.P. (dotted curve labeled $\rho(u)$). Note that $(Q_i^*)_{opt}$ is normalized with respect to $(Q_i^*)_{max}$. Thus it has been shown mathematically and illustrated graphically that a judicious redistribution of electrical resistivity -- even though small -- acts to increase the heat pumping capacity of a thermoelement.

3c. Optimized C.O.P. for $\rho(u) = \left[\bar{\rho} \left(1 + \gamma_\rho \left(u - \frac{1}{2} \right) \right) \right]$

It is of interest to determine the effect of a spatially dependent resistivity on the optimum coefficient of performance.

As defined previously, the C.O.P. is the ratio of the heat pumped Q_i to the total electrical power input P_i . That is,

$$\text{C.O.P.} = \frac{Q_i}{P_i} \quad (6-22)$$

But

$$P_i = I \bar{S} (T_h - T_c) + \frac{I^2 L}{A} \int_0^1 \rho(u) du \quad (6-22a)$$

The first term in Eq. (6-22a) represents the electrical power dissipated in overcoming the Seebeck voltage which occurs because of the temperature difference across the element; the second term is the power dissipated in Joule heat. Using Eq. (6-6),

$$P_i = I \bar{S} (T_h - T_c) + \frac{I^2 L \bar{\rho}}{A} \int_0^1 \left[1 + \gamma_\rho \left(u - \frac{1}{2} \right) \right] du \quad (6-22b)$$

By definition of $\rho(u)$, its integral over the element is $\bar{\rho}$. Thus,

$$P_i = I \bar{S} (T_h - T_c) + \frac{I^2 \bar{\rho} L}{A} \quad (6-22c)$$

Hence one may write,

$$\text{C.O.P.} = \frac{Q_1}{\frac{I^2 \bar{\rho} L}{A} + I \bar{S} (T_h - T_c)} \quad (6-23)$$

Multiplying the numerator and denominator of Eq. (6-23) by $L / \bar{k} A T_h$ and applying some of the dimensionless quantities defined previously, yields

$$\text{C.O.P.} = \frac{Q_1^*}{\frac{\alpha^2}{\bar{S} T_h} - \alpha \theta_c} \quad (6-24a)$$

By making use of Eq. (6-17), there results

$$\text{C.O.P.} = \frac{\alpha(\theta_c + 1) + \theta_c - \frac{\alpha^2}{2 \bar{\epsilon} T_h} \left(1 - \frac{\gamma_p}{6}\right)}{\frac{\alpha^2}{\bar{\epsilon} T_h} - \alpha \theta_c} \quad (6-24b)$$

The optimum value of the C.O.P. occurs if

$$\frac{\partial}{\partial \alpha} (\text{C.O.P.}) = 0$$

and is given by

$$(\alpha)_{\text{opt}} = \frac{\theta_c}{\frac{\theta_c}{2} \left(1 + \frac{\gamma_p}{6}\right) + 1} \left[\sqrt{1 + \bar{\epsilon} T_h \left\{ \frac{\theta_c}{2} \left(1 + \frac{\gamma_p}{6}\right) + 1 \right\}} + 1 \right] \quad (6-25)$$

The validity of Eq. (6-25) may be easily checked by allowing $\gamma_p = 0$.

When this is done, Eq. (6-25) reduces to

$$(\alpha)_{\text{opt}} = \frac{2(T_h - T_c)}{T_c + T_h} \left[\sqrt{1 + \bar{\epsilon} \left(\frac{T_c + T_h}{2} \right) + 1} \right] \quad (6-26)$$

which is the usual expression for the optimum current in a constant property infinite fin thermoelement operated at maximum C.O.P.

Eq. (6-25) may be substituted into Eq. (6-24b) to obtain an expression for $(\text{C.O.P.})_{\text{opt}}$. However, such a substitution yields a rather long equation that does not easily contribute additional insight into the physical situation. Therefore, a computer program was written that first calculated $(\alpha)_{\text{opt}}$ from Eq. (6-25) and then substituted this value into Eq. (6-24b), to obtain $(\text{C.O.P.})_{\text{opt}}$. To implement this program, it was

assumed, as before that $T_h = 300^\circ \text{K}$, $T_c = 250^\circ \text{K}$ and $\bar{z} = 3 \times 10^{-3} \text{ } ^\circ\text{K}^{-1}$; γ_ρ was used as the argument. Fig. 29 illustrates the effect of a spatially dependent resistivity on the optimum coefficient of performance normalized with respect to $(\text{C.O.P.})_{\text{max}}$; that is, $\gamma_\rho = 0$. This figure shows that the assumed variation in $\rho(u)$ always causes an increase in $(\text{C.O.P.})_{\text{opt}}$. Hence, even a small predetermined redistribution of electrical resistivity acts to increase the optimum coefficient of performance. Notice in Fig. 29 that if the thermoelement is operated at the condition of optimum heat pumping (dotted curve labeled $\rho(u)$) the C.O.P. is virtually independent of the variation in γ_ρ . On the other hand, Fig. 28 shows that if the thermoelement is operated at the condition of optimum C.O.P. (dotted curve labeled $\rho(u)$) the heat pumping capacity increases as γ_ρ increases.

4. Effect of Spatially Dependent $k(x)$ on the Performance Criteria: ρ and S constant

The purpose of this section is to examine the effect of a linear variation in $k(x)$ with axial position on the no-load temperature difference, the heat pumped, and the C.O.P.; ρ and S are considered to remain constant. The thermal conductivity, $k(x)$ is assumed to vary linearly such that the average thermal conductivity \bar{k} remains the same. Essentially this section illustrates the effect of redistributing the thermal conductivity. Using the $k(x)$ assumption,

$$k(x) = \bar{k} + \frac{\Delta k}{L} \left(\frac{L}{2} - x \right) \quad (6-27)$$

Graphically Eq. (6-27) appears as shown in Fig. 25.

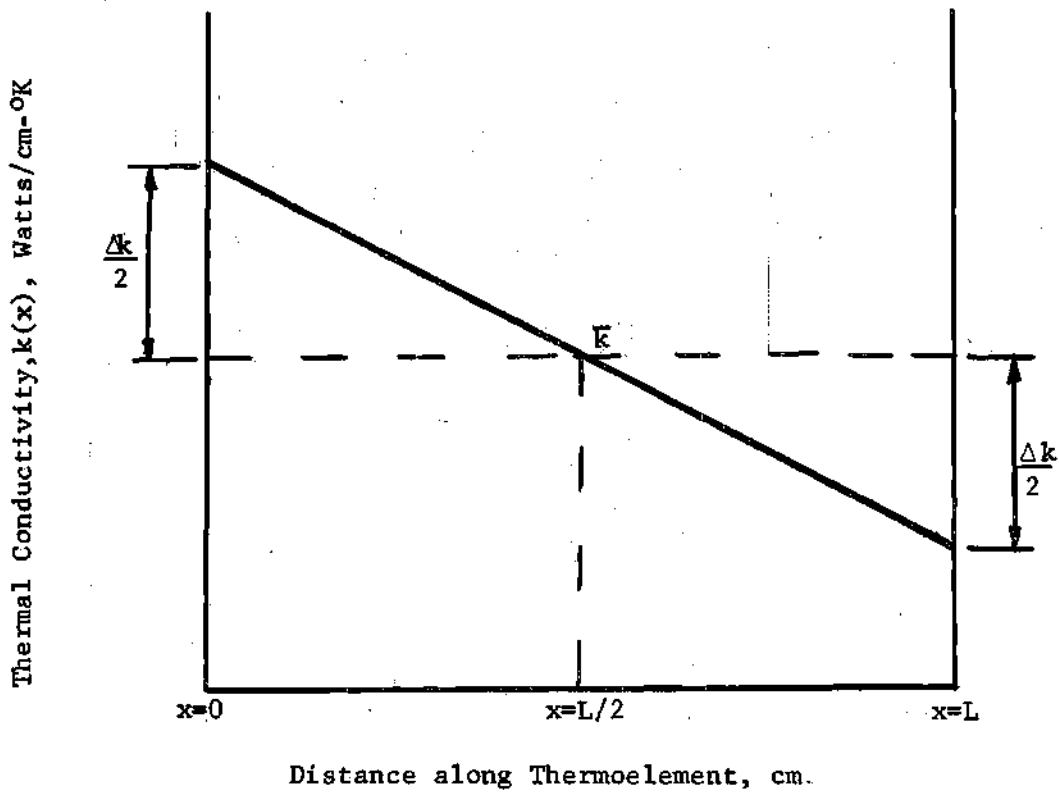


Fig. 25. Assumed Spatial Dependence of $k(x)$.

The physical model to be studied in this section is shown in Fig. 23. The differential equation describing this system subject to the assumptions of this section is obtained by reduction of Eq. (6-1) and is

$$\frac{d}{dx} \left[k(x) \frac{dT}{dx} \right] = \frac{-I^2 \bar{\rho}}{A^2} \quad (6-28)$$

Eq. (6-28) is subject to the boundary conditions

$$Q_i = \bar{T}_c - k(x) A \left. \frac{dT}{dx} \right|_{x=0} \quad (6-2a)$$

$$T(L) = T_h \quad (6-2b)$$

When most of the dimensionless definitions introduced in section 3 are applied to the above equations, Eq. (6-27) becomes

$$k(u) = \bar{k} \left[1 + \gamma_k \left(\frac{1}{2} - u \right) \right] \quad (6-29)$$

where $\gamma_k = \Delta k / \bar{k}$. Eq. (6-28) becomes

$$\frac{d}{du} \left[\left(1 - \gamma'_k u \right) \frac{d\theta}{du} \right] = -f \quad (6-30)$$

where $\gamma'_k = \gamma_k / (1 + \gamma_k/2)$ and $f = \frac{\alpha^2}{\bar{z} T_h \left(1 + \frac{\gamma_k}{2} \right)}$. Equation (6-2) becomes

$$\frac{Q_i^*}{\left(1 + \frac{\gamma_k}{2} \right)} = \frac{\alpha}{\left(1 + \frac{\gamma_k}{2} \right)} (\theta_c + 1) - \left. \frac{d\theta}{du} \right|_{u=0} \quad (6-31a)$$

$$\theta(1) = \theta_h = -1 \quad (6-31b)$$

Using the Green's function as outlined in Appendix D, the dimensionless temperature distribution $\theta(u)$, may be written as,

$$\theta(u) = \int_0^1 G(u, \varepsilon) (f) d\varepsilon + \frac{(Q_i^* - \alpha) \ln \left(\frac{1 - \gamma'_k u}{1 - \gamma'_k} \right)}{\gamma_k \left[1 + \frac{\alpha}{\gamma_k} \ln (1 - \gamma'_k) \right]} \quad (6-32a)$$

where

$$G(u, \varepsilon) = \begin{cases} \frac{\ln\left(\frac{1 - \gamma_k' \varepsilon}{1 - \gamma_k'}\right) \ln\left\{\frac{e}{(1 - \gamma_k' u)^{\alpha/\gamma_k'}}\right\}}{\ln\left\{\frac{e}{(1 - \gamma_k')^{\alpha/\gamma_k'}}\right\}^{\gamma_k'}} & 0 \leq u < \varepsilon \\ \frac{\ln\left(\frac{1 - \gamma_k' u}{1 - \gamma_k'}\right) \ln\left\{\frac{e}{(1 - \gamma_k' \varepsilon)^{\alpha/\gamma_k'}}\right\}}{\ln\left\{\frac{e}{(1 - \gamma_k')^{\alpha/\gamma_k'}}\right\}^{\gamma_k'}} & \varepsilon < u \leq 1 \end{cases}$$

It is interesting to note that Eq. (6-32a) can also represent the solution for the temperature distribution in a thermoelement with a spatially dependent electrical resistivity in addition to the assumed $k(u)$ variation; this may be accomplished by simply replacing f by the desired $f(\varepsilon)$ in Eq. (6-32a).

Performing the indicated integration in Eq. (6-32a) yields the dimensionless temperature distribution in the following form

$$\theta(u) = \frac{f \left[(u-1) + \frac{\alpha'+1}{\gamma_k'} \ln(1 - \gamma_k' u) - \frac{(\alpha' u+1)}{\gamma_k'} \ln(1 - \gamma_k') \right] + (Q_1^* - \alpha) \ln\left(\frac{1 - \gamma_k' u}{1 - \gamma_k'}\right)}{\gamma_k' \left[1 - \frac{\alpha}{\gamma_k'} \ln(1 - \gamma_k') \right]} \quad (6-32b)$$

where

$$\alpha' = \frac{\alpha}{1 + \frac{\gamma_k'}{2}}$$

4#. Optimized No-Load Temperature Difference for $k(u) = \bar{k} \left[1 + \gamma_k \left(\frac{1}{2} - u \right) \right]$

In this section the no-load temperature difference, as previously

defined, is examined. Letting $Q_1^* = 0$ and $u = 0$ in Eq. (6-32b) and applying the definition of θ_{NL} gives

$$\theta_{NL} = \frac{\alpha \ln(1 - \gamma'_k) - \frac{\alpha^2}{2 T_h} \left[1 + \frac{\ln(1 - \gamma'_k)}{\gamma'_k} \right]}{\gamma_k \left[\frac{\alpha}{\gamma_k} \ln(1 - \gamma'_k) - 1 \right]} \quad (6-33a)$$

The optimum value of θ_{NL} occurs if

$$\frac{\partial \theta_{NL}}{\partial \alpha} = 0 \quad (6-33b)$$

The dimensionless current which yields the optimum value of θ_{NL} is

$$(\alpha)_{opt} = \frac{\gamma_k}{\ln \left(\frac{2 - \gamma_k}{2 + \gamma_k} \right)} \left[1 - \sqrt{1 - \frac{\bar{z} T_h \ln^2 \left(\frac{2 - \gamma_k}{2 + \gamma_k} \right)}{\gamma_k + \left(1 + \frac{\gamma_k}{2} \right) \ln \left(\frac{2 - \gamma_k}{2 + \gamma_k} \right)}} \right] \quad (6-34)$$

where

$$\frac{2 - \gamma_k}{2 + \gamma_k} = (1 - \gamma'_k)$$

Substitution of Eq. (6-34) into Eq. (6-33a) gives the optimum value of θ_{NL} (after considerable algebra) as,

$$(\theta_{NL})_{opt} = - \frac{\left\{ \sqrt{1 - \varphi_k} - 1 \right\}^2}{\varphi_k} \quad (6-35)$$

where

$$\varphi_k = \frac{\bar{k} T_h \ln^2 \left(\frac{2 - \gamma_k}{2 + \gamma_k} \right)}{\gamma_k + \left(1 + \frac{\gamma_k}{2} \right) \ln \left(\frac{2 - \gamma_k}{2 + \gamma_k} \right)}$$

In order to determine the effect of the assumed spatially dependent $k(u)$ on $(\theta_{NL})_{opt}$, it is expedient to compare $(\theta_{NL})_{opt}$ as given by Eq. (6-35) with $(\theta_{NL})_{max}$ for constant properties; this latter expression is given by Eq. (6-15).

Fig. 27 illustrates the effect of a spatially dependent thermal conductivity on $(\theta_{NL})_{opt}$. Before discussing Fig. 27, it is very important to consider two facts. First, the region of practical variation in $k(u)$ is approximately confined to $\gamma_k < 1$; the same as for γ_ρ . Based on Eq. (6-29), variations of γ_k much greater than one (1) are not presently feasible. However the region $\gamma_k > 1$ is included for present interest and possible future use. Second, one must recall (see Fig. 22) that spatial variations in thermal conductivity are not as great as the spatial variations in the Seebeck coefficient and the electrical resistivity for a given change in carrier concentration. Therefore in Fig. 27, one must not compare the variations in $(\theta_{NL})_{opt}$ at a specific value of the abscissa, say $\gamma_k = \gamma_\rho$, because for a given change in carrier concentration γ_k will be less than γ_ρ ; the degree of discrepancy would have to be calculated for a specific case. In the region ($\gamma_k < 1$), Fig. 27 shows that the assumed variation in $k(u)$ decreases $(\theta_{NL})_{opt}$.

4b. Optimized Heat Pumped for $k(u) = \bar{k} \left[1 + \gamma_k \left(\frac{1}{2} - u \right) \right]$

In this section the effect of a spatially dependent resistivity

on the optimum amount of heat that a thermoelement can pump across a specified temperature difference is determined. The energy balance at the cold junction as given by Eq. (6-31a) can be obtained readily by letting $u = 0$ in Eq. (6-32b) and solving for Q_i^* . Thus, the dimensionless heat pumped at the cold junction is given by

$$Q_i^* = \alpha \left[\theta_c + 1 \right] - \frac{\gamma_k \theta_c}{\ln \left(\frac{2 - \gamma_k}{2 + \gamma_k} \right)}$$

$$= \frac{\alpha^2 \left[1 + \left(\frac{2 + \gamma_k}{2 \gamma_k} \right) \ln \left(\frac{2 - \gamma_k}{2 + \gamma_k} \right) \right]}{\bar{z} T_h \ln \left(\frac{2 - \gamma_k}{2 + \gamma_k} \right)} \quad (6-36)$$

The optimum value of Q_i^* occurs if

$$\frac{\partial Q_i^*}{\partial \alpha} = 0 \quad (6-37)$$

The current which yields the optimum value of Q_i^* is

$$(\alpha)_{\text{opt}} = \frac{\bar{z} T_h (\theta_c + 1) \ln \left(\frac{2 - \gamma_k}{2 + \gamma_k} \right)}{2 \left[1 + \left(\frac{2 + \gamma_k}{2 \gamma_k} \right) \ln \left(\frac{2 - \gamma_k}{2 + \gamma_k} \right) \right]} \quad (6-38)$$

Substitution of Eq. (6-38) into Eq. (6-36) gives the optimum value of

$(Q_i^*)_{\text{opt}}$ as

$$(Q_i^*)_{\text{opt}} = \frac{\bar{z} T_h (\theta_c + 1)^2 \ln \left(\frac{2 - \gamma_k}{2 + \gamma_k} \right)}{4 \left[1 + \left(\frac{2 + \gamma_k}{2 \gamma_k} \right) \ln \left(\frac{2 - \gamma_k}{2 + \gamma_k} \right) \right]} - \frac{\gamma_k \theta_c}{\ln \left(\frac{2 - \gamma_k}{2 + \gamma_k} \right)} \quad (6-39a)$$

By arranging Eq. (6-39a) in another form the effect of γ_k on Q_i^* may be estimated. Thus, one may write

$$(Q_i^*)_{\text{opt}} = \epsilon_k \left[\frac{\bar{z} T_h (\theta_c + 1)^2}{2} - \frac{\gamma_k \theta_c}{\epsilon_k \ln \left(\frac{2 - \gamma_k}{2 + \gamma_k} \right)} \right] \quad (6-39b)$$

where

$$\epsilon_k = \frac{\ln \left(\frac{2 - \gamma_k}{2 + \gamma_k} \right)}{2 \left[1 + \left(\frac{2 + \gamma_k}{2 \gamma_k} \right) \ln \left(\frac{2 - \gamma_k}{2 + \gamma_k} \right) \right]}$$

For very small variations in γ_k , say as $\gamma_k \rightarrow 0$, it may be shown that $\epsilon_k \rightarrow +1.0$ from below. In addition $\gamma_k / \ln \left(\frac{2 - \gamma_k}{2 + \gamma_k} \right) \rightarrow -1.0$. Hence when γ_k is very small Eq. (6-39b) is multiplied by a quantity (ϵ_k) which is less than one (1). Therefore for small γ_k (near zero) it is reasonable to assume that the heat pumping capacity is reduced. Fig. 28 shows quantitatively the variations in $(Q_i^*)_{\text{opt}}$ and Q_i^* that may be expected for various γ_k ; in addition Fig. 28 substantiates the mathematical analysis above and illustrates the expected decrease in $(Q_i^*)_{\text{opt}}$ for various γ_k values. Thus it has been shown mathematically and illustrated graphically that the assumed redistribution of the thermal conductivity acts to

decrease the optimum heat pumped and the heat pumped for the condition of $(C.O.P.)_{opt}$ (dotted curve labeled $k(u)$).

4c. Optimized C.O.P. for $k(u) = \bar{k} \left[1 + \gamma_k \left(\frac{1}{2} - u \right) \right]$

This section is concerned with determining the effect of a spatially dependent conductivity on the optimum coefficient of performance. Using a development almost identical to that in the variable resistivity section, the C.O.P. may be written as

$$C.O.P. = \frac{\alpha(\theta_c + 1) - \frac{\gamma_k \theta_c}{\ln\left(\frac{2 - \gamma_k}{2 + \gamma_k}\right)} - \frac{\alpha^2}{2 \bar{z} T_h \epsilon_k}}{\frac{\alpha^2}{2 T_h} - \alpha \theta_c} \quad (6-40)$$

The optimum value of the C.O.P. occurs if

$$\frac{\partial}{\partial \alpha} (C.O.P.) = 0 \quad (6-41)$$

The current which yields the optimum value of the C.O.P. is given by

$$(\alpha)_{opt} = -\beta_k \theta_c \left[1 + \sqrt{1 + \frac{\bar{z} T_h}{\beta_k}} \right] \quad (6-42)$$

where

$$\beta_k = \frac{\gamma_k}{\left[\frac{\theta_c}{2 \epsilon_k} - \theta_c - 1 \right] \ln\left(\frac{2 - \gamma_k}{2 + \gamma_k}\right)}$$

Substitution of Eq. (6-42) into Eq. (6-40) gives the optimum value of (C.O.P.)_{opt} as

$$(C.O.P.)_{opt} = -\frac{1}{2\varepsilon_k} \frac{\left\{ 1 + \frac{2\bar{\varepsilon} T_h \varepsilon_k (\theta_c + 1)}{\beta_k \theta_c \left[1 + \sqrt{1 + \frac{\bar{\varepsilon} T_h}{\beta_k}} \right]} \right\}}{\left\{ 1 + \frac{\bar{\varepsilon} T_h}{\beta_k \left[1 + \sqrt{1 + \frac{\bar{\varepsilon} T_h}{\beta_k}} \right]} \right\}} \quad (6-43)$$

Fig. 29 illustrates the effect of a spatially dependent thermal conductivity on the optimum C.O.P. and on the C.O.P. for optimum heat pumping. This figure shows that the general effect of the assumed variation in $k(u)$ is to decrease (C.O.P.)_{opt} until approximately $\gamma_k = 0.6$. For $\gamma_k > 0.6$ there is a slight increase in (C.O.P.)_{opt} in the range of γ_k that is of practical interest; that is, $\gamma_k < 1$. Notice also that if the thermoelement is operated at the condition of optimum heat pumping (dotted curve labeled $k(u)$) the C.O.P. is virtually independent of the variation in γ_k for $\gamma_k < 1$; this same result was obtained for $\rho(u)$.

5. Effect of Spatially Dependent $S(x)$ on the Performance Criteria: ρ and k constant

In this section the effect of a linear variation in $S(x)$ on the no-load temperature difference, the heat pumped, and the C.O.P. is determined with ρ and k constant. The Seebeck coefficient, $S(x)$ is assumed to vary linearly in such a manner that the average Seebeck coefficient remains the same. Essentially this section illustrates the effect of

redistributing the Seebeck coefficient. Using the above $S(x)$ assumption,

$$S(x) = \bar{S} + \frac{\Delta S}{L} \left(x - \frac{L}{2} \right) \quad (6-44)$$

Graphically Eq. (6-44) appears as shown in Fig. 26.

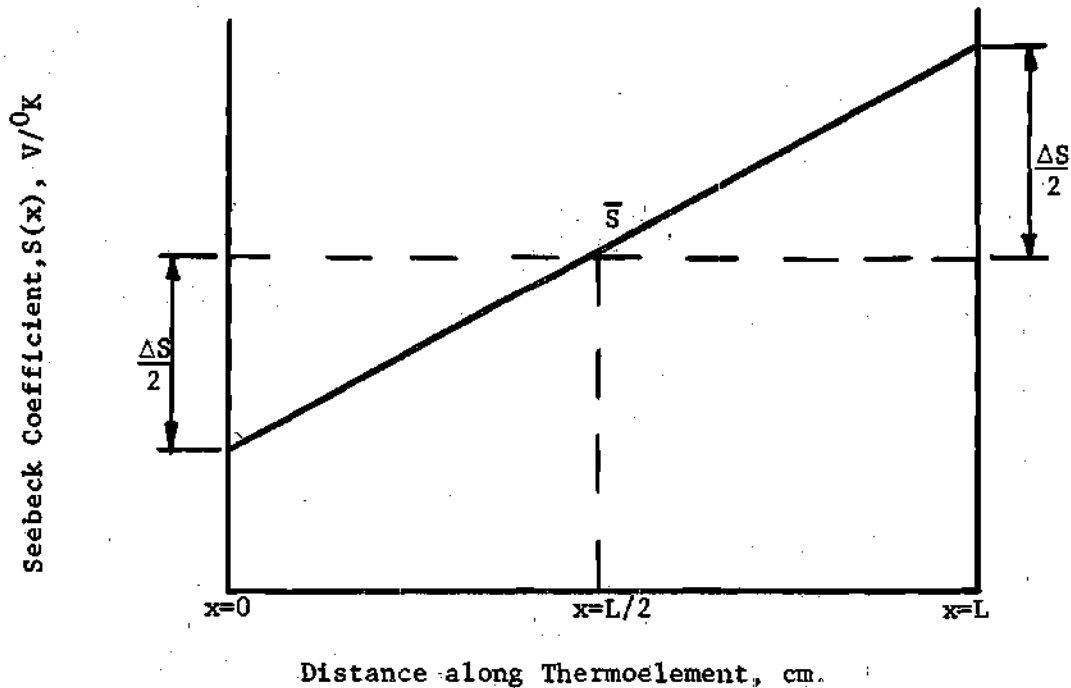


Fig. 26. Assumed Spatial Dependence of $S(x)$.

The physical model to be studied in this section is shown in Fig. 23. The differential equation describing this system subject to the assumptions of this section is obtained by reduction of Eq. (6-1) and is

$$\frac{d^2 T}{dx^2} - \frac{I}{kA} \left(\frac{dS}{dx} \right) T = - \frac{I^2 \rho}{kA^2} \quad (6-45)$$

Equation (6-45) is subject to the boundary conditions

$$Q_i = I S(o) T_c - \bar{k} A \left. \frac{dT}{dx} \right|_{x=0} \quad (6-46a)$$

and

$$T(L) = T_h \quad (6-46b)$$

When most of the dimensionless definitions introduced in section 3 are applied to the above equations, Eq. (6-44) becomes

$$S(u) = \bar{S} \left[1 + \gamma_S \left(u - \frac{1}{2} \right) \right] \quad (6-47)$$

where

$$\gamma_S = \Delta S / \bar{S}$$

Eq. (6-45) becomes

$$\frac{d^2\theta}{du^2} - \lambda^2 \theta = -f \quad (6-48)$$

where

$$f = \frac{\lambda^4}{\bar{S} T_h \gamma_S^2} - \lambda^2$$

Eq. (6-46) becomes

$$Q_i^* = \frac{\lambda^2}{\gamma_S} (\theta_c + 1) - \left. \frac{d\theta}{du} \right|_{u=0} \quad (6-49a)$$

$$\theta(1) = 0 \quad (6-49b)$$

The additional dimensionless quantities λ and γ'_S have been introduced because they help to simplify some of the following equations; they are defined as

$$\lambda \equiv \sqrt{\alpha \gamma_S} \quad (6-50a)$$

$$\gamma'_S \equiv \gamma_S / \left(1 - \frac{\gamma_S}{2}\right) \quad (6-50b)$$

A good reason for the assumed spatial dependence of $S(u)$ becomes apparent by examination of the forcing function f in Eq. (6-48). With the variation assumed the effect of the Joule heating $\lambda^4/\bar{\epsilon} T_h \gamma_S^2$ is opposed by the contribution of the linear variation in $S(u)$ represented by λ^2 . Obviously a linear variation of $S(u)$ with a negative slope in Fig. 26 would be undesirable.

Using the Green's function, the dimensionless temperature distribution $\theta(u)$, may be expressed as,

$$\theta(u) = \int_0^1 G(u, \epsilon) f \, d\epsilon + \frac{\left(Q_1^* - \frac{\lambda^2}{\gamma_S}\right) \left[\tanh(\lambda) \cosh(\lambda u) - \sinh(\lambda u)\right]}{\lambda \left[1 + \frac{\lambda}{\gamma'_S} \tanh(\lambda)\right]} \quad (6-51a)$$

where

$$G(u, \epsilon) = \begin{cases} \frac{\left[\tanh(\lambda) \cosh(\lambda \epsilon) - \sinh(\lambda \epsilon) \right] \left[\frac{\lambda}{\gamma_S} \sinh(\lambda u) + \cosh(\lambda u) \right]}{\lambda \left[1 + \frac{\lambda}{\gamma_S} \tanh(\lambda) \right]} & 0 \leq u < \epsilon \\ \frac{\left[\tanh(\lambda) \cosh(\lambda u) - \sinh(\lambda u) \right] \left[\frac{\lambda}{\gamma_S} \sinh(\lambda \epsilon) + \cosh(\lambda \epsilon) \right]}{\lambda \left[1 + \frac{\lambda}{\gamma_S} \tanh(\lambda) \right]} & \epsilon < u \leq 1 \end{cases}$$

It is interesting to note that Eq. (6-51a) can also represent the solution for the temperature distribution in a thermoelement with a spatially dependent electrical resistivity in addition to the assumed $S(u)$ variation.

Performing the indicated integration in Eq. (6-51a), the dimensionless temperature distribution is

$$\theta(u) =$$

$$\frac{f \left[\left(1 - \frac{\cosh(\lambda u)}{\cosh(\lambda)} \right) \left(\frac{1}{\lambda} \right) + \frac{1}{\gamma_S \cosh(\lambda)} \left\{ \left(1 - \cosh(\lambda u) \right) \sinh(\lambda) - \left[1 - \cosh(\lambda) \right] \sinh(\lambda u) \right\} \right]}{\lambda \left[1 + \frac{\lambda}{\gamma_S} \tanh(\lambda) \right]} + \frac{\left(Q_i^* - \frac{\lambda^2}{\gamma_S} \right) \left[\tanh(\lambda) \cosh(\lambda u) - \sinh(\lambda u) \right]}{\lambda \left[1 + \frac{\lambda}{\gamma_S} \tanh(\lambda) \right]} \quad (6-51b)$$

5a. Optimized No-Load Temperature Difference for $S(u) = \bar{S} \left[1 + \gamma_S \left(u - \frac{1}{2} \right) \right]$

In this section, the no-load temperature difference, as previously defined, is examined. Letting $Q_1^* = 0$ and $u = 0$ in Eq. (6-51b) and applying the definition of θ_{NL} gives

$$\theta_{NL} = \frac{\left(\frac{\lambda^2}{\bar{z} T_h \gamma_S^2} - 1 \right) \left(\operatorname{sech}(\lambda) - 1 \right) + \lambda \left(\frac{1}{\gamma_S} - \frac{1}{2} \right) \tanh(\lambda)}{1 + \lambda \left(\frac{1}{\gamma_S} - \frac{1}{2} \right) \tanh(\lambda)} \quad (6-52)$$

The optimum value of θ_{NL} occurs if

$$\frac{\partial \theta_{NL}}{\partial \lambda} = 0 \quad (6-53)$$

A transcendental equation results when one attempts to satisfy Eq. (6-53). Of course, this transcendental equation can not be solved explicitly for λ_{opt} ; therefore, it is necessary to employ a numerical technique to determine λ_{opt} . The mechanics of the numerical technique used are explained in Appendix E. It should be added that this optimizing procedure was checked by recalculating the optimum values in sections 3a. through 3c which had already been determined in closed form; the results agreed to five decimal places.

For various values of γ_S , Eq. (6-52) was optimized with respect to the dimensionless current λ . The results are given in Fig. 27. This figure represents the effect of a spatially dependent Seebeck coefficient on $(\theta_{NL})_{opt}$. Fig. 27 shows that the assumed variation $S(u)$, acts to increase $(\theta_{NL})_{opt}$ in the γ_S region of practical interest ($\gamma_S < 1$). Thus,

a predetermined redistribution of electrical resistivity -- even though small -- effects an increase in the optimum no-load temperature difference.

$$5b. \text{ Optimized Heat Pumped for } S(u) = \bar{S} \left[1 + \gamma_S \left(u - \frac{1}{2} \right) \right]$$

The purpose of this section is to ascertain the effect of a spatially dependent Seebeck coefficient on the optimum amount of heat that a thermoelement can pump across a specified temperature difference. The energy balance at the cold junction as given by Eq. (6-49a) can be obtained readily by letting $u = 0$ in Eq. (6-51b) and solving for Q_1^* . Thus, the dimensionless heat pumped at the cold junction is given by

$$Q_1^* = \lambda \left[\frac{\lambda}{2\gamma_S} (2 - \gamma_S) (\theta_c + 1) + \frac{\theta_c}{\tanh(\lambda)} + \left(1 - \frac{\lambda^2}{2 T_h \gamma_S^2} \right) \tanh\left(\frac{\lambda}{2}\right) \right] \quad (6-54)$$

The optimum value of Q_1^* occurs for the value of λ which satisfies

$$\frac{\partial Q_1^*}{\partial \lambda} = 0 \quad (6-55)$$

As in the previous section, a transcendental equation results when one attempts to satisfy Eq. (6-55). However, Eq. (6-54) may be optimized by employing the numerical technique discussed in Appendix E.

Equation (6-54) was optimized with respect to the dimensionless current λ using γ_S as the argument. The results of this optimization are illustrated in Fig. 28. This figure shows quantitatively the variations in $(Q_1^*)_{\text{opt}}$ and Q_1^* (the heat pumped for the condition of

optimum C.O.P.) that may be expected for various γ_S values. In the range of practical interest ($\gamma_S < 1$), Fig. 28 indicates that $(Q_1^*)_{\text{opt}}$ and Q_1^* may both be increased.

5c. Optimized C.O.P. for $S(u) = \bar{S} \left[1 + \gamma_S \left(u - \frac{1}{2} \right) \right]$

This section is concerned with determining the effect of a spatially dependent Seebeck coefficient on the optimum C.O.P. Employing the definition of C.O.P. given previously one may write

$$\text{C.O.P.} = \frac{Q_1^*}{P_1^*} \quad (6-56)$$

where Q_1^* is given by Eq. (6-54). The dimensionless electrical power input P_1^* is defined as

$$P_1^* = \frac{\lambda^4}{\bar{z} T_h \gamma_S^2} - \frac{\lambda^2 \theta_c}{\gamma_S} \int_0^1 \left[1 + \gamma_S \left(u - \frac{1}{2} \right) \right] du \quad (6-57)$$

By definition the value of the integral is one (1). Substitute Eqs. (6-54) and (6-57) into Eq. (6-56) to obtain a more explicit form.

$$\text{C.O.P.} = \frac{\frac{\lambda}{2\gamma_S} \left(\theta_c + 1 \right) \left(2 - \gamma_S \right) + \frac{\theta_c}{\tanh(\lambda)} + \left(1 - \frac{\lambda^2}{\bar{z} T_h \gamma_S^2} \right) \tanh\left(\frac{\lambda}{2}\right)}{\lambda \left[\frac{\lambda^2}{\bar{z} T_h \gamma_S^2} - \frac{\theta_c}{\gamma_S} \right]} \quad (6-58)$$

Next it is desired to optimize Eq. (6-58) with respect to λ . The value of λ which optimizes this equation must satisfy

$$\frac{\partial(\text{C.O.P.})}{\partial\lambda} = 0 \quad (6-59)$$

Again a transcendental equation results when one attempts to satisfy Eq. (6-59). Therefore the numerical technique discussed in Appendix E was employed to optimize the C.O.P. The results of this optimization are shown in Fig. 29; γ_S is used as the argument. Figure 29 shows that the effect of the assumed variation $S(u)$, is to increase $(\text{C.O.P.})_{\text{opt}}$. Notice, however, that if the thermoelement is operated at the condition of optimum heat pumping (dotted curve labeled $S(u)$), the C.O.P. is virtually independent of the variation in γ_S . This latter effect is also present for a variable electrical resistivity and is discussed later.

6a. Effect of a Simultaneous Variation of $S(x)$ and $\rho(x)$ on the

Performance Criteria: k constant

At this point a brief discussion may give the reader a clearer physical insight into the purpose of this section. In sections 1 and 4a, it was pointed out that the thermal conductivity does not change its spatial dependence in the same proportion as the Seebeck coefficient and the electrical resistivity for a given change in carrier concentration. In addition, the theory of thermoelectric device performance (as set forth in reference (3) for instance) indicates that the magnitude of the figure of merit, $Z = S^2/\rho k$, is a guide to the performance capabilities of a device. The performance increases as Z increases. The veracity of this last statement is readily checked by referring to Eq. (6-15) or Eq. (6-21). From the definition of Z , it can be seen that variations in S have a distinct effect on Z . It is shown in the section on variable electrical resistivity that small predetermined

variations in the electrical resistivity can significantly increase device performance. On the other hand, small variations in the thermal conductivity are not as important.

In view of the above discussion, the purpose of this section is to examine the performance criteria for the case of the simultaneous spatial dependence of the Seebeck coefficient and the electrical resistivity; the thermal conductivity is assumed constant. As before, both $\rho(x)$ and $S(x)$ are allowed to vary linearly such that their respective average values $\bar{\rho}$ and \bar{S} remain the same over the length of the thermoelement. The equations describing $\rho(x)$ and $S(x)$ are the same as before and are given by Eq. (6-3) and Eq. (6-44) respectively.

The physical model to be studied in this section is shown in Fig. 23. The differential equation describing this system is obtained by reduction of Eq. (6-1) and is

$$\frac{d^2 T}{dx^2} - \frac{I}{kA} \left(\frac{dS}{dx} \right) T = - \frac{I^2 \rho(x)}{k A^2} \quad (6-60)$$

Equation (6-60) is subject to the boundary conditions

$$Q_i = IS(o)T_c - k A \left. \frac{dT}{dx} \right|_{x=0} \quad (6-61a)$$

$$T(L) = T_h \quad (6-61b)$$

Utilizing the dimensionless quantities, Eq. (6-60) can be expressed as

$$\frac{d^2 \theta}{du^2} - \chi^2 \theta = - f(u) \quad (6-62)$$

where

$$\beta = (1 - \frac{\gamma_p}{2}) / \bar{z} T_h \gamma_S^2 \quad (6-63a)$$

and

$$f(u) = \lambda^4 \beta (1 + \gamma_p' u) - \lambda^2 \quad (6-63b)$$

In dimensionless form, the boundary conditions become

$$Q_i^* = \frac{\lambda^2}{\gamma_T} (\theta_c + 1) - \frac{d\theta}{du} \Big|_{u=0} \quad (6-64a)$$

and

$$\theta(1) = 0 \quad (6-64b)$$

One advantage of the Green's function solution is illustrated rather clearly at this time. One should notice the only difference in Eq. (6-48) and (6-62) is that Eq. (6-62) has a variable forcing function $f(u)$ because of $\rho(u)$; the boundary conditions for these two equations are the same. Hence the Green's function or the kernel $[G(u, \varepsilon)]$ is the same for both differential equations. Therefore, the dimensionless temperature distribution $\theta(u)$ for this section may be written down by inspection and is

$$\theta(u) = \int_0^1 G(u, \varepsilon) f(\varepsilon) d\varepsilon + \frac{\left(Q_i^* - \frac{\lambda^2}{\gamma_T}\right) \left[\tanh(\lambda) \cosh(\lambda u) - \sinh(\lambda u) \right]}{\lambda \left[1 + \frac{\lambda}{\gamma_T} \tanh(\lambda) \right]} \quad (6-65)$$

where

$$f(\epsilon) = f(u) \Big|_{u=\epsilon}$$

The kernel $G(u, \epsilon)$ is the same as for Eq. (6-51a). Observe that Eqs. (6-51a) and (6-65) appear almost identical; the variable forcing function $f(\epsilon)$ is the only difference; but it is an important difference. When the indicated integration is performed, Eq. (6-65) may be written as

$$\begin{aligned} \theta(u) = & (\lambda^2 \beta - 1) \left[\frac{1 + \frac{\lambda}{\gamma_S} \sinh(\lambda u) \left[1 - \frac{1}{\cosh(\lambda)} \right] - \cosh(\lambda u) \left(\frac{1}{\cosh(\lambda)} + \frac{\lambda}{\gamma_S} \tanh(\lambda) \right)}{\left[1 + \frac{\lambda}{\gamma_S} \tanh(\lambda) \right]} \right] \\ & + \lambda^2 \beta \gamma'_\rho \left[\frac{u - \frac{\cosh(\lambda u)}{\cosh(\lambda)} + \frac{\cosh(\lambda u)}{\lambda} \left(\tanh(\lambda) - \tanh(\lambda u) \right) + \frac{\lambda}{\gamma_S} \left(u \tanh(\lambda) - \frac{\sinh(\lambda u)}{\cosh(\lambda)} \right)}{\left[1 + \frac{\lambda}{\gamma_S} \tanh(\lambda) \right]} \right] \\ & + \left(Q_i^* - \frac{\lambda^2}{\gamma_S} \right) \left\{ \frac{\tanh(\lambda) \cosh(\lambda u) - \sinh(\lambda u)}{\lambda \left[1 + \frac{\lambda}{\gamma_S} \tanh(\lambda) \right]} \right\} \quad (6-66) \end{aligned}$$

6b. Optimized θ_{NL} , Q_i^* , and C.O.P. for Variable $\rho(u)$ and $S(u)$

In this section, the performance criteria, as previously defined, are examined. To determine the expression for θ_{NL} , let $Q_i^* = 0$ and $u = 0$ in Eq. (6-66) and apply the definition of θ_{NL} to obtain

$$\theta_{NL} = \frac{(1 - \lambda^2 \beta) \left\{ \frac{\cosh(\lambda) - 1}{\cosh(\lambda)} \right\} - \lambda^2 \beta \gamma_p' \left[\frac{\tanh(\lambda)}{\lambda} - \frac{1}{\cosh(\lambda)} \right] + \frac{\lambda \tanh(\lambda)}{\gamma_s'}}{1 + \frac{\lambda}{\gamma_s'} \tanh(\lambda)} \quad (6-67)$$

The heat pumped across a specified temperature difference is the next performance criterion of interest. The energy balance as given by Eq. (6-64a) can be obtained readily by letting $u=0$ in Eq. (6-66) and solving for Q_i^* . Thus, the dimensionless heat pumped at the cold junction is given by

$$Q_i^* = \frac{\lambda^2}{\gamma_s'} + \frac{\lambda \theta_c}{\tanh(\lambda)} \left[1 + \frac{\lambda}{\gamma_s'} \tanh(\lambda) \right] - \lambda (\beta \lambda - 1) \tanh\left(\frac{\lambda}{2}\right) - \frac{\lambda^2 \beta \gamma_p'}{\tanh(\lambda)} \left[\tanh(\lambda) - \frac{\lambda}{\cosh(\lambda)} \right] \quad (6-68)$$

Finally, it is desired to determine the effect of the simultaneous variation in $\rho(u)$ and $S(u)$ on the coefficient of performance. Employing the definition of C.O.P. given previously,

$$\text{C.O.P.} = \frac{Q_i^*}{P_i^*} \quad (6-69)$$

where Q_i^* is given by Eq. (6-68). For the given conditions, the dimensionless electrical power input P_i^* is defined as

$$P_i^* = \frac{\lambda^4}{z T_h \gamma_s^2} \int_0^1 \left[1 + \gamma_p' \left(u - \frac{1}{2} \right) \right] du - \frac{\lambda \theta_c}{\gamma_s} \int_0^1 \left[1 + \gamma_s' \left(u - \frac{1}{2} \right) \right] du \quad (6-70)$$

By definition, both integrals are equal to one. Substitute Eqs. (6-68) and (6-70) into Eq. (6-69) to obtain a more explicit form.

$$\text{C.O.P.} = \frac{\lambda \left[\frac{\theta_c + 1}{\gamma_s} \right] + \frac{\theta_c}{\tanh(\lambda)} - (\lambda^{2\beta} - 1) \tanh\left(\frac{\lambda}{2}\right) - \frac{\lambda^{2\beta} \gamma_d}{\tanh(\lambda)} \left[\tanh(\lambda) - \frac{\lambda}{\cosh(\lambda)} \right]}{\frac{\lambda}{\gamma_s} \left[\frac{\lambda^2}{2 T_h \gamma_s} - \theta_c \right]} \quad (6-71)$$

For any given set of conditions, in order to find the value of current λ that optimizes any given performance criterion, the first derivative of Eqs. (6-67), (6-68), and (6-71) with respect to λ can be set equal to zero. In each case a transcendental equation results. Thus it is not possible to solve for λ_{opt} explicitly. The numerical technique discussed in Appendix E is employed to optimize Eqs. (6-67), (6-68), and (6-71); during this optimization, assume that $\gamma_s = \gamma_\rho$ for the sake of simplicity. The effect of the equal simultaneous variation of $\rho(u)$ and $S(u)$ on $(\theta_{\text{NL}})_{\text{opt}}$, $(Q_i^*)_{\text{opt}}$, and $(\text{C.O.P.})_{\text{opt}}$ is shown in Figs. 27 through 29 respectively; in addition, Figs. 28 and 29 give the heat pumped at optimum C.O.P. and the C.O.P. at optimum heat pumping respectively.

Fig. 27 shows that the assumed spatial dependence of $\rho(u)$ and $S(u)$ significantly increases $(\theta_{\text{NL}})_{\text{opt}}$ even for small $\gamma_s = \gamma_\rho$ values.

Fig. 28 illustrates that the optimum heat pumped may be substantially augmented by the assumed simultaneous variation of $\rho(u)$ and $S(u)$. It also predicts an improvement in heat pumped for the condition of operation at optimum C.O.P.

Fig. 29 indicates that the assumed simultaneous variation of $\rho(u)$ and $S(u)$ substantially increases the optimum C.O.P. On the other

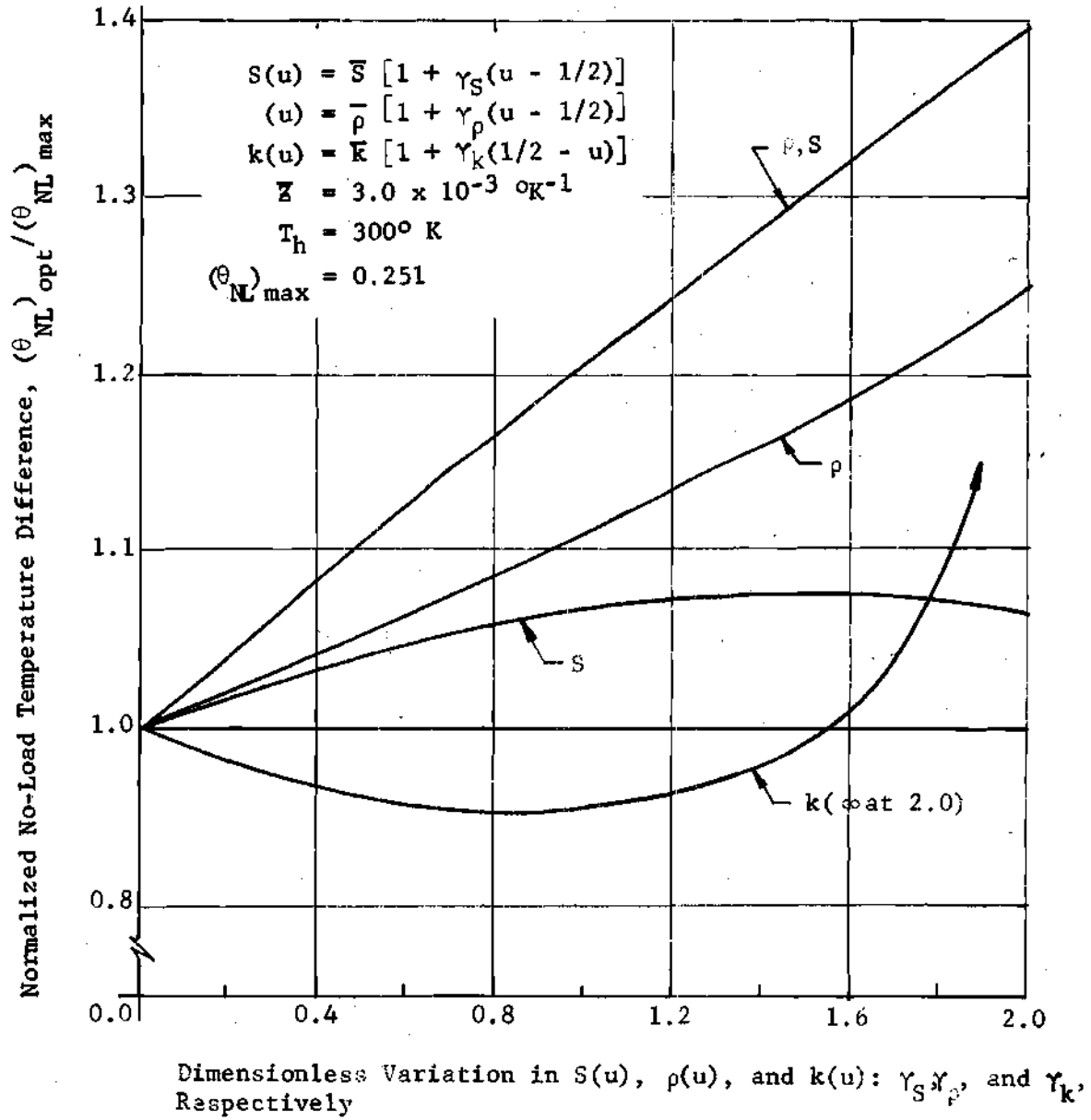


Fig. 27. Effect of the Distribution of $S(u)$, $\rho(u)$, and $k(u)$ with Position on the Optimum No-Load Temperature Difference.

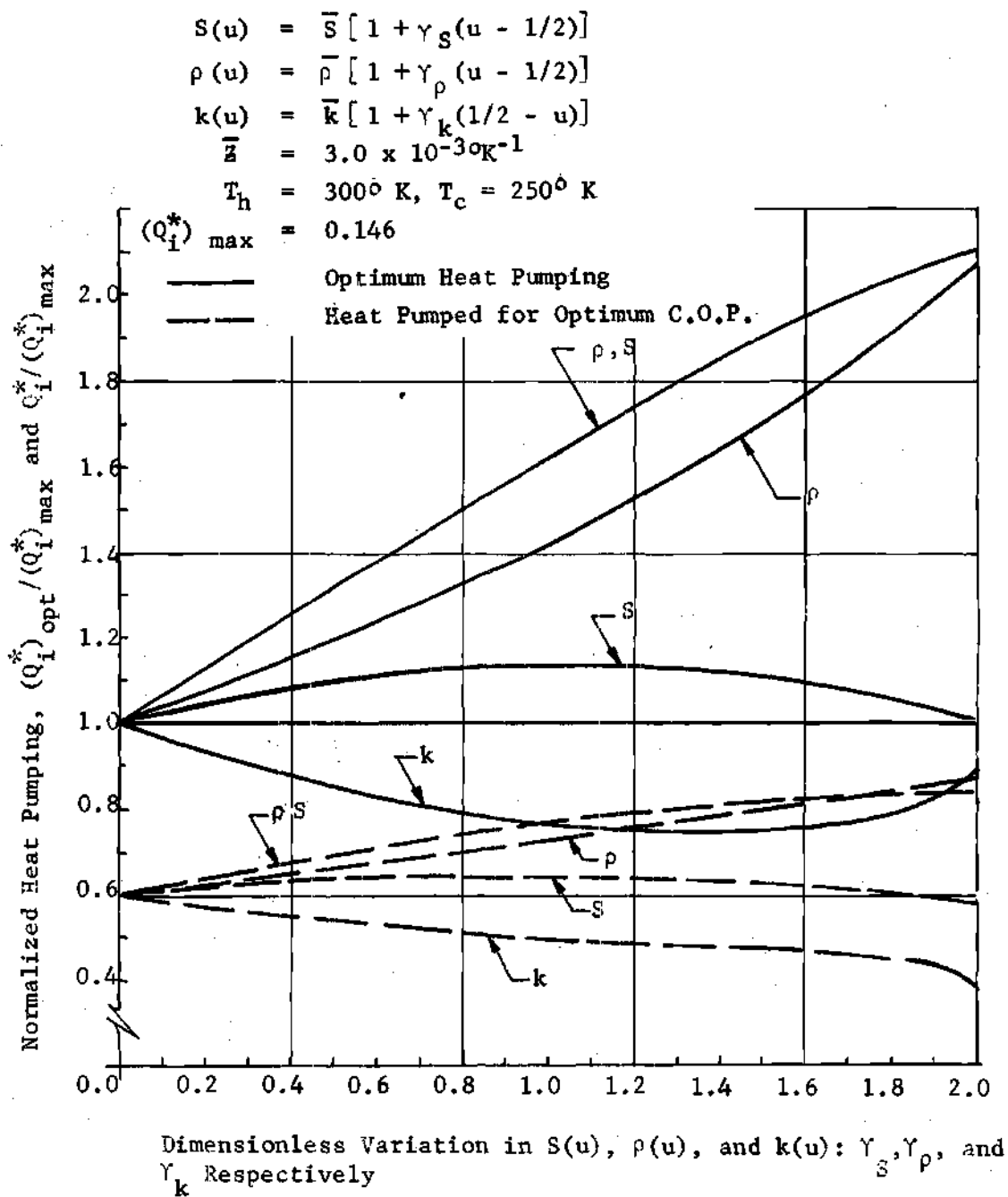


Fig. 28. Effect of the Distribution of $S(u)$, $\rho(u)$, and $k(u)$ with Position on Heat Pumping.

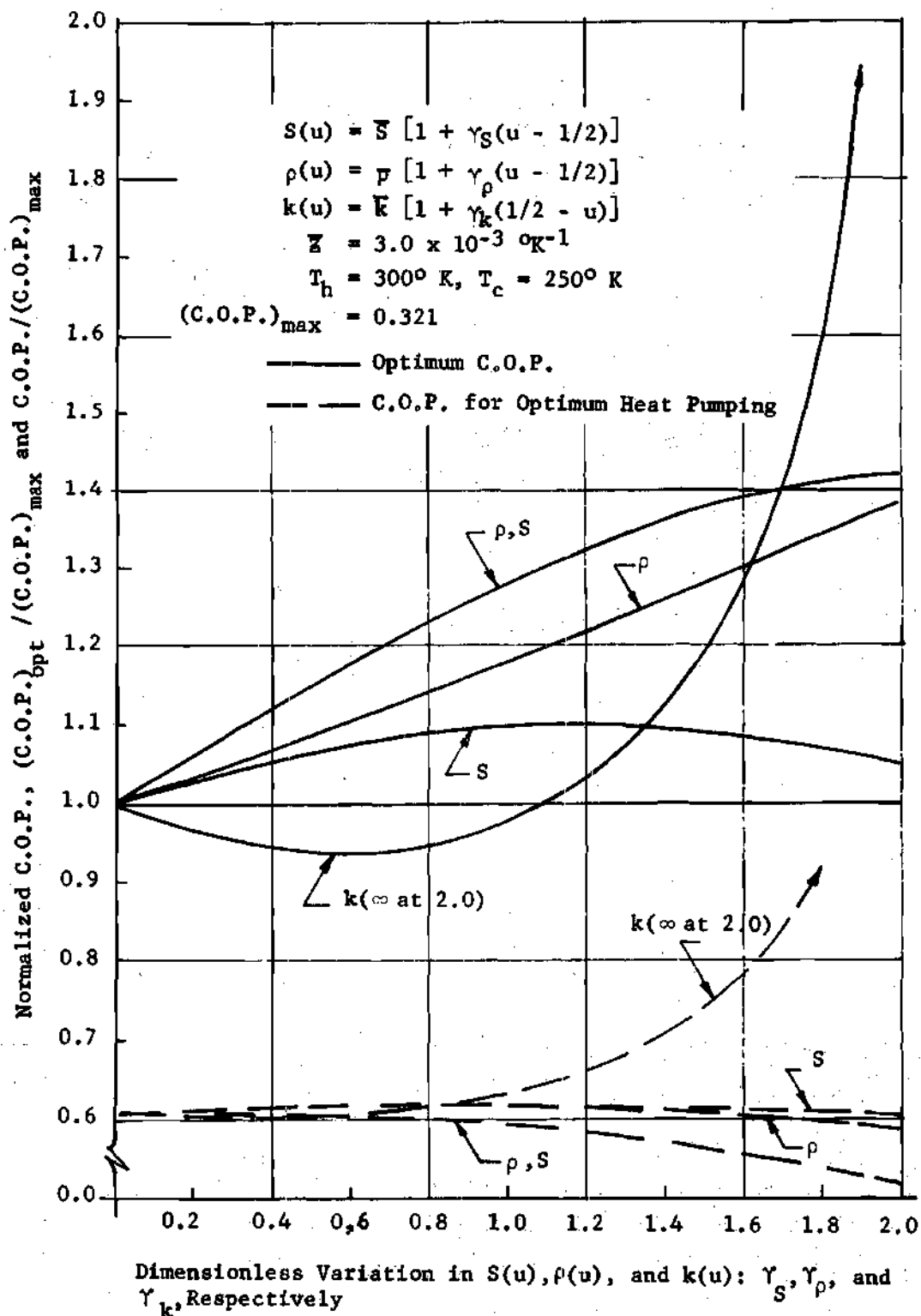


Fig. 29. Effect of the Distribution of $S(u)$, $\rho(u)$, and $k(u)$ with Position on the Coefficient of Performance.

hand, it shows the C.O.P. for the condition of optimum heat pumping is virtually independent of γ_S and γ_p in the region of practical interest ($\gamma_p, \gamma_S < 1$).

7a. Performance Criteria and the Variation of $S(x)$ and $\rho(x)$ such that Z Remains Constant

Strictly speaking, the analysis to be considered in this section is a special case of the previous section (6a), although, it is intimately related to the other sections of the chapter also. In section 6a, it is pointed out that the three performance criteria θ_{NL} , Q_i^* , and C.O.P. are all functions of Z . In fact as Z increases, it is easy to show that the values of the performance criteria become more favorable. Consider for a moment the definition of $\rho(u)$ and $S(u)$ from section 6a. Using these definitions, and assuming $\gamma_S = \gamma_p = \gamma$, Z may be written as

$$Z = \frac{\bar{S}^2 \left[1 + \gamma \left(u - \frac{1}{2} \right) \right]^2}{\bar{\rho} \bar{k} \left[1 + \gamma \left(u - \frac{1}{2} \right) \right]} = \bar{Z} \left[1 + \gamma \left(u - \frac{1}{2} \right) \right] \quad (6-72)$$

Certainly the average value of the figure of merit, Z , over the length of thermoelement is \bar{Z} . However, over approximately one-half of the thermoelement ($u > \frac{1}{2}$), the value of Z is greater than \bar{Z} . It is clear that Z is also less than \bar{Z} over approximately one-half of the thermoelement ($u < \frac{1}{2}$). But one could legitimately claim that the improvement in the three performance criteria shown thus far is due to the increase in Z over one-half of the thermoelement and not to the judicious redistribution of the thermoelectric properties; that is, one could legitimately make this claim in the absence of an analysis to the contrary.

The purpose of this section is to examine the performance criteria when the Seebeck coefficient and the electrical resistivity vary such that Z is constant; the thermal conductivity is assumed constant.

The objective of the problem at hand is to show that even if ρ and S are chosen such that Z is a constant it is still possible to augment the performance of a device. To accomplish this end, it is not necessary to use the formalism that has been used up to now. Specifically, a linear variation in a property is selected such that the integral of the variation over the length of the thermoelement is equal to the average value of the property. For the following analysis, it proves just as rigorous and easier to assume that $S(x)$ has the variation

$$S(x) = S(0) + \frac{\Delta S}{L} x \quad (6-73)$$

and $\rho(x)$ has the variation*

$$\rho(x) = \rho(0) + 2\Delta\rho\left(\frac{x}{L}\right) + \frac{\Delta\rho^2}{\rho(0)}\left(\frac{x}{L}\right)^2 \quad (6-74)$$

$S(0)$, $\rho(0)$ represent the values of the respective properties at the cold junction ($x=0$) and $S(L)$, $\rho(L)$ represent the values of the respective properties at the hot junction ($x=L$). As a first approximation it may be assumed that

$$\gamma = \frac{\Delta S}{S(0)} = \frac{\Delta\rho}{\rho(0)} \quad (6-75)$$

Inspection of Fig. 22 indicates that this is a good assumption. Employing this approximation allows Eq. (6-73) and Eq. (6-74) to be

*The author is aware that such a variation has physical significance only for small values of $\Delta\rho$; nevertheless it is extremely convenient for the present analysis.

written respectively as
$$S(u) = S(0) [1 + \gamma u] \quad (6-76)$$

$$\rho(u) = \rho(0) [1 + \gamma u]^2 \quad (6-77)$$

Now if one substitutes Eq. (6-76) and Eq. (6-77) into the definition of Z ,

$$Z = \frac{S^2(0) [1 + \gamma u]^2}{k \rho(0) [1 + \gamma u]^2} = \frac{S^2(0)}{k \rho(0)} \quad (6-78)$$

Thus for the property variations assumed in this section, the figure of merit Z , is a constant independent of u and γ .

The physical model to be studied in this section is shown in Fig. 23. The differential equation describing this system subject to the assumptions of this section is identical in form to Eq. (6-62). However, two changes must be made for Eq. (6-62) to be applicable to this section. First, eliminate the subscripts in γ_s and γ_ρ . Second, define a new forcing function as

$$f(u) = \frac{\lambda^4}{Z T_h \gamma^2} [1 + \gamma u]^2 - \lambda^2 \quad (6-79)$$

The boundary conditions for this section are exactly the same as Eqs. (6-64a) and (6-64b) if γ_s is replaced by γ in Eq. (6-64a). Thus, the differential equation and boundary conditions from section 6a. are similar to the governing differential equation and boundary conditions for this system. Again, the advantage of the Green's function solution is apparent because by inspection the dimensionless temperature distribution $\theta(u)$ for this section may be written as

$$\theta(u) = \int_0^1 G(u,\varepsilon) f(\varepsilon) d\varepsilon + \frac{\left(Q_i^* - \frac{\lambda^2}{\gamma}\right) \left[\tanh(\lambda) \cosh(\lambda u) - \sinh(\lambda u) \right]}{\lambda \left[1 + \frac{\lambda}{\gamma} \tanh(\lambda) \right]} \quad (6-80)$$

The kernel $G(u, \varepsilon)$ is the same as for Eq. (6-51a). The forcing function $f(\varepsilon) = f(u) \Big|_{u=\varepsilon}$ is given by Eq. (6-79).

7b. Optimized θ_{NL} , Q_i^* , and C.O.P. for variable $S(u)$ and $\rho(u)$ and constant Z

The performance criteria as previously defined are derived and optimized in this section. To determine the expression for θ_{NL} ; perform the indicated integration in Eq. (6-80); let $Q_i^* = u = 0$; and apply the definition of θ_{NL} to obtain,

$$\theta_{NL} = \frac{\left[1 - \cosh(\lambda) \right] \left[\frac{\lambda^2}{\gamma^2} + 2 - Z T_h \right] - \frac{2\lambda}{\gamma} \sinh(\lambda) + \frac{\lambda^2(2 + \gamma)}{\gamma}}{Z T_h \left\{ \cosh(\lambda) + \frac{\lambda}{\gamma} \sinh(\lambda) \right\}} + \frac{\tanh(\lambda)}{\gamma \left[1 + \frac{\lambda}{\gamma} \tanh(\lambda) \right]} \quad (6-81)$$

The next performance criteria to be determined is the heat pumped across a specified temperature difference. The energy balance as given by Eq. (6-64a) (with γ'_3 replaced by γ) can be readily obtained by performing the indicated integration in Eq. (6-80) and letting $u = 0$. Solving for Q_i^* , gives the dimensionless heat pumped at the cold junction as

$$Q_i^* = \lambda \left[\frac{\lambda}{\gamma} - \frac{1}{Z T_h} \left\{ \left(\frac{\lambda^2}{\gamma} + 2 - Z T_h \right) \tanh\left(\frac{\lambda}{2}\right) + \frac{2\lambda}{\gamma} - \frac{\lambda^2(2 + \gamma)}{\gamma \sinh(\lambda)} \right\} \right] + \frac{\lambda \theta_c \left[1 + \frac{\lambda}{\gamma} \tanh(\lambda) \right]}{\tanh(\lambda)} \quad (6-82)$$

Finally, it is desired to determine the effect of the assumed variation of $\rho(u)$ and $S(u)$ on the C.O.P. Utilizing the definition of C.O.P. given previously, one may write

$$\text{C.O.P.} = \frac{Q_i^*}{P_i^*} \quad (6-69)$$

where Q_i^* is given by Eq. (6-82). For the given conditions, the dimensionless electrical power input P_i^* is given by

$$P_i^* = \frac{\lambda^4}{z T_h \gamma^2} \int_0^1 (1 + \gamma u)^2 du - \frac{\lambda^2 \theta_c}{\gamma} \int_0^1 (1 + \gamma u) du \quad (6-83a)$$

When the integration is performed, one may write

$$P_i^* = \frac{\lambda^4}{z T_h \gamma^2} \left(1 + \gamma + \frac{\gamma^2}{3} \right) - \frac{\lambda^2 \theta_c}{\gamma} \left(1 + \frac{\gamma}{2} \right) \quad (6-83b)$$

A more explicit form for the C.O.P. may be obtained by substituting Eqs. (6-82) and (6-83b) into Eq. (6-69) to obtain

C.O.P. =

$$\frac{\frac{\lambda}{\gamma} - \frac{1}{z T_h} \left\{ \left(\frac{\lambda^2}{\gamma} + 2 - z T_h \right) \tanh\left(\frac{\lambda}{2}\right) + \frac{2\lambda}{\gamma} - \frac{\lambda^2(2 + \gamma)}{\gamma \sinh(\lambda)} \right\} + \frac{\theta_c \left[1 + \frac{\lambda}{\gamma} \tanh(\lambda) \right]}{\tanh(\lambda)}}{\frac{\lambda}{\gamma} \left[\frac{\lambda^2}{z T_h \gamma^2} \left(1 + \gamma + \frac{\gamma^2}{3} \right) - \theta_c \left(1 + \frac{\gamma}{2} \right) \right]} \quad (6-84)$$

The three performance criteria above may be optimized with respect to the current λ by equating the first derivative of Eqs. (6-81), (6-82), and (6-84) with respect to λ equal to zero. As in section 6b, a transcendental equation results in each case. Thus, it is not possible to solve for λ_{opt} explicitly. The numerical technique discussed in Appendix E is employed to optimize Eqs. (6-81), (6-82) and (6-84). The effect of the assumed variation of $\rho(u)$ and $S(u)$ on $(\theta_{NL})_{opt}$, $(Q_1^*)_{opt}$, and $(C.O.P.)_{opt}$ is shown in Figs. 30 through 32 respectively; in addition, Figs. 31 and 32 give the heat pumped at optimum C.O.P. and the C.O.P. at optimum heat pumping respectively.

Fig. 30 shows that the assumed spatial dependence of $\rho(u)$ and $S(u)$ significantly increases $(\theta_{NL})_{opt}$ even though the figure of merit Z remains constant.

Fig. 31 illustrates that both the optimum heat pumped and the heat pumped at optimum C.O.P. are substantially increased by the assumed spatial dependence of $\rho(u)$ and $S(u)$.

Fig. 32 indicates that the assumed variation of $\rho(u)$ and $S(u)$ augments the optimum C.O.P. In addition, it shows the C.O.P. for the condition of optimum heat pumping is virtually independent of γ . Thus Figs. (30-32) indicate that all three of the optimized performance criteria increase even though the figure of merit Z remains constant.

8. Simultaneous Variation of $S(x)$, $\rho(x)$, and $k(x)$

In this section equations describing the combined effects of the spatially dependent thermoelectric properties $\rho(x)$, $k(x)$, and $S(x)$ on the performance criteria are presented and discussed. The equations are

$$\begin{aligned}
 S(u) &= S(0) [1 + \gamma u] \\
 \rho(u) &= \rho(0) [1 + \gamma u]^2 \\
 \bar{\alpha} &= 3.0 \times 10^{-3} \text{ } ^\circ\text{K}^{-1} \\
 T_h &= 300^\circ \text{K} \\
 (\theta_{NL})_{\text{max}} &= 0.251
 \end{aligned}$$

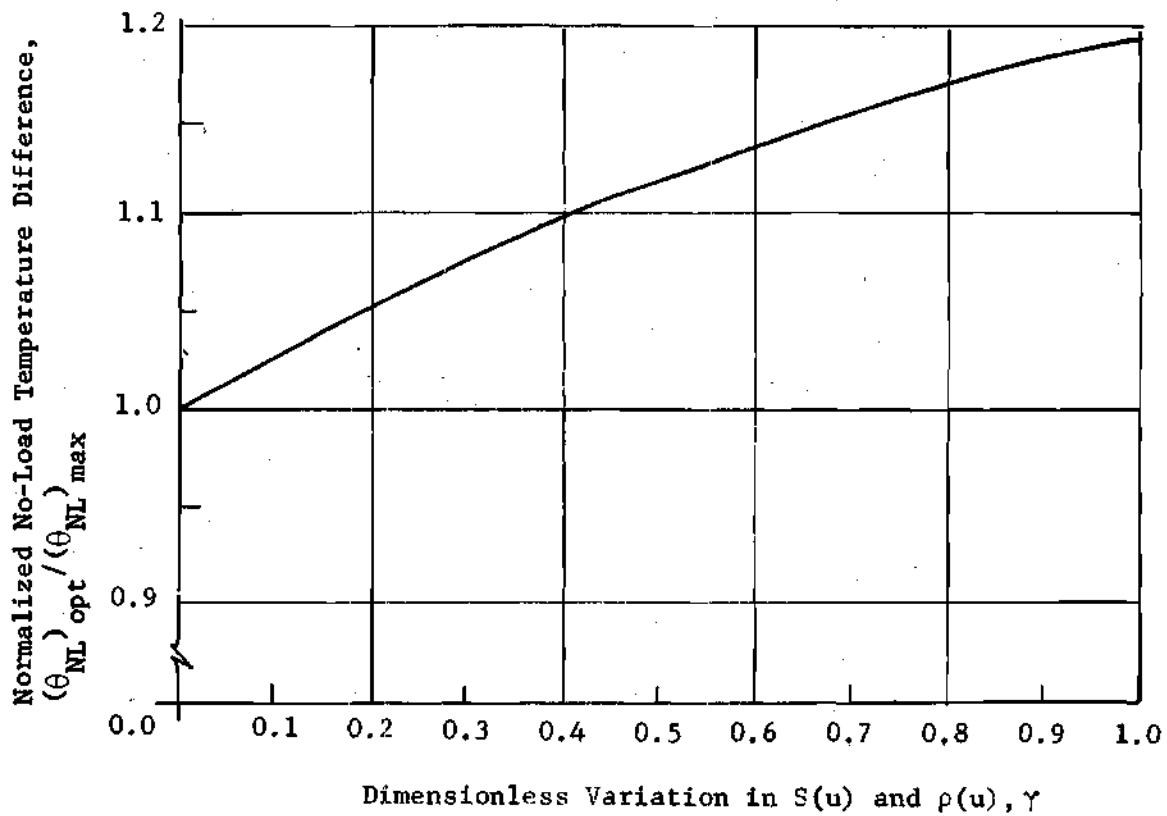


Fig. 30. Effect of the Distribution of $S(u)$, and $\rho(u)$ with Position on the Optimum No-Load Temperature Difference when $S^2(u)/\rho(u) = \text{Constant}$.

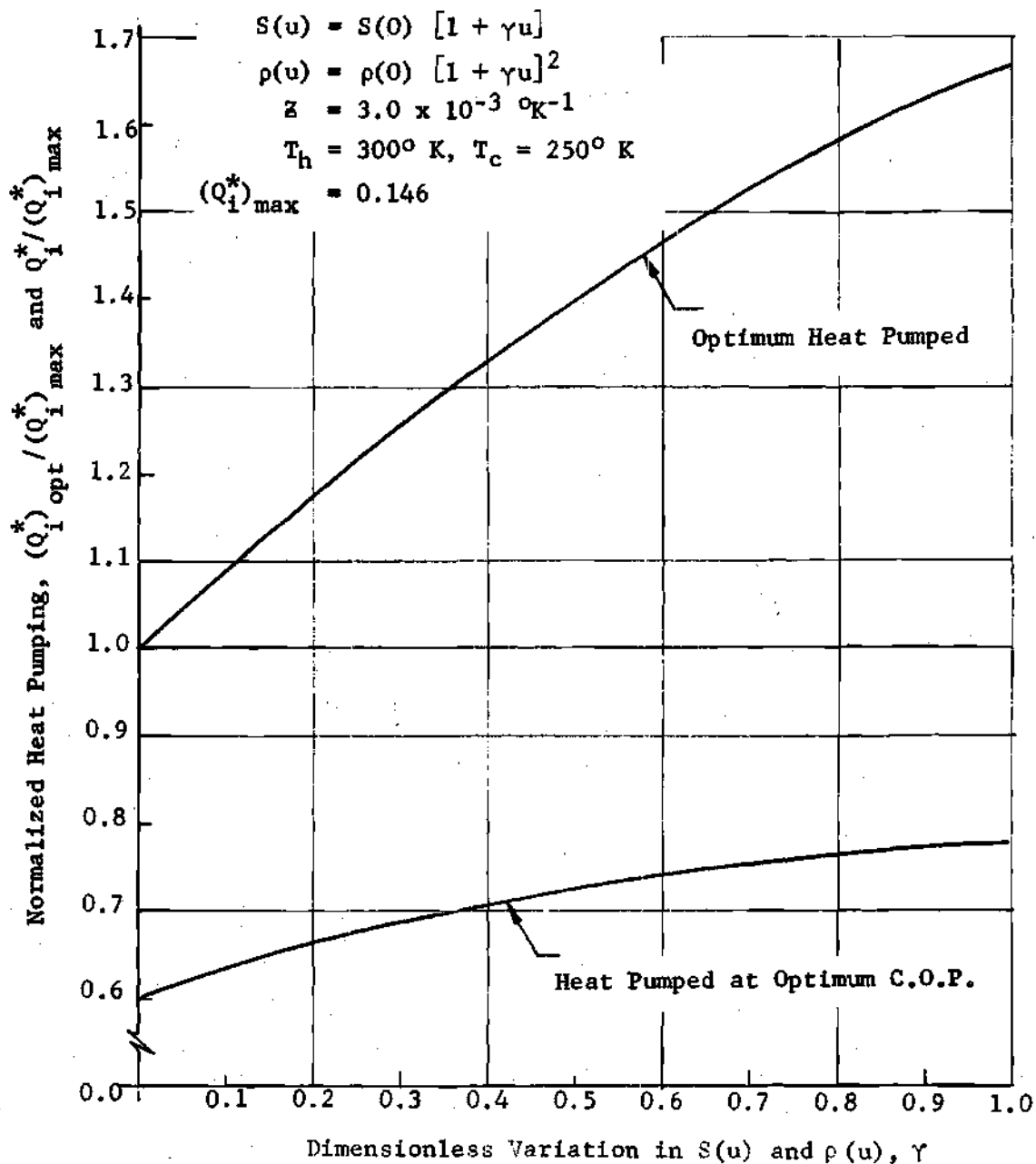


Fig. 31. Effect of the Distribution of $S(u)$ and $\rho(u)$ with Position on Heat Pumping When $S^2(u)/\rho(u) = \text{Constant}$.

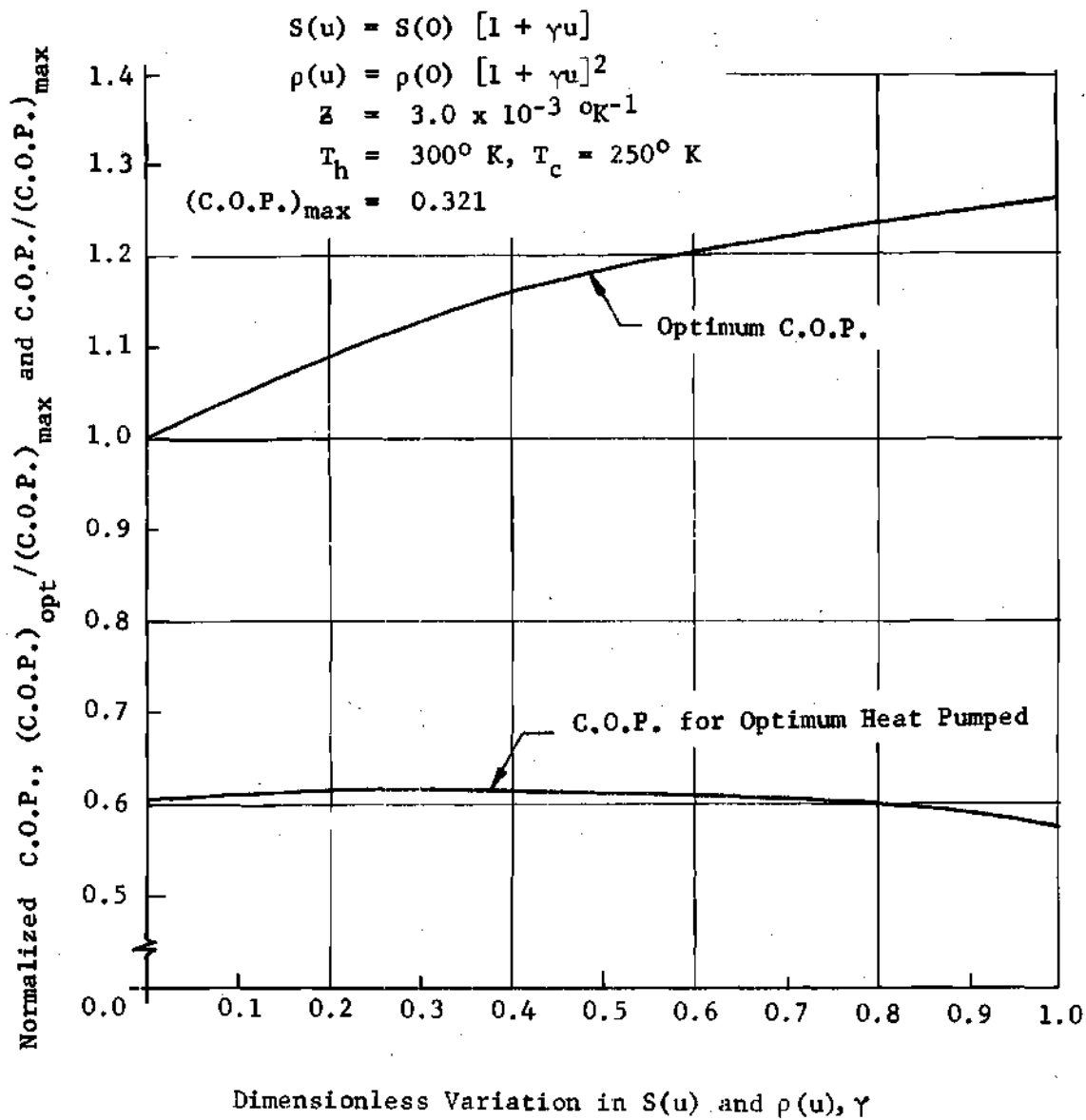


Fig. 32. Effect of the Distribution of $S(u)$ and $\rho(u)$ with Position on the Coefficient of Performance when $S^2(u)/\rho(u) = \text{Constant}$.

developed using the spatial property dependence for $\rho(x)$, $k(x)$, and $S(x)$ given by Eqs. (6-3), (6-27), and (6-44) respectively; or in dimensionless form, by Eqs. (6-6), (6-29), and (6-47) respectively. The differential equation describing the physical model (see Fig. 23) is given by Eq. (6-1) and is subject to boundary conditions (6-2a) and (6-2b). Making use of dimensionless quantities defined previously, Eq. (6-1) becomes

$$\frac{d}{du} \left[(1 - \gamma'_k u) \frac{d\theta}{du} \right] - \lambda^2 \theta = \lambda^2 - \lambda^4 \beta_1 (1 + \gamma'_\rho u) \quad (6-85)$$

where

$$\beta_1 = (1 - \frac{\gamma'_\rho}{2}) (1 + \frac{\gamma'_k}{2}) / \bar{z} T_h$$

The boundary conditions Eqs. (6-1a) and (6-1b) become

$$Q_i^* = \frac{\lambda^2}{\gamma'_s} (\theta_c + 1) - \frac{d\theta}{du} \Big|_{u=0} \quad (6-86a)$$

$$\theta(1) = 0 \quad (6-86b)$$

Equation (6-85) is solved by standard techniques rather than by use of the Green's function. The solution of Eq. (6-85) is not apparent by inspection. However, by an appropriate change of the independent variable; one may transform Eq. (6-85) to a special case of the familiar Bessel differential equation. The transformation is

$$r = \frac{2i \sqrt{\lambda^2 (1 - \gamma'_k u)}}{\gamma'_k} \quad (6-87)$$

*This transformation may be deduced from Eq. (1a) on page 440 of Reference (28).

Application of the Eq. (6-87) to Eq. (6-85) leads to the differential equation

$$\frac{d^2\theta}{dr^2} + \frac{1}{r} \frac{d\theta}{dr} + \theta = \lambda^2 \beta_1 \left[1 + \frac{\gamma_p}{\gamma_k} \right] - 1 + \frac{\beta_1 \gamma_p \gamma_k r^2}{4} \quad (6-88)$$

The homogeneous portion of Eq. (6-88) is the well-known Bessel differential equation of zero order. Since the argument is imaginary the modified Bessel functions of the first and second kind are more convenient in expressing the solution to the homogeneous portion of Eq. (6-88). Using the principle of superposition, the general solution of Eq. (6-88) is

$$\theta(r) = C_1 I_0(r) + C_2 K_0(r) + \frac{\beta_1 \gamma_p \gamma_k}{4} (r^2 - 4) + \lambda^2 \beta_1 + \frac{\lambda^2 \beta_1 \gamma_p}{\gamma_k} - 1 \quad (6-89)$$

Using the definition of r , Eq. (6-89) may be written

$$\theta(u) = C_1 I_0 \left[\frac{2\sqrt{\lambda^2(1-\gamma_k^2 u)}}{\gamma_k} \right] + C_2 K_0 \left[\frac{2\sqrt{\lambda^2(1-\gamma_k^2 u)}}{\gamma_k} \right] + \lambda^2 \beta_1 (1+\gamma_p u) - \beta_1 \gamma_p \gamma_k - 1 \quad (6-90)$$

where C_1 and C_2 are constants of integration and I_0 and K_0 are modified zero order Bessel functions of the first and second kind respectively. Solving Eq. (6-90) subject to boundary conditions (6-86a) and (6-86b) allows the constants of integration C_1 and C_2 to be determined; they are written on the following page. Equation (6-90) in conjunction with Eqs. (6-91) and (6-92) is sufficient to determine the steady-state temperature distribution in the thermoelement for any specific set of conditions.

$$c_1 = \frac{\left[1 + \beta_1 \gamma_\rho' \gamma_k' - \lambda^2 \beta_1 (1 + \gamma_\rho') \right] \left[\frac{\lambda^2}{\gamma_S'} K_0 \left(\frac{2\lambda}{\gamma_k'} \right) - \lambda K_1 \left(\frac{2\lambda}{\gamma_k'} \right) \right] - \left[Q_i^* + \lambda^2 \beta_1 \left\{ \gamma_\rho' - \frac{1}{\gamma_S'} (\lambda^2 - \gamma_\rho' \gamma_k') \right\} \right] \left[K_0 \left(\frac{2\lambda \sqrt{1 - \gamma_k'}}{\gamma_k'} \right) \right]}{\left[I_0 \left(\frac{2\lambda \sqrt{1 - \gamma_k'}}{\gamma_k'} \right) \right] \left[\frac{\lambda^2}{\gamma_S'} K_0 \left(\frac{2\lambda}{\gamma_k'} \right) - \lambda K_1 \left(\frac{2\lambda}{\gamma_k'} \right) \right] - \left[K_0 \left(\frac{2\lambda \sqrt{1 - \gamma_k'}}{\gamma_k'} \right) \right] \left[\frac{\lambda^2}{\gamma_S'} I_0 \left(\frac{2\lambda}{\gamma_k'} \right) + \lambda I_1 \left(\frac{2\lambda}{\gamma_k'} \right) \right]} \quad (6-91)$$

$$c_2 = \frac{\left[Q_i^* + \lambda^2 \beta_1 \left\{ \gamma_\rho' - \frac{1}{\gamma_S'} (\lambda^2 - \gamma_\rho' \gamma_k') \right\} \right] \left[I_0 \left(\frac{2\lambda \sqrt{1 - \gamma_k'}}{\gamma_k'} \right) \right] - \left[1 + \beta_1 \gamma_\rho' \gamma_k' - \lambda^2 \beta_1 (1 + \gamma_\rho') \right] \left[\frac{\lambda^2}{\gamma_S'} I_0 \left(\frac{2\lambda}{\gamma_k'} \right) + \lambda I_1 \left(\frac{2\lambda}{\gamma_k'} \right) \right]}{\left[I_0 \left(\frac{2\lambda \sqrt{1 - \gamma_k'}}{\gamma_k'} \right) \right] \left[\frac{\lambda^2}{\gamma_S'} K_0 \left(\frac{2\lambda}{\gamma_k'} \right) - \lambda K_1 \left(\frac{2\lambda}{\gamma_k'} \right) \right] - \left[K_0 \left(\frac{2\lambda \sqrt{1 - \gamma_k'}}{\gamma_k'} \right) \right] \left[\frac{\lambda^2}{\gamma_S'} I_0 \left(\frac{2\lambda}{\gamma_k'} \right) + \lambda I_1 \left(\frac{2\lambda}{\gamma_k'} \right) \right]} \quad (6-92)$$

8a. Performance Criteria for variable $\beta(u)$, $k(u)$, and $S(u)$

The no-load temperature difference, the heat pumped, and the coefficient of performance are the performance criteria to be examined. Letting $u = 0 = Q_1^*$ in Eq. (6-90), and applying the definition of θ_{NL} gives the no-load temperature difference as

$$\theta_{NL} = 1 + \beta_1(\gamma_p' \gamma_k' - \lambda^2) - C_1' I_0 \left(\frac{2\lambda}{\gamma_k'} \right) - C_2' K_0 \left(\frac{2\lambda}{\gamma_k'} \right) \quad (6-93)$$

The quantities C_1' and C_2' are given by Eqs. (6-94) and (6-95); notice that these quantities simply represent C_1 and C_2 evaluated for $Q_1^* = 0$ respectively.

$$C_1' = C_1 \Big|_{Q_1^*=0} \quad (6-94)$$

$$C_2' = C_2 \Big|_{Q_1^*=0} \quad (6-95)$$

The rate of heat pumped from the cold environment, Q_1^* (dimensionless) can be determined by evaluating Eq. (6-86a). Using Eqs. (6-90), (6-91), (6-92), (6-94), and (6-95), the following expression for Q_1^* can be found

$$Q_1^* = \frac{\psi \left[\theta_c + 1 + \beta_1 \gamma_p' \gamma_k' - \lambda^2 \beta_1 - C_1' I_0 \left(\frac{2\lambda}{\gamma_k'} \right) - C_2' K_0 \left(\frac{2\lambda}{\gamma_k'} \right) \right]}{I_0 \left(\frac{2\lambda \sqrt{1 - \gamma_k'}}{\gamma_k'} \right) K_0 \left(\frac{2\lambda}{\gamma_k'} \right) - K_0 \left(\frac{2\lambda \sqrt{1 - \gamma_k'}}{\gamma_k'} \right) I_0 \left(\frac{2\lambda}{\gamma_k'} \right)} \quad (6-96)$$

where

$$\psi = I_0 \left(\frac{2\lambda \sqrt{1 - \gamma_k^2}}{\gamma_k^2} \right) \left[\frac{\lambda^2}{\gamma_s^2} K_0 \left(\frac{2\lambda}{\gamma_k} \right) - \lambda K_1 \left(\frac{2\lambda}{\gamma_k} \right) \right] \\ - K_0 \left(\frac{2\lambda \sqrt{1 - \gamma_k^2}}{\gamma_k^2} \right) \left[\frac{\lambda^2}{\gamma_s^2} I_0 \left(\frac{2\lambda}{\gamma_k} \right) + \lambda I_1 \left(\frac{2\lambda}{\gamma_k} \right) \right]$$

As in previous sections the C.O.P. in dimensionless form is given by

$$\text{C.O.P.} = \frac{Q_i^*}{P_i^*} \quad (6-97)$$

In this section, the dimensionless power input P_i^* , is given by

$$P_i^* = \frac{\lambda^2}{\gamma_s} \left(1 + \frac{\gamma_k}{2} \right) \left[\frac{\lambda^2 \left(1 + \frac{\gamma_k}{2} \right)}{\bar{z} T_h \gamma_s} - \theta_c \right] \quad (6-98)$$

Thus, the dimensionless C.O.P. is given by

$$\text{C.O.P.} = \frac{\gamma_s Q_i^*}{\lambda^2 \left(1 + \frac{\gamma_k}{2} \right) \left[\frac{\lambda^2 \left(1 + \frac{\gamma_k}{2} \right)}{\bar{z} T_h \gamma_s} - \theta_c \right]} \quad (6-99)$$

where Q_i^* is given by Eq. (6-96). Equations (6-93), (6-96), and (6-99) are sufficient to determine the performance criteria for any given set of conditions.

In order to find the value of the dimensionless current λ that optimizes any given performance criteria, the first derivative of Eqs. (6-93), (6-96) and (6-99) may be set equal to zero. Inspection of the above equations shows that it is not feasible to solve the

resulting extremum conditions explicitly for λ_{opt} . It is clear that λ_{opt} could be obtained by using the numerical technique in Appendix E. Subroutines for the required Bessel functions are not available at the Rich Electronic Computing center. Furthermore, the parameters to be used are of such a nature that the customary approximating relationships for Bessel functions of very small or very large arguments may not be used.

In the opinion of the author, the actual optimization of Eqs. (6-93), (6-96) and (6-99) would only serve to further substantiate the results of the previous sections. A greater physical insight into the quantitative effects of spatial property dependence on the performance criteria would not result; although it must be admitted that more qualitative results would be feasible because of the more accurate model. The latter fact was not the purpose of this chapter.

8b. Summary of Results

In this chapter, the effect of spatial property dependence on the performance of a single-element thermoelectric heat pump has been analyzed. The summary of the results is clearer if the three principal parts of the analysis are reiterated in their order of presentation.

First, only one of the three properties is considered a specified function of x : the other two are considered constant. For this condition the performance criteria are derived and optimized. This procedure rotates until the effect of the spatial dependence of each individual property is analyzed.

Second, based on the results of the initial analysis, it is established that the spatial dependence of the Seebeck coefficient and

the electrical resistivity affect the performance criteria far more than the spatial dependence of the thermal conductivity. Thus, the thermal conductivity is assumed constant and simultaneous variations in the Seebeck coefficient and the electrical resistivity are investigated. The results of these two parts are summarized in Figs. 27 through 32. All of the following discussion is relegated to values of γ_ρ , γ_k , and γ_S less than one.

The results indicate that $(\theta_{NL})_{opt}$ can be improved by using spatial property dependence except in the case of variable thermal conductivity. The optimum amount of heat $(Q_I^*)_{opt}$, an element can pump across a specified temperature difference may be substantially increased through the use of spatial property dependence except in the case of variable thermal conductivity. It should be noted that the improvement in the heat pumping capacity is not as large when the element is operated to yield the optimum C.O.P.; the heat pumped still decreases for variable thermal conductivity. The optimum coefficient of performance $(C.O.P.)_{opt}$ is also increased by using spatial property dependence except in the case of variable thermal conductivity. However, when the element is operated to obtain the optimum heat pumping effect the C.O.P. is virtually independent of the property variations.

Third, equations describing the effects of the simultaneous variation of the thermoelectric properties on the performance criteria are derived. These equations are derived for specific linear variations in the thermoelectric properties and may be optimized for any given set of conditions. Solutions to these general equations are not presented because a greater physical insight into the quantitative effects of

spatial property dependence on the performance criteria would not result.

CHAPTER VII

SUMMARY

The objectives of this investigation have been to determine the effects of finite fins, finite fins and surface heat transfer, and the spatial dependence of S , ρ , and k on the optimum performance of a thermoelectric heat pump. Three separate analyses were made.

The first analysis presented analytical solutions that could be used to predict the optimum performance of a completely insulated thermoelement used as a heat pump with finite fins at the hot and cold junctions. In addition, the equations could be applied to a heat pump with unknown hot and cold junction temperatures, arbitrary hot and cold junction fin surface areas, and arbitrary surface heat transfer coefficients over the hot and cold junction fins. The results showed that the performance of an element may be altered significantly depending on the values of the dimensionless parameters, H_h and H_c . The results were applied to a numerical example. For the set of conditions considered, increasing the fin conductances H_c and H_h to a value greater than 20 would improve the performance by only a small amount. For other design applications, curves similar to those presented could be constructed, and from these curves, the amount of fin surface area needed for optimum performance could be determined.

The analysis presented in the second phase of this investigation could be used to predict the optimum performance of thermoelectric heat

pumps that have finite fins at the hot and cold junctions and are fully or partially insulated. The results showed that substantial gains in heat pumping capacity and C.O.P. could be achieved when the thermoelement had insulation extending a specified distance along its surface from the cold junction. The effect of fin conductance on optimum performance was also shown. One of the interesting aspects of the analysis was the significance of the value u_L . As u_L increased, the gains realized from surface heat transfer increased greatly and vice versa. For $u_L = 1$, surface heat transfer offered no improvements in performance compared to devices using fully insulated elements. However, for $u_L \geq 3$ large improvements in performance could result through the use of surface heat transfer. Improvements in performance, resulting from the use of surface heat transfer predicted in this analysis, were conservative for two reasons. First, it was assumed that thermal and electrical contact resistance at the junction of the elements were negligible. Second, it was assumed that the fins used at the hot and cold junctions were isothermal. Thus, the actual benefits gained by using surface heat transfer could be somewhat greater than those predicted in this analysis.

The final analysis determined the quantitative effect of spatially dependent thermoelectric properties on the optimized performance criteria. The analysis was quantitative primarily because the longitudinal surface of the thermoelement was insulated and both fin conductances were infinite. The effect of the positional dependence of each property on the performance criteria was determined individually, and then, in physically significant combinations. Results showed that a specific small positional dependence in S and ρ acted to increase all the performance criteria. However, a

specific small variation in k (consistent with Fig. 22) decreased the performance criteria. Also, it was shown that the positional dependence of k was not nearly as important as the positional dependence of S and ρ . Thus, a net increase in the performance criteria might be feasible through the controlled use of spatially dependent properties. Finally, the properties of S , ρ , and k were assumed to have a small linear positional dependence (consistent with Fig. 22) and equations describing the performance criteria of a thermoelement used as a heat pump were developed. Because these equations are dimensionless, computations based on them may be used over a wide range of parameter values.

APPENDICES

APPENDIX A

DERIVATION OF DIFFERENTIAL EQUATION FOR
 ONE-DIMENSIONAL TEMPERATURE DISTRIBUTION
 IN AN INHOMOGENEOUS THERMOELEMENT

In the derivation to follow, it is assumed that the thermoelement is cylindrical and has a negligible radius of curvature; the electrical current I is constant; the properties $\rho(x,T)$, $k(x,T)$ and $S(x,T)$ are arbitrary functions of axial position x and absolute temperature T ; and the element can exchange heat by convection with an environment at temperature T' .

Fig. 33 shows a differential segment of a thermoelement of length Δx . The rate at which energy is convected from the surface of the differential element is

$$hp(T - T')\Delta x \quad (A-1)$$

The rate at which electrical energy leaves the element at x is

$$IV \Big|_x \quad (A-2)$$

The rate at which carriers transport energy from the element at x is

$$IST \Big|_x \quad (A-3)$$

The rate at which energy is conducted from the element at x is

$$kA \left. \frac{dT}{dx} \right|_x \quad (A-4)$$

The rate at which energy is conducted into the element at $x + \Delta x$ is

$$kA \left. \frac{dT}{dx} \right|_{x + \Delta x} \quad (A-5)$$

The rate at which carriers transport energy into the element at $x + \Delta x$ is

$$IST \left|_{x + \Delta x} \quad (A-6)$$

The rate at which electrical energy enters the element at $x + \Delta x$ is

$$IV \left|_{x + \Delta x} \quad (A-7)$$

The rate at which the energy of the element is increasing is

$$\bar{\rho} c A \Delta x \frac{\partial T}{\partial t} \quad (A-8)$$

Conservation of energy requires that

$$\left[\begin{array}{c} \text{rate of} \\ \text{energy in} \end{array} \right] - \left[\begin{array}{c} \text{rate of} \\ \text{energy out} \end{array} \right] = \left[\begin{array}{c} \text{rate of accumulation} \\ \text{of energy} \end{array} \right] \quad (A-9)$$

Substituting Eqs. (A-1) through (A-8) into Eq. (A-9) gives

$$\begin{aligned} kA \left. \frac{\partial T}{\partial x} \right|_{x+\Delta x} - kA \left. \frac{\partial T}{\partial x} \right|_x + IST \left|_{x+\Delta x} - IST \left|_x + IV \left|_{x+\Delta x} - IV \left|_x - hp(T-T')\Delta x \right. \right. \\ = \bar{\rho} c A \Delta x \frac{\partial T}{\partial t} \quad (A-9a) \end{aligned}$$

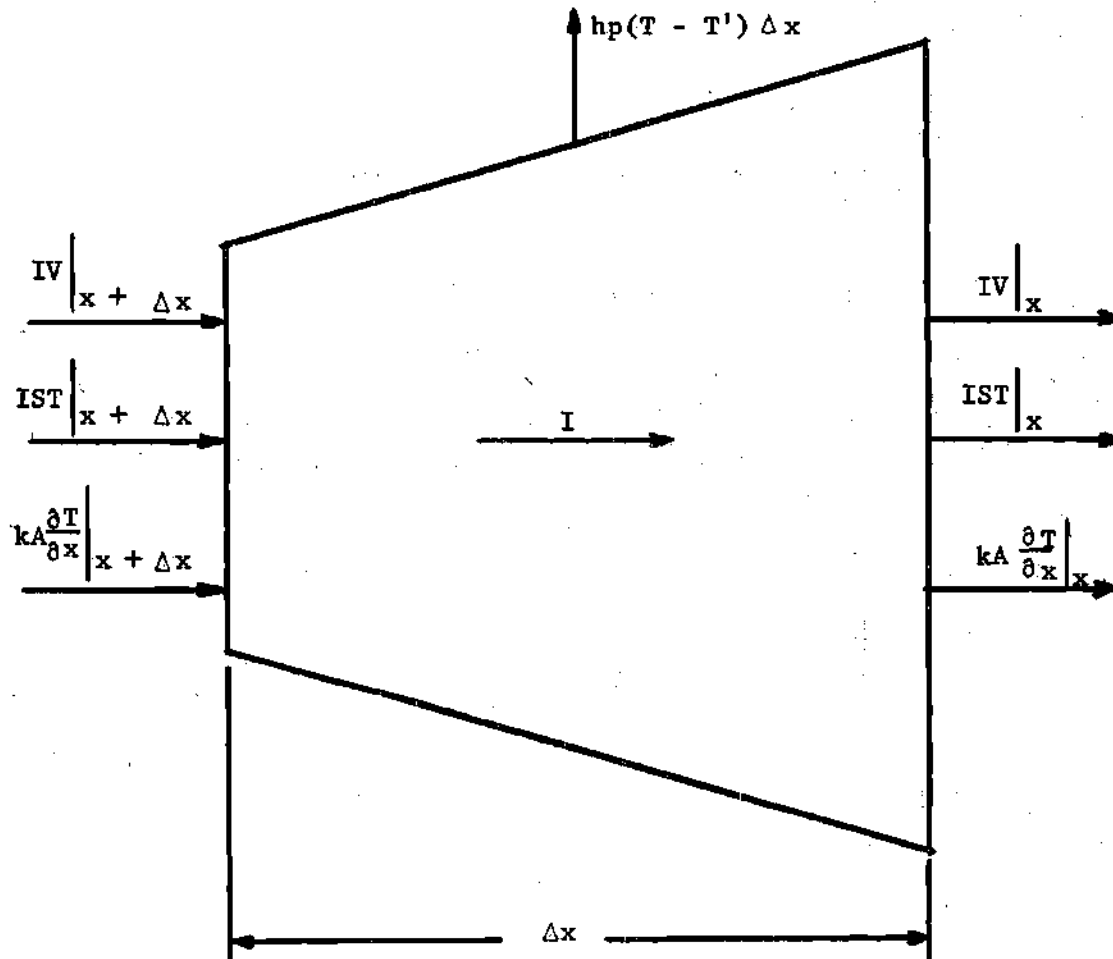


Fig. 33. Energy Balance for a Differential Thermoelement.

Next divide by Δx , take the limit as $\Delta x \rightarrow 0$, and apply the definition of a derivative to obtain

$$\frac{\partial}{\partial x} \left(kA \frac{\partial T}{\partial x} \right) + IS \frac{\partial T}{\partial x} + IT \frac{\partial S}{\partial x} + I \frac{\partial V}{\partial x} - hp(T - T') = \bar{\rho} cA \frac{\partial T}{\partial t} \quad (\text{A-9b})$$

The conjugate flows and reciprocal relationships developed by Lee and Sears from irreversible thermodynamics allow us to write

$$\frac{\partial V}{\partial x} = I \frac{\partial R}{\partial x} - S \frac{\partial T}{\partial x} \quad (\text{A-10a})$$

with

$$R = \int_0^x \frac{\rho}{A} dx \quad (\text{A-11})$$

thus,

$$\frac{\partial V}{\partial x} = \frac{I\rho}{A} - S \frac{\partial T}{\partial x} \quad (\text{A-10b})$$

Substituting Eq. (A-10b) into Eq. (A-9b) gives

$$\frac{\partial}{\partial x} (kA \frac{\partial T}{\partial x}) + IT \frac{\partial S}{\partial x} - hp(T - T') + \frac{I^2 \rho}{A} = \bar{\rho} cA \frac{\partial T}{\partial t} \quad (\text{A-12})$$

Since it was assumed that $S = S(x, T)$, it follows that

$$\frac{\partial S}{\partial x} = \left. \frac{\partial S}{\partial x} \right|_T + \left. \frac{\partial S}{\partial T} \right|_x \frac{\partial T}{\partial x} \quad (\text{A-13})$$

when Eq. (A-13) is substituted into Eq. (A-12) and the functional dependence of S , ρ , and k is shown there results

$$\begin{aligned} \frac{\partial}{\partial x} \left[k(x, t) A(x) \frac{\partial T}{\partial x} \right] + IT \left. \frac{\partial S}{\partial x} \right|_T + IT \left. \frac{\partial S}{\partial T} \right|_x \frac{\partial T}{\partial x} - hp(x) (T - T') \\ + \frac{I^2 \rho(x, T)}{A(x)} = \bar{\rho} cA(x) \frac{\partial T}{\partial t} \end{aligned} \quad (\text{A-14})$$

Notice that only the second and third terms in Eq. (A-14) depend on the direction of the current in the thermoelement. The second term is referred to as the "Volume Peltier heating effect" by Domenicali (16). The third term is the usual Thomson heating effect. If the current is reversed in Fig. (33), replace I by $-I$ in Eq. (A-14) and obtain

$$\frac{\partial}{\partial x} \left[k(x, t) A(x) \frac{\partial T}{\partial x} \right] - IT \frac{\partial S}{\partial x} \Big|_T - IT \frac{\partial S}{\partial T} \Big|_x \frac{\partial T}{\partial x} - hp(x) (T - T')$$

$$+ \frac{I^2 \rho(x, T)}{A(x)} = \bar{\rho} c A(x) \frac{\partial T}{\partial t} \quad (A-15)$$

The second and third terms in Eq. (A-15) are now referred to as the Volume Peltier cooling effect and the Thomson cooling effect respectively.

Equations (A-14) and (A-15) are general expressions for the production of energy and absorption of energy, respectively, in an inhomogeneous thermoelement.

APPENDIX B

PHYSICAL SIGNIFICANCE OF THE FIN CONDUCTANCE AND EQUATIONS FOR
THE MAXIMUM PERFORMANCE OF A COMPLETELY INSULATED THERMOELEMENT

A. Fin Conductance

In order to attach a physical significance to typical values of fin conductance, for generality, consider a shorter thermoelement 0.635 cm long by 0.635 cm in dia. If $k = 0.015 \text{ W/cm} \cdot ^\circ\text{K}$ and $A = 0.317 \text{ cm}^2$, then

$$H_h = 66.8 h_h A_h$$

and

$$H_c = 66.8 h_c A_c$$

In air, the heat-transfer coefficient h ranges in value from about $0.00284 \text{ W/cm}^2 \cdot ^\circ\text{K}$ for natural convection to about $0.0284 \text{ W/cm}^2 \cdot ^\circ\text{K}$ for forced convection. Letting $A_h = A_c = 138 \text{ cm}^2$ for forced convection gives

$$H = 262$$

Letting $A_h = A_c = 353 \text{ cm}^2$ for natural convection gives

$$H = 67$$

B. Equations for Maximum Performance of a Completely Insulated Thermoelement

If the hot and cold junction fin conductances are considered infinite, then Eq. (4-11) reduces to

$$(\dot{Q}_i^*)_{\max} = 1 + \phi y - \frac{\alpha y^2}{2} \quad (\text{B-1})$$

and Eq. (4-13) reduces to

$$(\text{C.O.P.})_{\max} = \frac{1 + \phi y - \alpha y^2/2}{\alpha y^2 - y} \quad (\text{B-2})$$

In addition, if the cold junction is considered insulated from the cold-junction environment ($H_c = 0$), then Eq. (4-10) reduces to

$$(\dot{Q}_{\text{NL}})_{\max} = \frac{y(\phi - 1) - (\alpha/2)y^2}{1 + y} \quad (\text{B-3})$$

The expression for y_{opt} for Eqs. (4-17), (4-18) and (4-19) may be obtained by a corresponding reduction in Eqs. (4-15), (4-16), and (4-14) respectively.

APPENDIX C

DEFINITIONS OF CONSTANTS IN CHAPTER V

The following definitions are given for D_m , E_m , R_m ($m=1,2,3,4$), W_m ($m=1,2,3,4$), and z_m ($m=1,2,\dots,15$).

$$D_1 = (u_L/G) \left[\cosh(\dot{u}) + u_v \sinh(\dot{u}) \right]$$

$$D_2 = E_2 = u_L/G$$

$$D_3 = (u_L/G) \left[u_v^2/2 + (u_v - G) \tanh(\dot{u}/2) \right]$$

$$D_4 = -H_h + (u_L/G) (u_v - G) \tanh(\dot{u}/2)$$

$$E_1 = -u_L \cosh(\dot{u})/G$$

$$E_3 = - (u_L/G) \left[u_v^2/2 + \left\{ u_v + \tanh(\dot{u}/2) \right\} \tanh(\dot{u}) \right] \cosh(\dot{u})$$

$$E_4 = (u_L/G) \left[\cosh(\dot{u}) - 1 \right]$$

$$G = - (\tanh(\dot{u}) + u_v) \cosh(\dot{u})$$

$$R_1 = \alpha u_L (E_3 - D_3)$$

$$R_2 = \alpha \left[E_3 (D_1 - D_2 - H_h) - D_3 (E_1 + E_2 + H_c) \right]$$

$$R_3 = u_L \left[E_4 + D_4 - \alpha (D_1 - D_2 - H_h - H_c - E_1 - E_2) \right]$$

$$R_4 = E_4 (D_1 - D_2 - H_h) + D_4 (E_1 + E_2 + H_c)$$

$$W_1 = u_L \alpha E_3 H_c$$

$$W_2 = H_c \left[\alpha \left\{ E_3 (D_1 - H_h) - D_3 E_2 \right\} - u_L^2 \phi \right]$$

$$W_3 = u_L \phi H_c (H_h - D_1 + E_2) + u_L E_4 (H_c + D_1 - 1)$$

$$\begin{aligned}
W_4 &= H_c \left[E_4 (D_1 - H_h) + E_2 D_4 \right] \\
Z_1 &= \alpha u_L E_3 \\
Z_2 &= \alpha E_3 (H_h - D_1) + \alpha D_3 E_2 + u_L^2 \phi \\
Z_3 &= u_L \left[\phi (H_h - D_1) + E_4 + \phi E_2 \right] \\
Z_4 &= E_4 (H_h - D_1) - E_2 D_4 \\
Z_5 &= u_L^2 \\
Z_6 &= u_L (H_h - H_c - D_1 - E_1) \\
Z_7 &= (H_c + E_1) (H_h - D_1) - D_2 E_2 \\
Z_8 &= \alpha u_L D_3 \\
Z_9 &= \phi u_L^2 - \alpha \left\{ D_3 (H_c + E_1) + D_2 E_3 \right\} \\
Z_{10} &= u_L (\phi H_c + D_4) \\
Z_{11} &= D_4 (H_c + E_1) - D_2 E_4 \\
Z_{12} &= Z_3 + u_L (E_1 + D_1 - H_h) \\
Z_{13} &= (E_4 + E_1) (D_1 - H_h) + E_2 (D_4 + D_2) \\
Z_{14} &= u_L (H_h - D_1 - E_1) \\
Z_{15} &= E_1 (H_h - D_1) - D_2 E_2
\end{aligned}$$

The quantities above were defined solely as a matter of convenience. They simplified the algebra of the solution considerably and were especially useful for the computer program used in evaluating the results; the quantities themselves do not have any physical significance.

APPENDIX D

DISCUSSION OF THE GREEN'S FUNCTION

There are a great many textbooks that adequately discuss the Green's function. Therefore, this appendix is included primarily for the convenience of the reader and it is not intended as a mathematical treatise on the subject. On the contrary, the purposes of this discussion are to introduce the reader to the concept of the Green's function; acquaint the reader with the properties of this function; and to work an illustrative example.

This discussion is limited to the one dimensional Green's function and its application to linear, second-order, non-homogeneous differential equations with two associated boundary conditions. In general consider the differential equation

$$\frac{d}{du} \left[P(u) \frac{d\theta}{du} \right] + q(u)\theta + f(u) = 0 \quad (D-1)$$

It is assumed that $P(u)$, $q(u)$, and $f(u)$ are continuous in the closed interval $a \leq u \leq b$; also, $P(u) \neq 0$ and neither a or b are infinite. If these assumptions are violated it is possible for the solution of Eq. (D-1) to become infinite; it is desirable to avoid this difficulty at present. Equation (D-1) is subject to two non-homogeneous boundary conditions at the points a and b of the form

$$\alpha_1 \theta(a) + \alpha_2 \left. \frac{d\theta}{du} \right|_{u=a} = Q_1(a) \quad (D-2)$$

$$\beta_1 \theta(b) + \beta_2 \left. \frac{d\theta}{du} \right|_{u=b} = Q_2(b) \quad (D-3)$$

where α_1 , α_2 , β_1 , and β_2 are given constants.

In order to obtain a convenient form of the solution of Eq. (D-1), an auxiliary differential equation is considered.

$$\frac{d}{du} \left[P(u) \frac{dG}{du} \right] + q(u)G + \delta(u - \varepsilon) = 0 \quad (D-4)$$

where $\delta(u - \varepsilon)$ is the familiar Dirac delta function.

Equation (D-4) is subject to the homogeneous boundary conditions

$$\alpha_1 G(a) + \alpha_2 \left. \frac{dG}{du} \right|_{u=a} = 0 \quad (D-5)$$

$$\beta_1 G(b) + \beta_2 \left. \frac{dG}{du} \right|_{u=b} = 0 \quad (D-6)$$

First an attempt is made to determine the function $G(u, \varepsilon)$ which, for a given number ε , is given by $G_1(u, \varepsilon)$ when $u < \varepsilon$ and by $G_2(u, \varepsilon)$ when $u > \varepsilon$ and which has the following properties:

1. The functions $G_1(u, \varepsilon)$ and $G_2(u, \varepsilon)$ satisfy Eq. (D-4) in their intervals of definition; that is

$$\frac{d}{du} \left[P(u) \frac{dG_1}{du} \right] + q(u) G_1 = 0 \quad \text{when } u < \varepsilon$$

and

$$\frac{d}{du} \left[P(u) \frac{dG_2}{du} \right] + q(u) G_2 = 0 \quad \text{when } u > \varepsilon$$

2. The function $G(u, \varepsilon)$ satisfies the homogeneous boundary conditions

prescribed at the end points $u = a$ and $u = b$; that is, $G_1(u, \epsilon)$ satisfies Eq. (D-5) and $G_2(u, \epsilon)$ satisfies Eq. (D-6).

3. The function $G(u, \epsilon)$ is continuous at $u = \epsilon$; that is, $G_1(\epsilon, \epsilon) = G_2(\epsilon, \epsilon)$.

4. The derivative of $G(u, \epsilon)$ has a discontinuity of magnitude $-1/P(\epsilon)$ at the point $u = \epsilon$; that is,

$$\left. \frac{dG_2}{du} \right|_{u=\epsilon} - \left. \frac{dG_1}{du} \right|_{u=\epsilon} = -\frac{1}{P(\epsilon)}$$

5. The function $G(u, \epsilon)$ is symmetric; that is,

$$G(u, \epsilon) = G(\epsilon, u).$$

Any function satisfying the above five properties is defined as the Green's function $G(u, \epsilon)$. It can easily be shown that if the function $G(u, \epsilon)$, in which ϵ appears as a parameter, exists, then the solution of Eq. (D-1) subject to boundary conditions (D-2) and (D-3) is

$$\theta(u) = \int_a^b G(u, \epsilon) f(\epsilon) d\epsilon + P(\epsilon) \left[G(u, \epsilon) \frac{d\theta}{d\epsilon} - \theta(\epsilon) \frac{dG}{d\epsilon} \right]_{\epsilon=a}^{\epsilon=b} \quad (D-7)$$

This form of the solution is valuable and concise. Notice that, for boundary conditions (D-2) and (D-3), Eq. (D-7) expresses the solution to Eq. (D-1) for all continuous $f(u)$; that is, Eq. (D-7) represents infinitely many solutions of Eq. (D-1).

The above technique is illustrated by verifying the Green's function for Eq. (6-9). The system to be solved consists of differential

Eq. (6-7) subject to boundary conditions (6-8a) and (6-8b). The auxiliary system is given by

$$\frac{d^2G}{du^2} = -\delta(u - \epsilon) \quad (D-8)$$

and the homogeneous boundary conditions

$$\alpha G(0) - \left. \frac{dG}{du} \right|_{u=0} = 0 \quad (D-9)$$

$$G(1) = 0 \quad (D-10)$$

By property 1,

$$G(u, \epsilon) = \begin{cases} Au + B & 0 \leq u < \epsilon \\ Cu + D & \epsilon < u \leq 1 \end{cases}$$

where A, B, C, and D are constants to be determined by satisfying properties 2 through 4.

By property 2,

$$A = \alpha B \text{ and } C = -D$$

Therefore,

$$G(u, \epsilon) = \begin{cases} B(\alpha u + 1) & 0 \leq u < \epsilon \\ C(u - 1) & \epsilon < u \leq 1 \end{cases}$$

By property 3, continuity exists at $x = \epsilon$, thus

$$B = C(\epsilon - 1) / (\alpha\epsilon + 1)$$

and

$$G(u, \varepsilon) = \begin{cases} \frac{C(\varepsilon - 1)(\alpha u + 1)}{\alpha \varepsilon + 1} & 0 \leq u < \varepsilon \\ C(u - 1) & \varepsilon < u \leq 1 \end{cases}$$

By property 4,

$$C - \frac{C\alpha(\varepsilon - 1)}{\alpha \varepsilon + 1} = -1$$

$$\therefore G(u, \varepsilon) = \begin{cases} \frac{(1 - \varepsilon)(\alpha u + 1)}{1 + \alpha} & 0 \leq u < \varepsilon \\ \frac{(1 - u)(\alpha \varepsilon + 1)}{1 + \alpha} & \varepsilon < u \leq 1 \end{cases}$$

Notice that property 5 is also satisfied; this is a convenient check.

Evaluating the second term in Eq. (D-7), using $P(\varepsilon) = 1$, and Eqs.

(6-8a), (6-8b), (D-9), and (D-10) gives

$$\theta(u) = \int_0^1 G(u, \varepsilon) f(\varepsilon) d\varepsilon + \frac{(\bar{Q}_1^* - \alpha)(1 - u)}{\alpha + 1}$$

which is identical to Eq. (6-9).

APPENDIX E

DISCUSSION OF A NUMERICAL OPTIMIZING TECHNIQUE

The numerical technique discussed below was suggested by Dr. K. R. Purdy of the Mechanical Engineering Department. In conjunction with Fig. 34, this method can be explained briefly as follows:

Assume a value of λ which is somewhat smaller than the expected λ_{opt} and calculate $\theta_{NL}(\lambda)$. Establish a λ grid of width $\Delta\lambda$. Calculate $\theta_{NL}(\lambda + \Delta\lambda)$. "Ask" the computer if $\theta_{NL}(\lambda + \Delta\lambda) \leq \theta_{NL}(\lambda)$. If the answer is false, instruct the computer to compute $\theta_{NL}(\lambda + 2\Delta\lambda)$, etc. until the answer is true. When the answer is true send the computer back several intervals and decrease the size of the $\Delta\lambda$ grid. Repeat this procedure until λ_{opt} is obtained to the desired accuracy; then calculate $(\theta_{NL})_{opt}$. It is clear that this method will only work when one has a continuous function and a knowledge of the location of the optimum value.

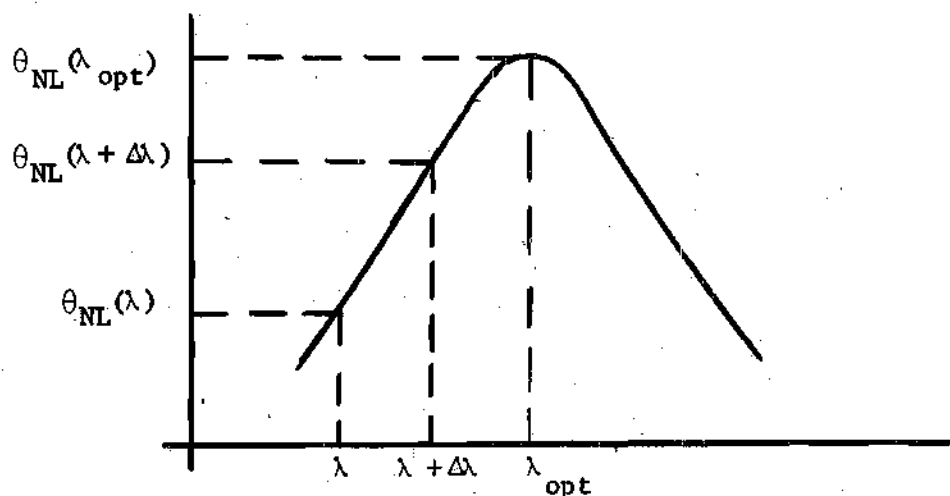


Fig. 34. Illustration of a Numerical Optimizing Technique.

LITERATURE CITED

1. E. Altenkirch, "Elektrothermische Kalteerzeugung und reversible elektrische Heizung", Physik, Z.12, 920-924, (1911).
2. P. O. Gelhoff, E. Justi, and M. Kohler, "Verfeinerte Theorie der elektrothermischen Kalteerzeugung", Abhandl, Braunschweig. Wiss. Ges., 2, 159-164, (1950).
3. A. F. Ioffe, Semiconductor Thermoelements and Thermoelectric Cooling, Inforsarch Ltd., London, (1957).
4. J. A. Brandt, "Solutions to the Differential Equations describing the Temperature Distribution, Thermal Efficiency, and Power Output of a Thermoelectric Element with Variable Properties and cross-sectional area", Advanced Energy Conversion, 2, 219-230, (1962).
5. C. N. Rollinger and J. E. Sunderland, "Performance of a Convectively Cooled Thermoelement used for Power Generation", Solid-State Electronics, 3, 268-277, (1961).
6. C. R. Crosby, M. H. Norwood, and B. R. West, "The Effects of Heat Transfer on Optimum Peltier Heat Pumping", American Society of Mechanical Engineers, P/62 - HT - 11, (1962).
7. R. Zito Jr., "Dynamic Behavior of a Thermoelectric Heat Pump", Electro-Technology, 71, 64-69, (1963).
8. L. J. Ybarrondo and J. E. Sunderland, "Effects of Surface Heat Transfer on the Performance of a Thermoelectric Generator", Solid-State Electronics, 5, 143-154, (1962).
9. C. O. Mackey, "Thermoelectric Cooling", A report published at the Sibley School of Mechanical Engineering, Cornell University under the auspices of the Salvatore Giordano Foundation, Inc., of Maspeth, New York, (April 1962).
10. T. C. Harmon, J. H. Cahn, and M. J. Logan, "Measurement of Thermal Conductivity by Utilization of the Peltier Effect", Journal of Applied Physics, 30, 1351-1359, (1959).
11. M. A. Kaganov, I. S. Lisker, and I. G. Mushkin, "On the Problem of Measuring Thermoelectric Properties of Semiconductors", Soviet Physics - Solid-State, 1, 905-907, (1959).
12. J. E. Parrott, "The Interpretation of the Stationary and Transient Behavior of Refrigerating Thermocouples", Solid-State Electronics, 1, 135-143, (1960).

13. H. B. Nottage, P. S. Starrett, and P. L. Winskell, "Thermoelectric Generators with Surface Heat Loss", ASME Journal of Heat Transfer, 84C, 193-206, (1962).
14. C. N. Rollinger and J. E. Sunderland, "The Performance of a Thermoelectric Heat Pump with Surface Heat Transfer", Solid-State Electronics, 6, 47-57, (1963).
15. T. C. Harmon, B. Paris, S. E. Miller and H. L. Goering, "Preparation and some Physical Properties of Bi_2Te_3 , Sb_2Te_3 , and As_2Te_3 ", Journal of Physics and Chemistry of Solids, 2, 181-190, (1957).
16. C. A. Domenicali, "Irreversible Thermodynamics of Thermoelectricity", Reviews of Modern Physics, 26, 237-275, (1954).
17. W. H. Clingman, "Entropy Production and Optimum Device Design", Advanced Energy Conversion, 1, 61-79, (1961).
18. B. Varga, A. D. Reich, and J. R. Madigan, "Thermoelectric and Thermomagnetic Heat Pumps", Journal of Applied Physics, 34, 3430-3441, (1963).
19. P. E. Gray, The Dynamic Behavior of Thermoelectric Devices, John Wiley and Sons, New York, (1960).
20. M. H. Norwood, "A Comparison of Theory and Experiment for a Thermoelectric Cooler", Journal of Applied Physics, 32, 2559-2563, (1961).
21. C. N. Rollinger, "Effect of Geometric Shape and Convective Heat Transfer on the Performance of a Thermoelement", Ph.D. Dissertation, Northwestern University, Evanston, Illinois, (1961).
22. R. B. Bird, W. E. Stewart, and E. N. Lightfoot, Transport Phenomena, John Wiley and Sons, Inc., New York, (1960).
23. H. S. Carslaw, and J. E. Jaeger, Conduction of Heat in Solids, Oxford Press, London, 2nd edn., (1959), p.21.
24. S. N. Levine, Selected Papers on New Techniques for Energy Conversion, Dover Publications, Inc., New York, (1961).
25. D. K. C. MacDonald, Thermoelectricity: An Introduction to the Principles, John Wiley and Sons, Inc., New York, (1960).
26. F. B. Hildebrand, Methods of Applied Mathematics, Prentice-Hall, New Jersey, (1961).
27. K. Yosida, Lectures on Differential and Integral Equations, Interscience Ltd., London, (1960).
28. E. Kamke, Differentialgleichungen Lösungsmethoden und Lösungen, Chelsea Publishing Co., New York, (1948).

OTHER REFERENCES

Cadoff, I. B., and Miller, E., Thermoelectric Materials and Devices, Reinhold Corp., New York, (1960).

Callen, H. B., Thermodynamics, John Wiley and Sons, Inc., New York, (1960).

Grobner, W., and Hofreiter, N., Integraltafel Erster Teil Unbestimmte Integrale, Zweite, verbesserte Auflage, Wein and Innsbruck, Springer-Verlag, (1957).

Heikes, R. R., Thermoelectricity: Science and Engineering, Interscience Publishers, Inc., New York, (1961).

Lee, J. F., and Sears, T. W., Thermodynamica, Addison-Wesley, Reading, Mass., (1955), pp. 180-185.

McLachlan, N. W., Bessel Functions for Engineers, Oxford Press, London, 2nd edn., (1961).

VITA

Lawrence J. Ybarrondo was born in Detroit, Michigan on July 15, 1937. He received a Bachelor of Mechanical Engineering degree from the University of Detroit in 1960. After graduation, he was employed by U. S. Rubber Company as a tire engineer until he entered graduate school. In 1962 he received the degree of Master of Science in Mechanical Engineering from Northwestern University. While attending graduate school at Northwestern University, he worked part-time as a research engineer at the Borg-Warner Corporation research center. His graduate work has resulted in the publication of three papers in the field of thermoelectricity.

Mr. Ybarrondo was married in 1958 to the former Mary Ann Mehall and they have two children.